Brazil Oil & Gas, tt_nrg and Norway Oil & Gas

EPRASHEED
signature series

2010 – Issue 12

Saudi Arabia oil & gas

www.saudiarabiaoilandgas.com

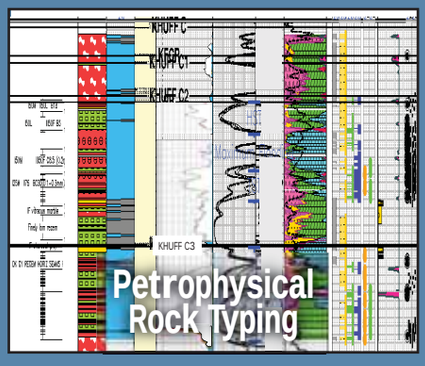

Petrophysical Rock Typing

Opening of Completions Base

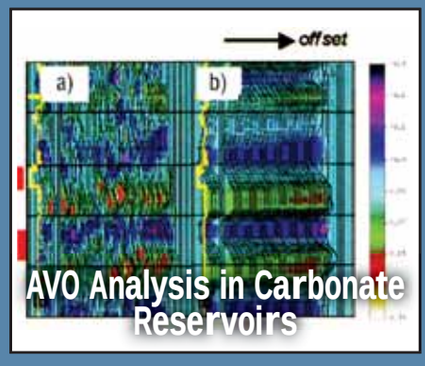

AVO Analysis in Carbonate Reservoirs

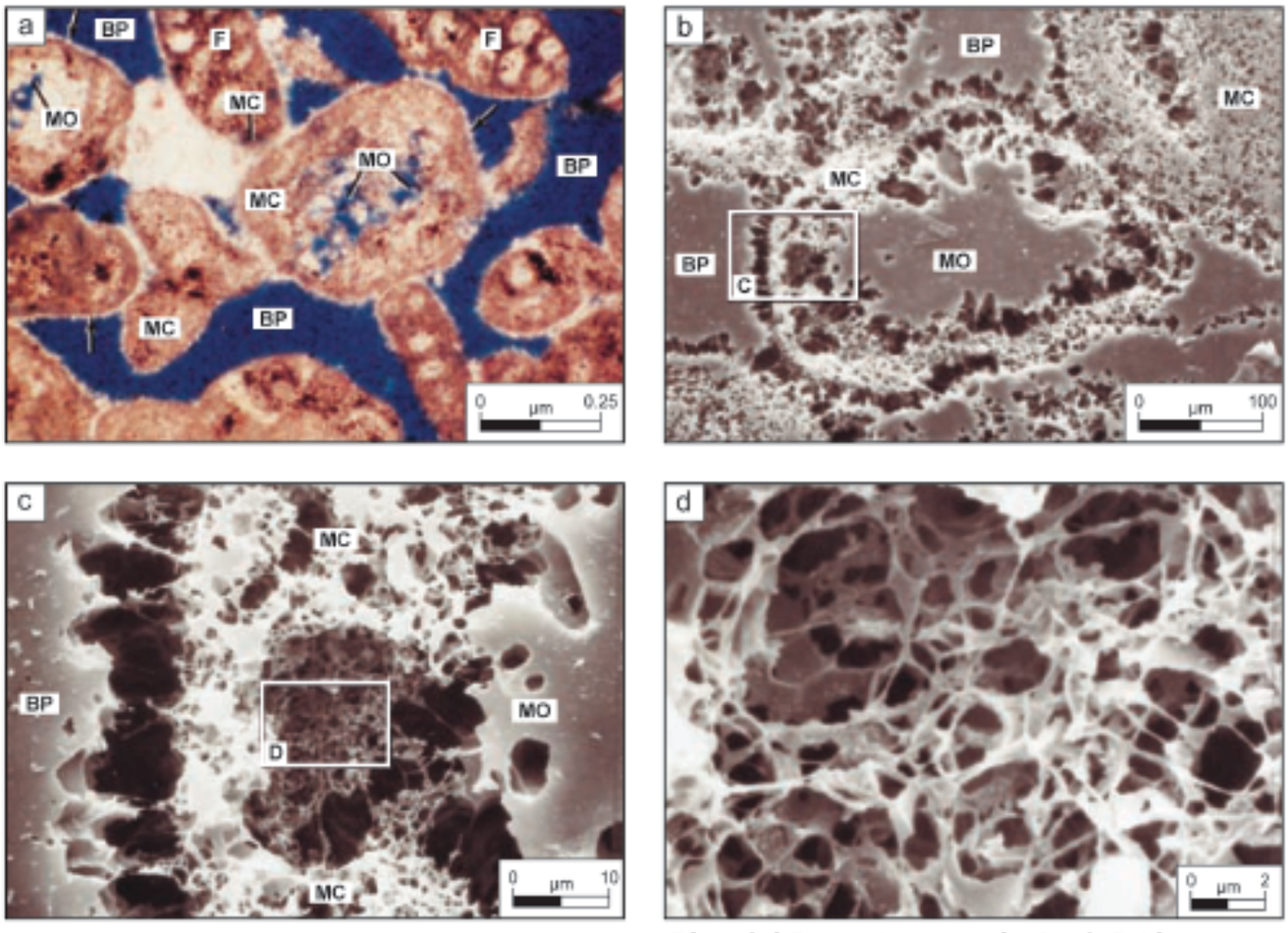

Bimodal Pore Systems in Arab-D Limestone

SMITH Means Superior Tubular Solutions

#1 A History of Excellence

For over 50 years the SMITH name and the Drilco® brand have been synonymous with excellence in tubular products and services. From the invention of Hevi-Wate™ drill pipe to the first use of continuous line heat treating for drill collar bars, to the comprehensive maintenance and repair facilities for BHA and down hole tools, SMITH has been continuously at the forefront of tubular sales and service.

#2 Extensive Product Range and Expertise

SMITH offers a full range of new tubulars including drill pipe, Hevi-Wate™, drill collars and kellys to optimize your drilling operations. SMITH also provides rental of these BHA products to reduce your overall inventory costs. In addition to our expert machine ship services, SMITH provides a full range of inspection and maintenance services for your drilling tools, including our new state-of-the-art mobile field hardbanding units which extend the life of your existing equipment inventory.

#3 Global Reach

SMITH has the worldwide infrastructure to support your operations no matter where you drill. With inventory and machine shop facilities strategically located around the globe, SMITH can be counted on to provide fast, dependable response to all your needs – 24 hours a day, 7 days a week.

Call your Smith representative today for
superior tubular solutions you can trust.

www.smith.com

THE POSSIBILITIES ARE ENDLESS

SMITH

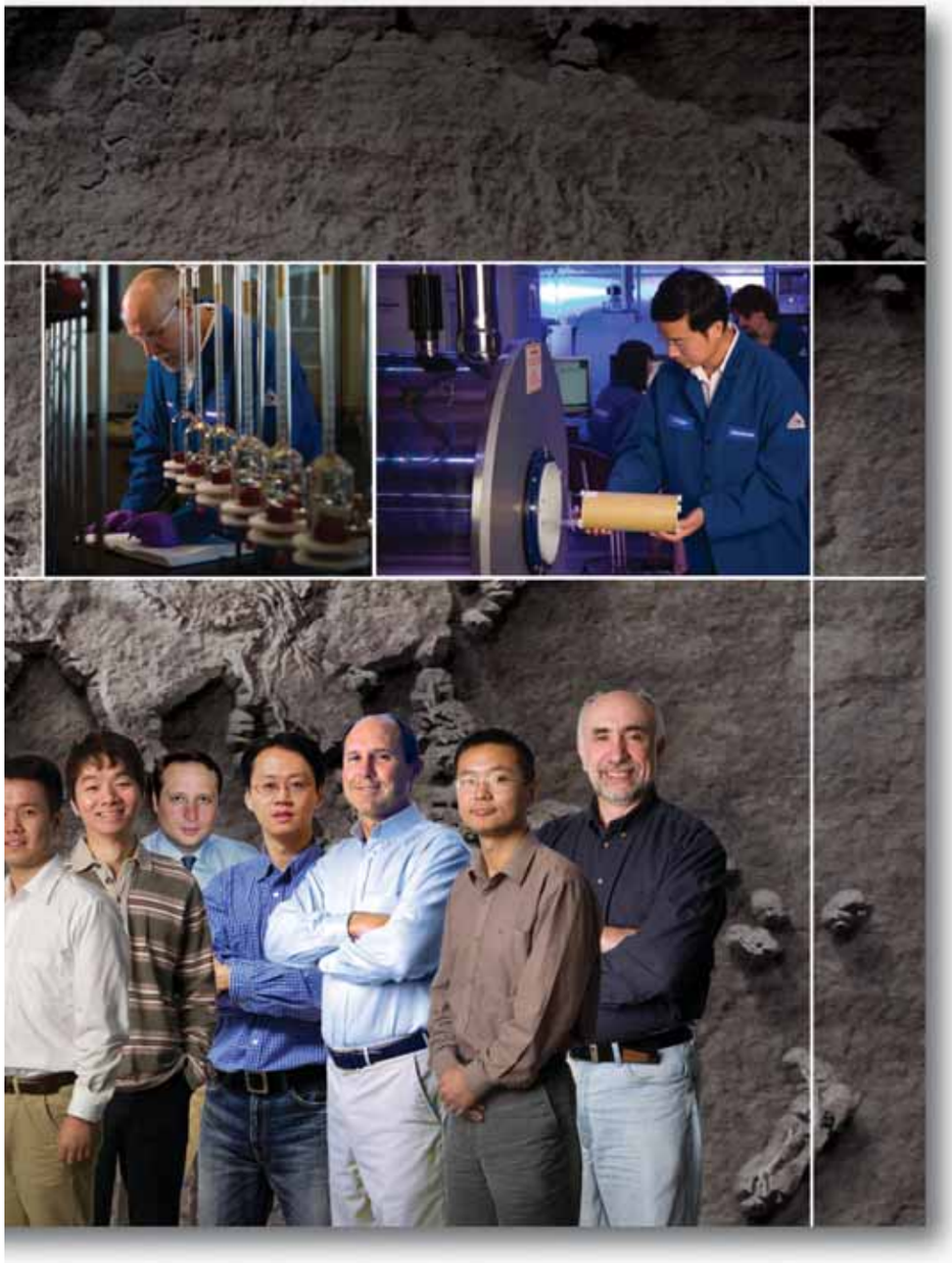

Carbonate Advisor

Schlumberger

2010 – Issue 12

Saudi Arabia oil & gas

EPRASHEED
signature series

www.saudiarabiaoilandgas.com

Contents

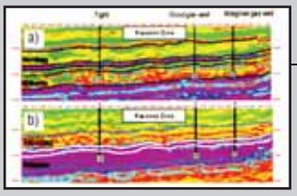

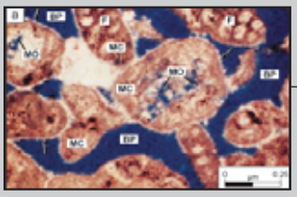

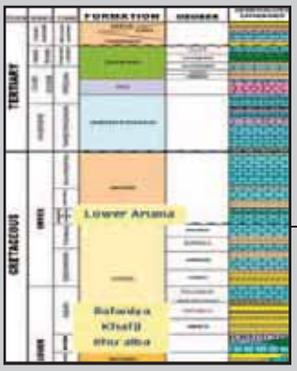

ADVERTISERS:

Contacts

CEO and Founder
EPRasheed
Wajid Rasheed
wajid.rasheed@eprasheed.com

Editors
JC Cunha (Technology)
Majid Rasheed
Mauro Martins

Design
Sue Smith

United Kingdom

- Head Office
Tel: (44) 207 193 1602

- Brian Passey
brian@bspmedia.com

- Sally Cole
sally@bspmedia.com

Saudi Arabia

- Akram ul Haq
PO BOX 3260, Jeddah 21471
akram.ul.haq@saudiarabiaoilandgas.com
Tel: (966) 557 276 426

- Mohanned AlSagri
mohanned.alsagri@saudiarabiaoilandgas.com

Houston

- David Jones
david.jones@eprasheed.com
Tel: (1) 281 793 4314

- William Bart Goforth
william.goforth@eprasheed.com
Tel: (1) 713 304 6119

Brazil

- Ana Felix
afelix@braziloilandgas.com
Tel: (55) 21 9714 8690

- Fabio Jones
fabio.jones@braziloilandgas.com
Tel: (55) 21 9392 7821

- Roberto S. Zangrando
rzangrando@braziloilandgas.com
Tel: (55) 22 8818 8507

NOTE FROM THE CHAIRMAN, 2010 SPE/DGS ANNUAL TECHNICAL SYMPOSIUM & EXHIBITION

Dear Colleagues,

I am pleased to announce the first Annual Technical Symposium and Exhibition organized jointly by the Society of Petroleum Engineers (SPE) Saudi Arabia Section and Dhahran Geoscience Society (DGS).

The SPE/DGS ATS&E 2010 will be held on 4-7 April 2010 in Khobar, Saudi Arabia. The symposium will consist of technical presentations, panel discussions, and poster sessions, focusing on technology applications and best practices.

Over the past 25 years, the ATS&E has become a central E&P technical gathering for regional and international industry professionals to discuss and exchange expertise and to promote the latest innovations and technologies. We anticipate hosting over 2000 delegates from across the region and around the world making the symposium one of the largest petroleum and gas industry gathering in Saudi Arabia.

This annual showcase will involve keynote speakers, technical presentations and posters, special technical sessions, panel discussions, technical courses, and field trips. An Exhibition will be also held along with the symposium that will involve leading companies showcasing their latest technological achievements.

On behalf of the Technical Program Committee, I would like to invite you to submit papers that address the symposium theme of "The Race to Ultimate Recovery: People, Technology, and Beyond".

I look forward to your support and commitment in making the 2010 SPE/DGS Annual Technical Symposium and Exhibition a grand success.

We would also like to express our gratitude to Saudi Arabia Oil and Gas as Official Publication and this issue contains call for papers and symposium information.

Sincerely,

Faisal N. Al-Nughaimish, Chairman

2010 SPE/DGS Annual Technical Symposium
& Exhibition

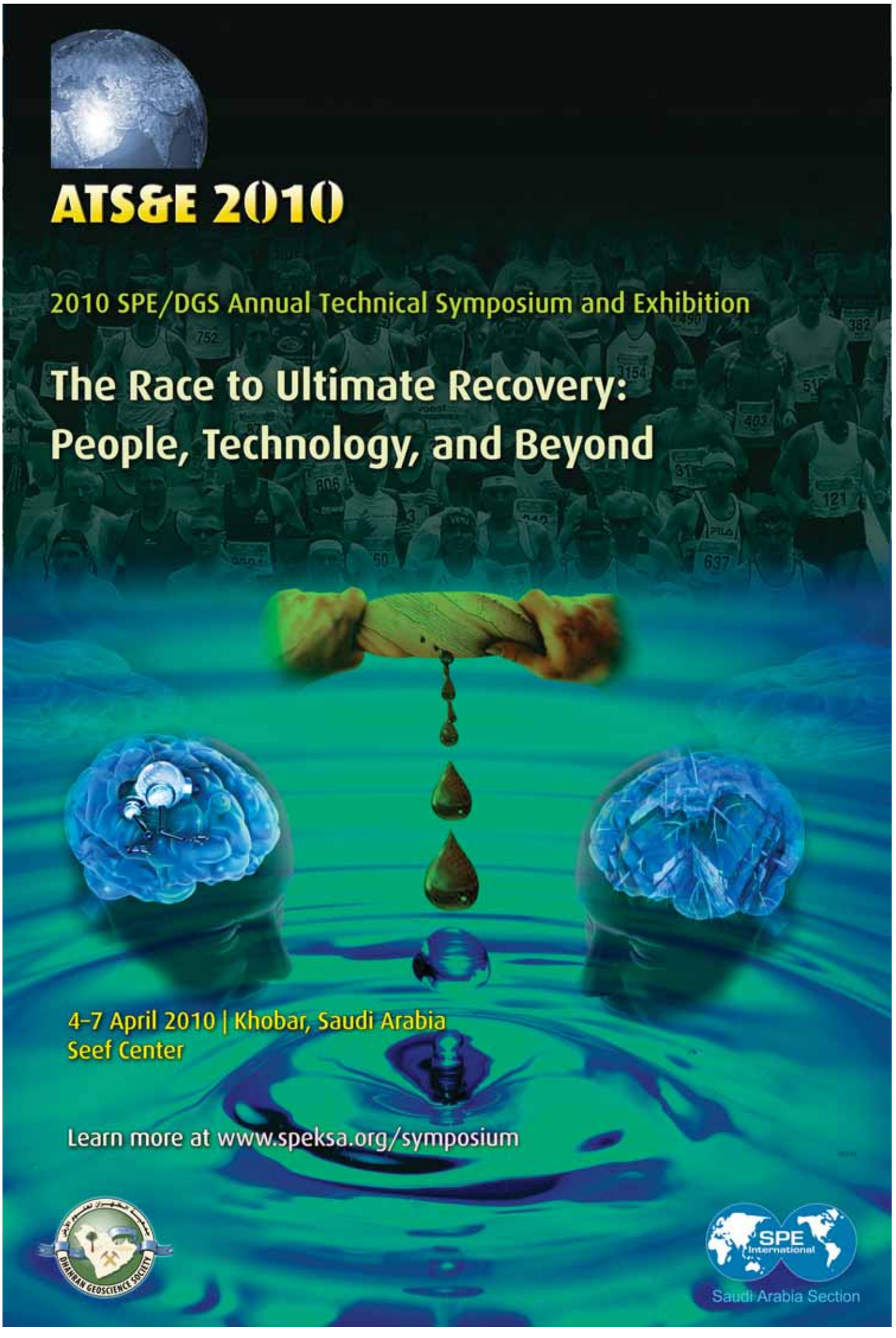
ATS&E 2010
2010 SPE/DGS Annual Technical Symposium and Exhibition
The Race to Ultimate Recovery:
People, Technology, and Beyond
4–7 April 2010 | Khobar, Saudi Arabia
Seef Center
Learn more at www.speksa.org/symposium
DHAHRAN GEOSCIENCE SOCIETY
SPE International
Saudi Arabia Section

Shoaibi Group – A Step Change to Innovation

Saudi Arabia Oil and Gas spoke exclusively with Walid Al-Shoaibi about the company's innovative strategy.

Saudi Arabia Oil and Gas: Can you provide some detail on Shoaibi's evolution and growth?

Walid Al-Shoaibi: Founded in 1973 in Saudi Arabia, Shoaibi Group was originally established to carry out industrial and commercial activities in KSA. The Shoaibi Group of companies currently works with global partners, predominately in the oil, gas & petrochemicals industry, and over the past 4 decades the Group's subsidiaries have steadily expanded to around 100 local and international partners in the fields of exploration, production, and support services to the oil and gas industry, oil refining and gas processing chemicals and petrochemicals, maritime services, and refined products and distribution. Recently, in recognizing the need for oil operators to control costs by becoming more efficient in the discovery and recovery processes, Shoaibi Group has become a developer of, partner to and investor in many innovative oil and gas technology companies with the objective of addressing the needs of the region's reservoirs.

Saudi Arabia Oil and Gas: What upstream solutions is Shoaibi innovating? What are the focus areas i.e. within Drilling and Completions?

Walid Al-Shoaibi: Shoaibi Group recently successfully sold its portfolio company Flotech to Tendeka. Founded in 2007, FloTech is an innovative reservoir completion company with proprietary technologies. The company's vision is to improve petroleum well efficiency through reservoir completion products, namely inflow control devices and mechanical packers, which combine design simplicity with superior performance. We are further investing in innovative technology companies such as Artificial Lift Company (Artificial lift ESP technology), Ingrain (Digital Core analysis – Shale and Tight Gas) and Fotech (Advanced Reservoir Monitoring).

Saudi Arabia Oil and Gas: How is Shoaibi partnering with Dhahran Techno-Valley (DTV) to research and develop such solutions?

Walid Al-Shoaibi: Recently Shoaibi Group has launched its own 'Incubator'. The Incubator Project is a R&D hub, located in Dhahran Techno Valley ('DTV'), Al-Khobar, to assist in bringing new technologies to local NOCs and the wider region through sponsorship and involvement of local and international universities such as King Fahd University of Petroleum & Minerals (KFUPM) in Dhahran, and other R&D centres. The purpose of this project is to incubate ideas either in-house or take existing technology and modify it towards an oilfield application. By understanding the current and future technology needs of Saudi Aramco, the 'incubator' serves to take these challenges to universities and other R&D centers to validate whether these challenges can be met. There is no better way to gain this understanding than by working alongside oil operators such as Saudi Aramco. If the technology is found to be suitable either as a concept or prototype, then the incubator team will secure funding to take the technology to the 'Technical and Commercial Feasibility' stage. Shoaibi Group collaborates with some of the world's leading venture capital companies in order to bring an added understanding of the specific needs of the MENA region, and a direction of funding to address these needs. Finally, once the technology/prototype has been developed and thoroughly tested it will be passed on to a company with sufficient funding from local

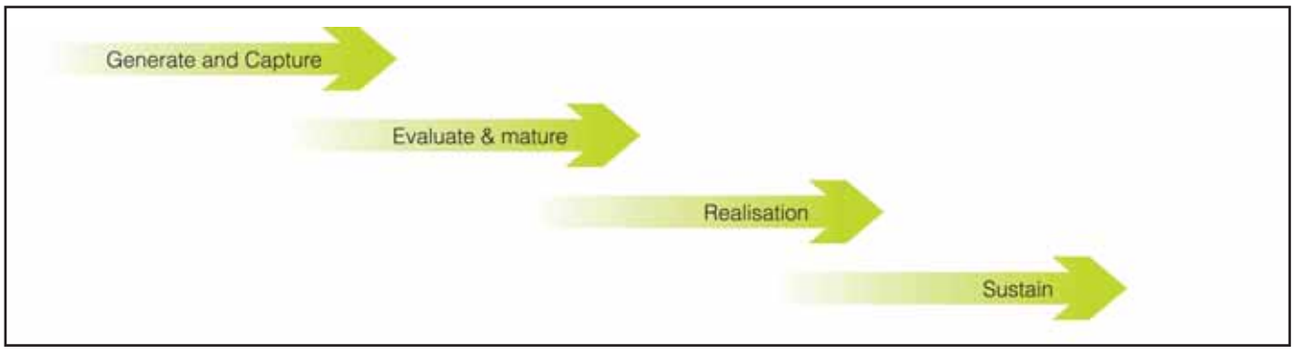

Research & Development Process - Capturing ideas to commercialisation.

and international investors with the objective to commercialise the product, delivering new value to NOCs and international oil companies (IOCs) in the region and globally. The Shoaibi Group, in working with Saudi Aramco and its various partners, very much aims to be a part of developing the innovative solutions.

Saudi Arabia Oil and Gas: How is end-user input helping research and development?

Walid Al-Shoaibi: The end user is key in the R&D process as it will ultimately decide the commercial viability of the new technology. A development process has been put in place where the end users input are 'funnelled' through key stages of the process. Another important note is to have the end users' input at these different development stages. Not only does this provide insight, it also encourages collaborative teamwork between the researchers and the end user. Sharing of knowledge enhances the success of the project.

Saudi Arabia Oil and Gas: What is the business case for the selected R&D and Innovations? How are prospective technologies evaluated?

Walid Al-Shoaibi: The business case for selected R&D projects is mainly driven by our 'development process'. There are four main key stages that any idea/innovation needs to pass through. The First is the 'Generate and Capture' stage, where ideas from industry, individuals, from conferences and from papers, etc, are captured and reviewed. The review process asks a certain number of key questions, e.g. is there a demand from the market for the technology for a particular business critical issue to be addressed. If the idea/innovation passes this stage, it enters the concept/feasibility stage.

This is where funds are provided to carry out small-scale experiments, build prototypes and test the design. Again a screening process is undertaken where certain criteria have to be met in order to pass through the concept/feasibility stage. The third stage is to define the detailed design and carry out further testing with the 'near final' prototype. Once the design is finalized, and tested, the technology is ready for field trials. During the field trail phase the technology is tested and evaluated under real well conditions. After a certain field trial period and assuming success of the trails, the product is commercialized.

Saudi Arabia Oil and Gas: What results has the innovation produced to date i.e. Field tests, Well Tests, Models, Patents, Trademarks, Designs, Process Improvements?

Walid Al-Shoaibi: Since the start of the Incubator project, we have produced seven patents and three com-

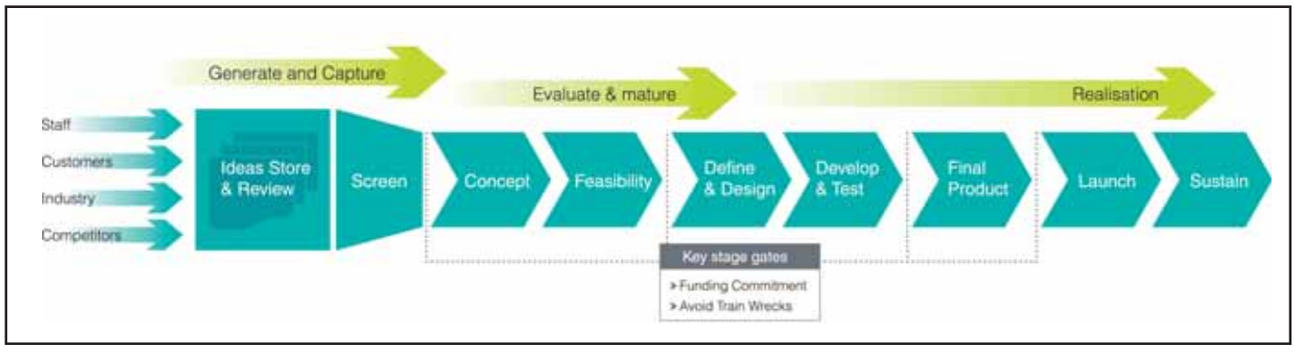

Research & Development Process – Go/No-Go key stage project phasing.

mercial products. We are in the process of field trialing new products in the view of commercialization in 2011. There are a number of ideas/innovations that we are screening in the development process and these will take their normal course over the next few months. The number of projects is expected to grow gradually as more ideas are fed into the development process. The Incubator project is expecting to grow with key recruitment of more scientists and engineers.

Saudi Arabia Oil and Gas: What kinds of issues are related to building a R&D infrastructure with qualified professionals?

Walid Al-Shoaibi: The issues in building an R&D infrastructure have been to establish professional working links with clients and universities. In order to recruit good scientists and engineers a base foundation is required. This foundation consists of local administration, office space and good working environments, but paramount in establishing any R&D structure is to ensure that the results of any such infrastructure will meet the commercial needs of the oil company. To ensure that Shoaibi Group is addressing these needs the Group has continued to build close commercial and collaborative working relationships across the respective organisations to promote the sharing of knowledge and experience.

Saudi Arabia Oil and Gas: What are the long-term plans for the company?

Walid Al-Shoaibi: To continue to represent and partner with the world's best technology companies in order to serve the region's oil, gas and petrochemicals industry and to further establish and invest in research and technology in order to be the leading game-changing oil field technology provider in the region.

> ...to serve the region's oil, gas and petrochemicals industry and to further establish and invest in research and technology in order to be the leading game-changing oil field technology provider in the region.

AVO Analysis in Carbonate Reservoirs

By Mohamed Elbaz, Geology Department , Mansoura University ,Egypt, Bandar Duraya Al-Anazi, King Abdulaziz City for Science & Technology, Saudi Arabia, Michael Arvanitis, Geomorph Instruments, Greece.

Introduction

Until recently, seismic analysis of data from carbonate reservoirs relied mainly on interpreting zero-offset (stacked) volumes. Common knowledge within the world of AVO suggests that zero offset information is often insufficient to differentiate shale from carbonate porosity, or to discriminate gas-saturated from brine saturated reservoirs. However, in the last few years, great efforts have been made to apply AVO analysis to carbonate reservoir characterization, but several issues must be addressed in investigating the feasibility, potential and sensitivity of the response of carbonate rock properties to porosity and fluid

First, a lack of carbonate rock property information is considered an obstacle in applying AVO to carbonate reservoir characterization. Second, the differences between clastic AVO and carbonate AVO need to be clarified. Third, procedures and calibration in seismic data processing and interpretation need to be developed. The situation has been greatly improved due to recent significant acquisition of dipole sonic logs. Below is the illustration of the application of AVO for carbonate reservoir including the summary of case study in the Western Canadian Sedimentary Basin (WCSB) given by Li et al (2003). Some issues such as physical relationships between rock properties, fluid sensitivity of the carbonate rock property, calibration and interpretation are reviewed and discussed.

Carbonate rock properties

Figure 1 shows a set of dipole well logs from the Foothills of the WCSB in which the mudrock line for clastics is $Vs = 0.862\ Vp - 1172.4$. A line with the relationship of $Vs = 0.4878\ Vp + 230.0$ is fitted to the carbonate lithology cluster. Similar to Castagna's, it can be seen that the carbonate line deviates from the clastic mudrock line with a slope significantly less than that of clastic rocks. In Figure 1, as is always observed, the data points of the gas sand in these two wells shift away from the clastic rock cluster and have a low *Vp* and a low *Vp*/*Vs* ratio in comparison with water-saturated sandstone.

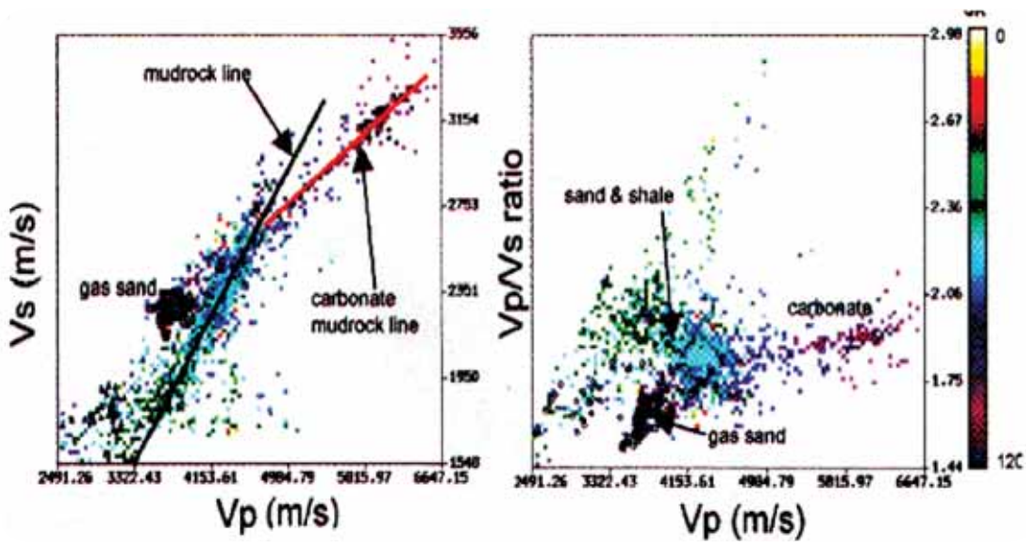

Figure 1. Velocities and *Vp*/*Vs* ratio of dipole well logs from Foothills, the WCSB (Li et al, 2003).

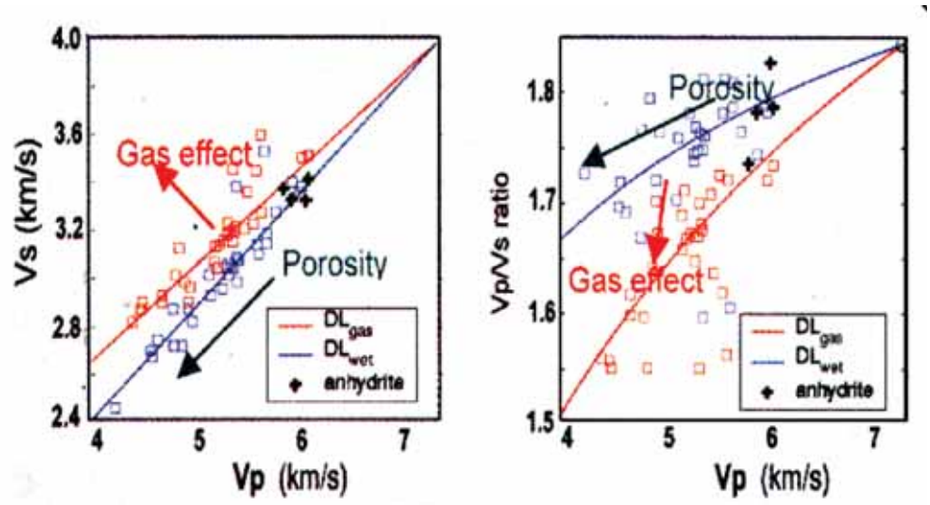

Figure 2. Gas effect of dolomite rock properties for the data set from Williston Basin (Li et al, 2003).

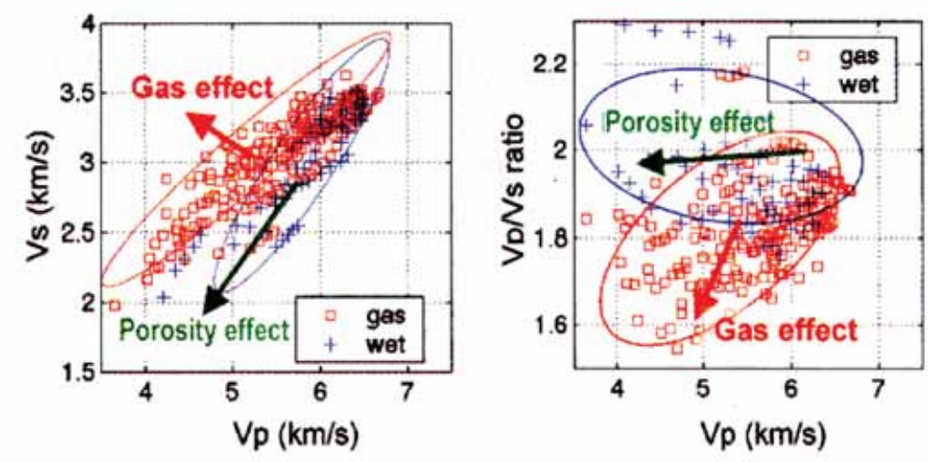

Figure 3. Gas effect of dolomite rock properties for a data set from the WCSB (Li et al, 2003)

Fluid effects in carbonates, especially gas effects, are contentious but of great interest. The common wisdom is that fluids have little or no effect on carbonate rock properties because carbonate rocks have very high moduli. In other words, the high velocity of the carbonate rock matrix causes seismic waves to travel primarily through the matrix where they are little influenced by pore fluids. However, an analysis of the dolomite data from the Williston Basin by Rafavich (1984) indicates that gas does influence carbonate rock properties and its effect is significant (Figure 2).

Further evidence of this can be seen in an analysis of a large data set of lab measurements on carbonate rocks from the WCSB. This data set includes limestones and dolomites. It represents a wide range of carbonate reservoirs and non reservoirs. An analysis of this data set indicates that the result is consistent with the data set of the Williston Basin (Figure 3). Notice that the behavior of dolomite rocks due to gas saturation is similar to that of sandstones. Namely, P-wave velocity and *Vp*/*Vs* ratio decrease, and S-wave velocity increases slightly due to decreasing density. In addition, the rocks are more sensitive to fluid with increasing porosity. The results of limestone are not shown. In general they are similar to dolomites except less sensitive to fluid.

The influence of fluid on carbonate rock properties described above implies that AVO response to gas and brine saturated rocks should be different. Figure 4 shows theoretical calculations to examine these for the most often encountered reservoir types (porous limestone and porous dolomite encased by tight limestone).

First, for limestone reservoirs encased by tight limestone, AVO gradient responses are similar for both gas and brine cases. Consequently, zero-offset amplitude becomes the attribute differentiating gas from brine. But, as porosity

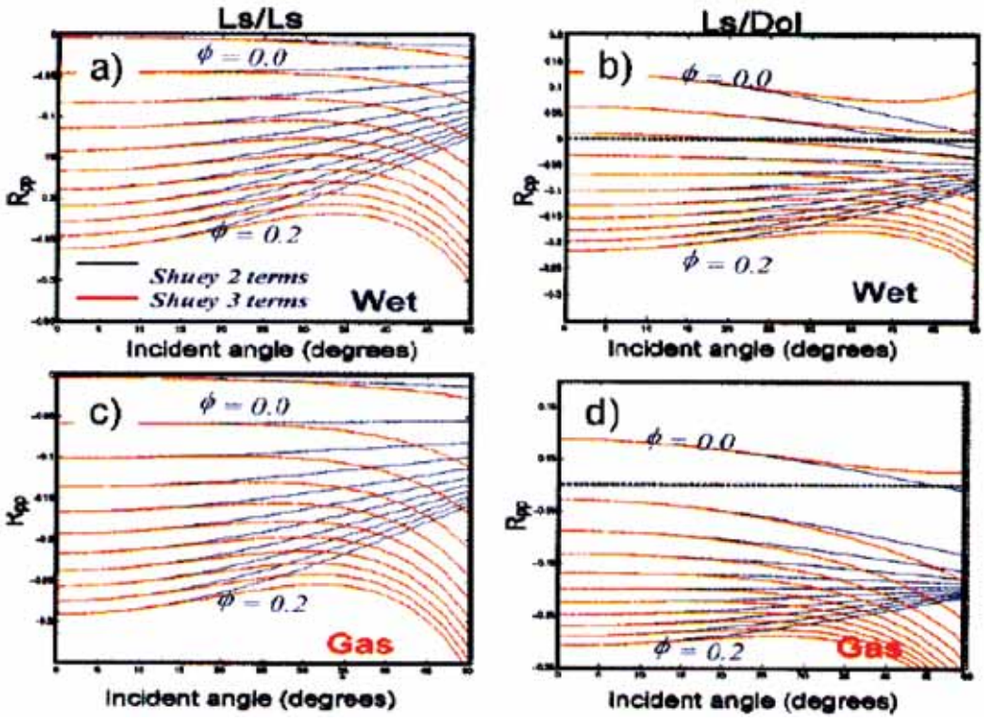

Figure 4. Theoretically calculated AVO responses for carbonate reservoirs (Li et al, 2003).

itself could produce the same response as fluid, zero-offset amplitude is ambiguous in determining fluid effect in a reservoir

In contrast, the fluid effect on offset amplitude or "gradient" in a dolomite reservoir encased by tight limestone is significant. With increasing porosity from 0 to 20%, all AVO classes (I-IV) are present. More specifically, a class III AVO mainly corresponds to porosity of 6–14%, and class III-IV to 14–20% (Figure 4d). In the WCSB, most carbonate reservoirs are in these porosity ranges. In addition, these AVO responses are accompanied by weak-to-strong zero-offset reflectivity. As a shale/limestone interface could produce a class II or III AVO response, care must be taken in standard AVO analysis. In Figure 4, Shuey's two-term AVO and three-term AVO calculations are shown as blue and red lines, respectively.

Analysis

Figure 5 shows selected dipole well logs that represent gas saturated dolomite reservoir at about 3700m and a brine saturated dolomite reservoir at 3000m. The gas saturated reservoir has a thickness of 30m, an average P-wave velocity of 5400m/s, density of 2.5–2.6 g/cc, and porosity of 8–16%. In Figure 5, the gas and wet dolomites are red and green squares respectively, tight limestone data points are black squares and small blue dots represent entire well logs. Empirical relationships for sand, shale and carbonates are overlain to establish a background where major lithologies are located. Such plots facilitate understanding relationships among different lithologies and fluid effect.

The empirical relationships of carbonates were developed from lab measurements and it can be seen that the log data agree with them There is no gas sand in these wells (refer to Figure 1). The observations that can be made from Figure 5 are:

(a) the gas effect is apparent in the Vp/Vs ratio, λ/μ ratio, and $\lambda\rho$ domain (λ is Lame's constant, μ is shear modulus, and ρ is density); (b) wet dolomite or wet limestone can be used as the background reference in order to quantitatively determine the degree of the gas effect; (c) the shear modulus of carbonates is higher than that of shale; and (d) shale and porous carbonate can be distinguished as they occupy different spaces in cross-plotting domains.

To determine a quantitative assessment of the influence of fluid on carbonate reservoir rocks, brine substitution (using the Biot-Gassmann equation and calibrated by the empirical relationship in Figure 2) was performed for the gas-charged dolomite in Figure 5. Figure 6 illustrates the sensitivity of rock properties in various domains. Figure 6 shows, in moving from the gas case to the brine-substituted case, that the density, velocities,

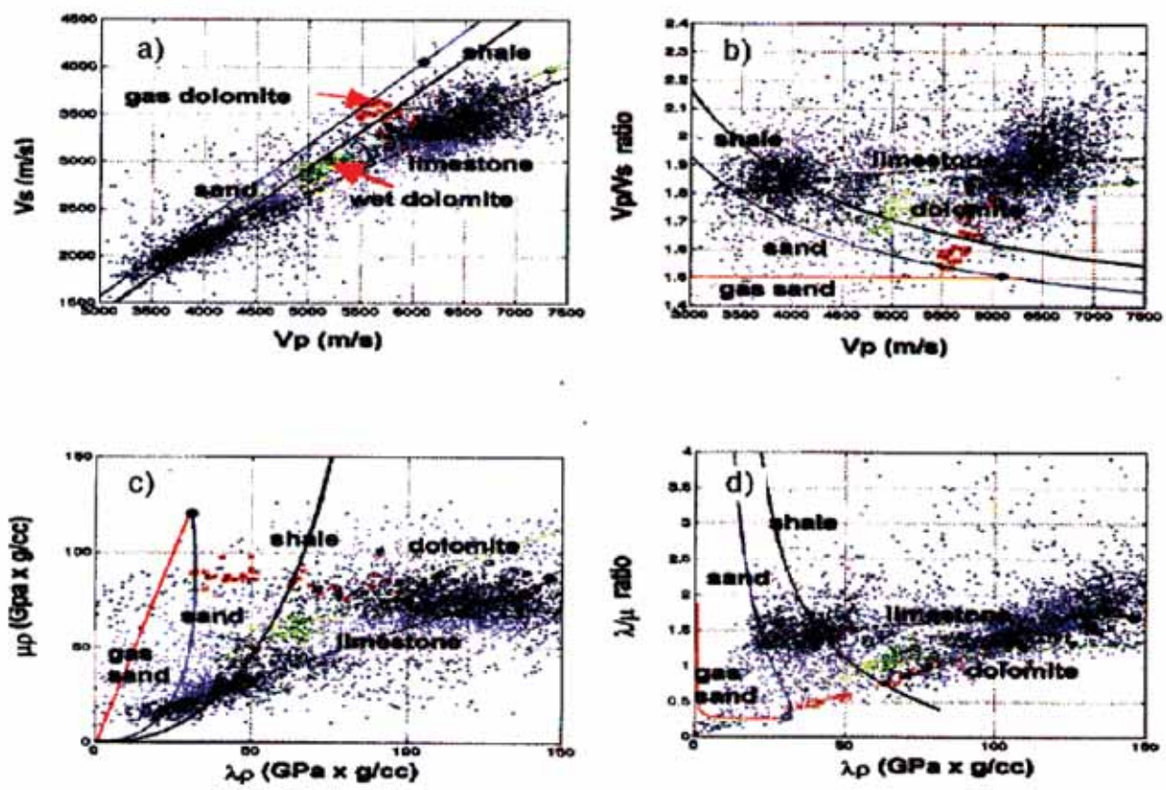

Figure 5. Gas-and brine-saturated dolomite reservoirs in velocity and modulus domains (Li et al, 2003).

Vp/*Vs* ratio and impedances change less than 10% in magnitude. The change in λρ, however, can be as great as 66%. The λρ contrast (relative variation) between encasing limestone and the gas-saturated dolomite is also significantly enhanced.

The high sensitivity of the reservoir rock and the enhancement of contrast between the encasing limestone and the gas-saturated reservoir in λρ domain are mainly contributed from the decreasing of *Vp*/*Vs* ratio (γ) of the reservoir rock. They are governed by the relation

$$\Delta\lambda\rho / \lambda\rho = ((2\gamma^{2} - 4\gamma) \quad / \quad (B(\gamma^{2} - 2))R_p$$

where *Rp* is P-wave reflectivity and *B* is the slope of the carbonate line. Based on this relation, a small decrease in *Vp*/*Vs* ratio will result in a large increase in Δλρ/λρ. The above observations are consistent with observations in clastic reservoirs. Consequently, for carbonate reservoir characterization, λρ and λμ ratio may be used as fluid indicators.

Synthetic gathers for the gas-charged, reservoir and the brine substituted case were then generated (Figure 7). A class III AVO at the base of the gas-charged reservoir changes to weak class II AVO after brine substitution. This is consistent with the theoretically calculated AVO response in Figure 4.

Figure 8 shows a real data example of a CDP gather at a dolomite gas well. The reservoir, at about 3000m, has a thickness of 20m and porosity of 12–14%. Figure 8a is the Ostrander gather and Figure 8b is the constructed gather using P-and S reflectivities (*Rp* and *Rs*) extracted using Fatti's AVO equation:

$$R_{pp}(\theta) = R_p(1 + \tan^2\theta) - 8(V_s / V_p)^2 R_s(\sin^2\theta).$$

As with the synthetic gather for the gas case in Figure 7, a class III AVO is at the base of this reservoir. This again confirms that a gas-charged dolomite reservoir does produce an AVO anomaly: the amplitude brightens at far offsets. At this specific well location, another class III AVO appears underneath the reservoir and suggests a new potential reservoir.

Figure 9 shows a 2D stack section with three CDP

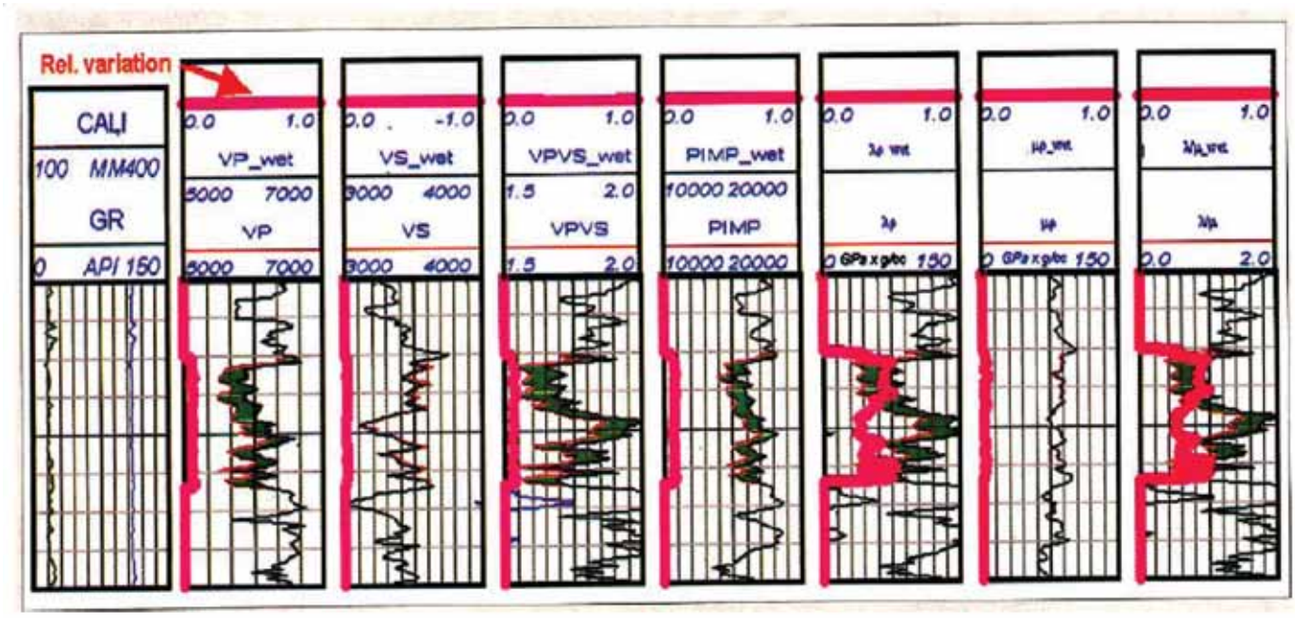

Figure 6. Sensitivity of rock properties in responding to fluid (Li et al, 2003).

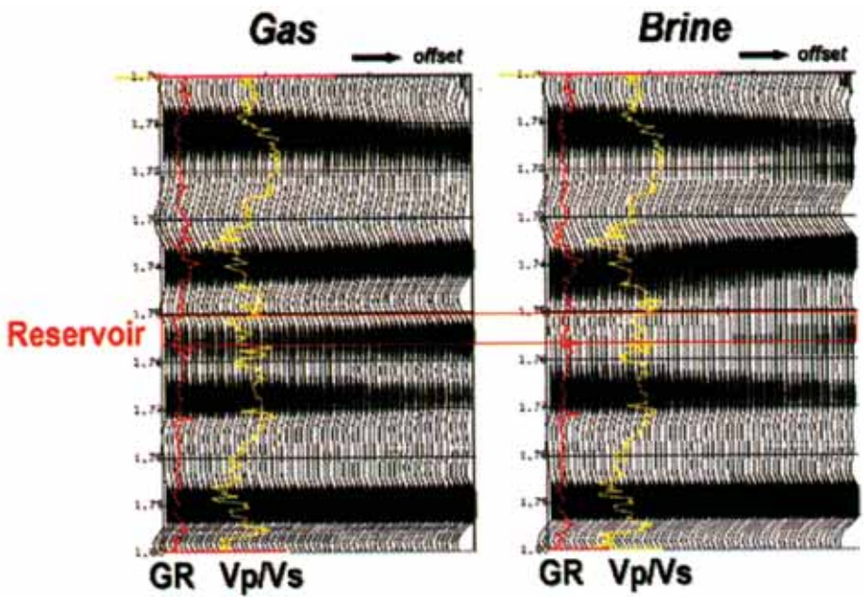

Figure 7. AVO responses of gas-charged and brine-saturated dolomite reservoir (Li et al, 2003).

gathers from two tight wells and one gas well. The gas dolomite discovery well produces 13 million cubic feet per day. The reservoir manifests as the highlighted bright spots on the stack. Without examining prestack gathers, the bright spots may be interpreted either as gas porosity, shale-filled channel, or gas charge reservoir. The CDP gather at the gas well shows class III AVO anomaly. In contrast, the seismic responses on the CDP gathers at the two tight wells are quiet. This example demonstrates that far offsets can contribute significantly to the amplitude anomaly of bright spots on a stacked section.

In an attempt to better define a carbonate reservoir, we analyzed the elastic property inversion method developed by Goodway et al (1994). The procedure is to first extract P- and S-reflectivities (*Rp* and *Rs*) from CDP gathers by using Fatti's AVO equation, invert these reflectivities into P- and S-impedances by introducing low-frequency background of P- and S-impedance, and finally calculate the modulus attributes, $\lambda\rho$, $\mu\rho$, and $\lambda\mu$ ratio using $\lambda\rho$ = Ip2-21s2 and $\mu\rho$ = Is2. This technique has been widely used in the WCSB clastic reservoirs. Its effectiveness is based on the fact that $\lambda\rho$ and λ/μ ratio are sensitive to fluid as shown in Figure 5

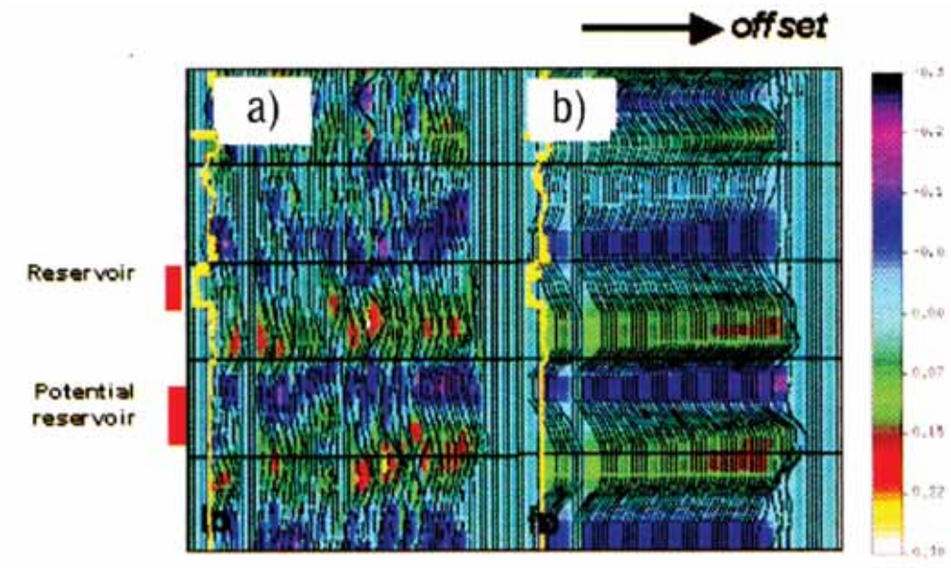

Figure 8. CDP gathers: (a) Ostrander gather and (b) the reconstructed gather using P and S reflectivities (Li et al, 2003)

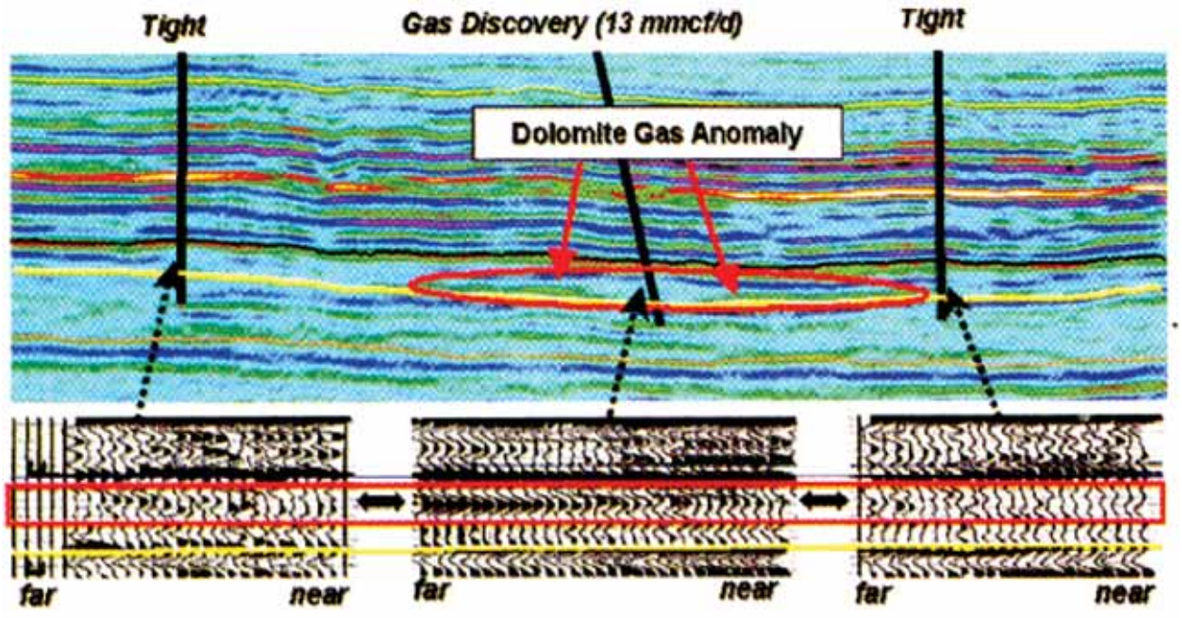

Figure 9. Stacked section and CDP gathers for a dolomite reservoir (Li et al, 2003)

Figure 10 shows λρ and μρ sections for a carbonate gas play. There are three wells: tight, good gas, and marginal gas. Direct observation indicate that the good gas well corresponds to the low λρ anomaly, and the tight and the marginal gas wells correspond with higher λρ values. However, μρ varies little within the reservoir zone. Since the shale formation may manifest itself as an amplitude anomaly on a stack section and low impedance in P-impedance section, the introduction of shear-wave information via AVO would help differentiate shale from carbonate. In Figure 10, there is low λρ and μρ shale zone under the reservoir zone. It can be seen that ambiguity between shale and reservoir prevents defining such a zone as a reservoir. However, cross plotting can solve this problem because the shear modulus of reservoir carbonate is higher than that of shale.

Figure 11 shows the crossplots of the λρ and μρ sections in Figure 10. There is good separation between shale and carbonates. For reservoir and non-reservoir carbonate

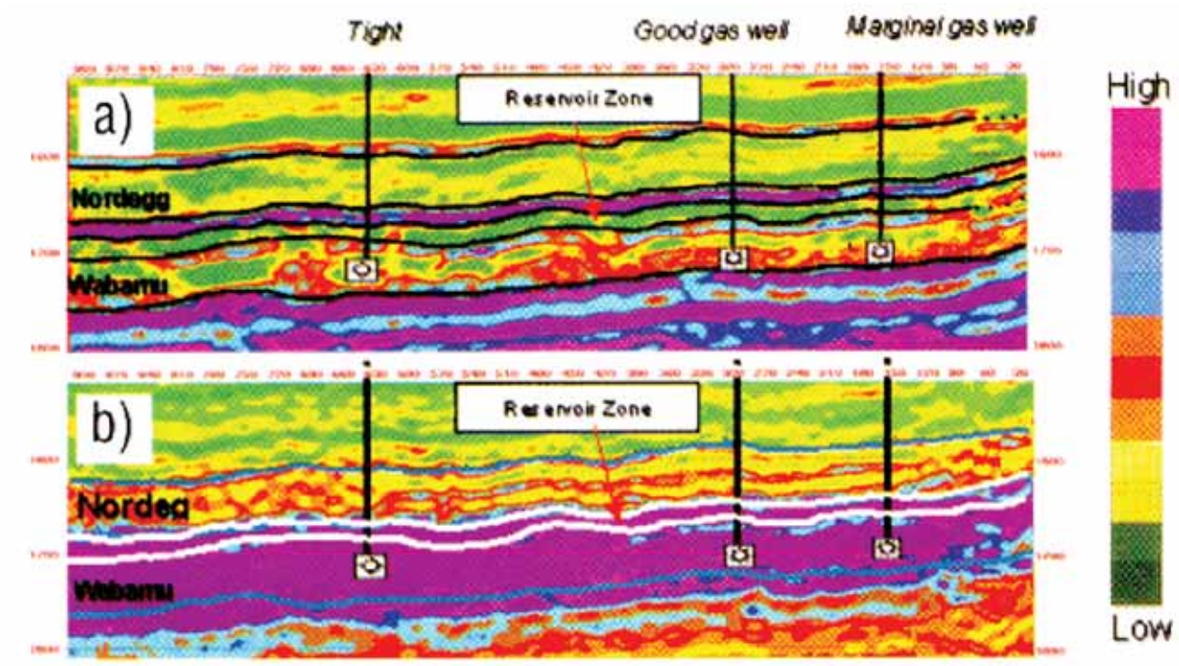

Figure 10. (a) section and (b) μ section with tight, good gas and marginal gas wells.

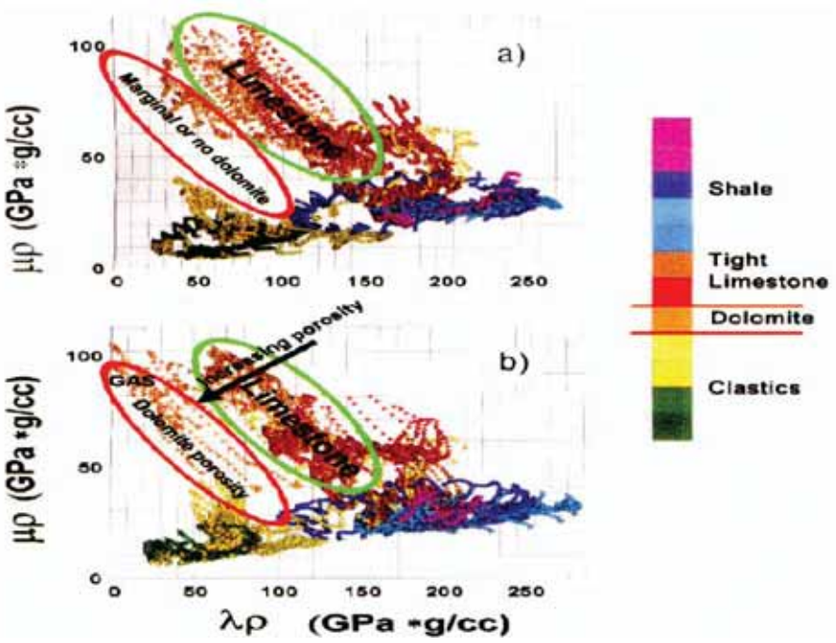

Figure 11. and μ crossplots at tight, marginal gas and good gas well locations (Li et al, 2003).

rocks, it can be seen that a space filled with data points from the gas well (lower half of Figure 11) has almost no points from tight and marginal gas wells (upper half of Figure 11). Furthermore, Figure 11 demonstrates that, in crossplot space, data points from the gas-charged dolomite reservoir are distinct from data from the tight limestone and marginal gas well. One can thus isolate the reservoir from non-reservoir rocks by projecting a polygon in the crossplot domain back into the 2D section or 3D volume.

Figure 12a has a polygon for the reservoir rocks indicated in Figure 11 and Figure 12b shows the projected results in a λρ section. Up to this stage the reservoir has been successfully isolated. It can be seen that a good gas well is located at the center of the most continuous low λρ zone; the marginal well is near a small gas zone but misses the target; and the location corresponding to the tight

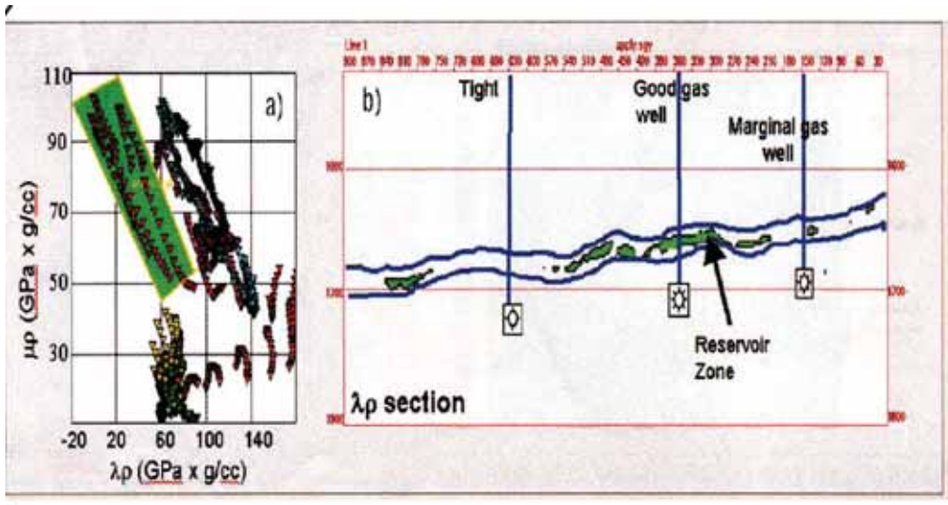

Figure 12. Projection of gas zone on section

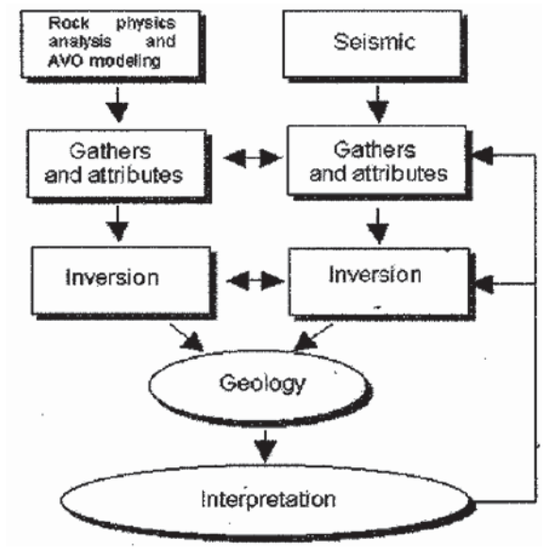

Figure 13. Flowchart of AVO processing and interpretation for carbonate reservoirs (Li et al, 2003).

well has no λρ anomaly. Figure 12b further suggests that potential drilling locations may exist at CDPs 500 and 810.

Calibrations

Calibration is a cross-examination between petrophysical rock properties, seismic rock properties, seismic, and inverted seismic rock properties. Figure 13, a flow chart for the calibration and interpretation in carbonate reservoirs using AVO, has two main branches: one for rock physics analysis and AVO modeling and one for seismic processing. Seismic interpretation should start from a stacked seismic in which a seismic amplitude anomaly and/or phase anomaly may already be seen. An AVO anomaly often can be determined through analyzing Ostrander or super gathers.

AVO modeling can be conducted at this stage to assist determining whether an AVO anomaly corresponds to a reservoir, The elastic rock property inversion provides P- and S- impedance, λρ, μρ and λ/μ ratio. As P-impedance cannot solve the ambiguity between shale and carbonate porosity, shear-wave information becomes crucial in discriminating reservoir from non reservoir. During the elastic rock property inversion, the relationship of P- and S-reflectivity trend may be used to check if offset-dependent amplitudes have been processed properly. The relationship between P-and S-impedance may be

used to check if the inversion was performed with the correct low-frequency background.

Conclusions

With better understanding of carbonate rock properties and advances in seismic data processing, carbonate reservoir characterization using AVO becomes more practical and less contentious. The fluid does affect carbonate rock properties and with significant magnitude given the rock property interpretation, the high shear modulus of reservoir carbonate rocks may be used to differentiate against shale intervals.

Low $\lambda\rho$ in combination with low λ/μ ratio or Vp/Vs ratio may be used to define a gas-charged dolomite reservoir. Rock physics analysis, seismic modeling, geologic input all are useful in constraining interpretation. By utilizing AVO techniques with correct data processing, geologic input and awareness of pitfalls, the risk of carbonate reservoir exploration may be reduced.

References

1. Sigit Sukmono , 2003 Reservoir analysis course.

2. Li, Y. et al, 2003, Recent application of AVO to carbonate reservoirs in the Western Canadian Sedimentary Basin, The Leading Edge, July 2003, vol.22, no.7, SEG.

3. Goodway, W., Chen, T., and Downton, J., 1997, Improved AVO fluid detection and lithology discrimination using Lamé petrophysical parameter, CSEG RECORDER, 22, No.7, 3-5.

4. Ruger, A., 1996, Reflection coefficients and azimuthal AVO analysis in anisotropic media: Ph.D. thesis, Colorado School of Mines.

5. Rafavich, F., Kendall, C.H. St. C., and Todd, T.P., 1984, The relationship between acoustic properties and the petrographic character of carbonate rocks, Geophysics, 49, 1622-1636.

6. Castagna, J., 2000, An introduction to this special section AVO: The next step, TLE, 19, 1187.

7. Hilterman, F., 2001, Seismic Amplitude Interpretation: 2000 Distinguished Instructor Short Course (DISC), SEG, Tulsa.

8. Verm, R., and Hilterman, F. J., 1995, Lithology color-coded seismic sections: The calibration of AVO crossplotting to rock properties, TLE, 14, 847-853.

9. Balz, O., Pivot, F., and Badolato, D., 2000, Fast identification of AVO-anomalies using classification of prestack waveforms. Expanded abstract, SEG annual convention, 4p.

10. Maria A. Pérez*, Vladmir Grechka, and Reinaldo J. Michelena, 1999, Fracture detection in a carbonate reservoir using a variety of seismic methods, Geophysics, v.64, no.4, 1266-1276.

Permeability, Relative Permeability, Microscopic Displacement Efficiency and Pore Geometry of M_1 Bimodal Pore Systems in Arab-D Limestone

By Edward A Clerke, Ph.D. SPE /Saudi Aramco

This paper was prepared for presentation at the 15th SPE Middle East Oil & Gas Show and Conference held in Bahrain International Exhibition Centre, Kingdom of Bahrain, 11–14 March 2007.

Abstract

Pore geometrical parameters for the M_1 petrophysical rock type of the Arab D limestone in Ghawar field have been related to static and dynamic reservoir properties and geological facies1. The M_1 bimodal pore system is the most common and important member of a new set of ultimate recovery petrophysical rock types (URPRT) which use a new pore system classification for the Arab D limestone. The dynamic reservoir property results for the bimodal M_1 are reviewed here. The roles played by the pore system parameters describing the macro (M) and micropores (Type 1)within the M_1, in: permeability, imbibition oil relative permeability and microscopic displacement efficiency, are examined in detail. All pore systems are analyzed by the Thomeer method using an extensive mercury injection capillary pressure data (MICP) set in conjunction with dynamic experiments performed on samples prepared using the same wettability restoration. Effects commonly ascribed to wettability changes are observed by changes in the distribution of porosity between the M and Type 1 subsystems. An extensive study of the pore systems of the Ghawar Arab D limestone gathered a large and comprehensive mercury injection capillary pressure data set (484 samples)1-6. All MICP data were type-curve matched by Thomeer functions.[1,7]

The study of this carefully prepared MICP data is the foundation for a new pore system classification. The new classification is built upon intrinsic, fundamental and separate maximum pore-throat diameter modal elements named porositons1,6. Porositons are stable and recurring modes in the statistics of the Thomeer maximum pore-throat diameter of these carbonate pore systems. Porositon combinations are used to construct meaningful petrophysical rock types.

Petrophysical rock types are defined by Clerke1 as ob-

jects or combinations of objects that are present in the three dimensional space of the Thomeer pore-system parameters.

Porositons are a new PRT object type; other PRT objects are clusters, trends and surfaces. By constructing PRTs from porositons, strong relationships are found connecting the geological facies, PRTs and reservoir-flow properties of these complex multimodal carbonate rocks1. These relationships demonstrate that these PRTs are important for defining ultimate recovery.

Introduction

Extensive and detailed pore system studies have been reported on the Arab D limestone pore systems in a major oil reservoir in Saudi Arabia.[1] That study created connections between the three major languages of the subsurface: depositional geological facies, petrophysical rock types and reservoir static and dynamic properties1-7 as required for integrated reservoir characterization. The connections were made possible by a fundamentally significant observation regarding the limestone pore system geometries.

The spectrum of maximum pore throat diameters (Log Pd's) captured in this large mercury injection capillary pressure data set (MICP) exhibited four distinct Gaussian modes that have been termed "porositons" (Figure 1). Petrophysical rock types (PRTs) are defined as combinations of porositons.

Porositons are distinct and separable maximum pore throat size distributions that are based on the four Gaussian modes in the Log (P_d) or maximum pore throat diameter frequency spectrum.

The studies indicate that a major portion of the depositional facies and pore volume can be identified with one PRT – M_1 – the Macro_Type 1 micro porositon combination.

The prevalent M_1 PRT is a bimodal pore system consisting of an instance from the distribution of Macro possibilities (M porositon) and an instance from the Type 1 micro porositon distribution. The M instance comes from the wide range of maximum pore-throat diameters within the M porositon. The Type 1 instance comes from a narrow range of smaller maximum pore-throat diameters within the Type 1 micro porositon. The maximum pore-throat diameters of the Type 1 micro porositon are on the average 53 times smaller than the M macro porositon average maximums. The Thomeer analyzed MICP data indicate that 17% is the average amount of porosity classified as M with a mean maximum pore-throat diameter of 58 microns. For Type 1 microporosity, 5.6% is the average pore volume with a mean maximum pore-throat diameter of 1.1 microns1. Both pore subsystems are well connected to themselves and each other. Thus, commonly and widely present in our Arab-D reservoir is a bimodal M_1 pore system with a very large contrast between a fine network of well-sorted small diameter tubular intraparticle Type 1 pores, connected and adjacent to much larger diameter moderately sorted interparticle M macropores. At many reservoir elevations oil is present in both pore subsystems. When oil is present in both subsystems, the oil in the Type 1 micropores has been emplaced at a significantly higher capillary pressure than that required to emplace a much larger volume of oil into the large M macropores. This large contrast between the mean maximum pore-throat diameters of the M and Type 1 pore subsystems and the related capillary entry pressure contrast, results in strong partitioning of the roles played by the two subsystems in the dynamic reservoir properties.

This porosity partitioning is first made manifest in a new M_1 permeability model which utilizes information primarily from the M porosition. The shape of the oil imbibition relative permeability curve is also shown to be controlled by the M porositon through the M controlled permeability in samples prepared with the same wettability restoration. However, properties of both M and Type 1 pore subsystems are necessary to completely characterize the full M_1 imbibition oil relative permeability behavior in terms of initial and final saturations.

Our pore-geometrical driven calculations use only the permeability (M attribute) and reproduce the single point normalized laboratory imbibition oil relative permeability over a range from 1 to 0.001 for seven out of eight waterflood composites. Unnormalized core plug centrifuge relative permeabilities variations are accounted for by including properties of the Type 1 micropores. Increasing amounts of Type 1 microporosity within the M_1 core plugs are related to shifts of the oil relative permeability curve to increasing water saturation and reduced residual oil saturation. These varying microporosity volumes produce an intrinsic "ineffective" water saturation offset to the relative permeability curve in these data. To widely implement our new approach to relative permeability in the M_1 reservoir intervals, we intend to investigate the possibility that the controlling pore subsystem properties could be extracted from appropriate processing of modern spectral porosity well log data[8,9,10].

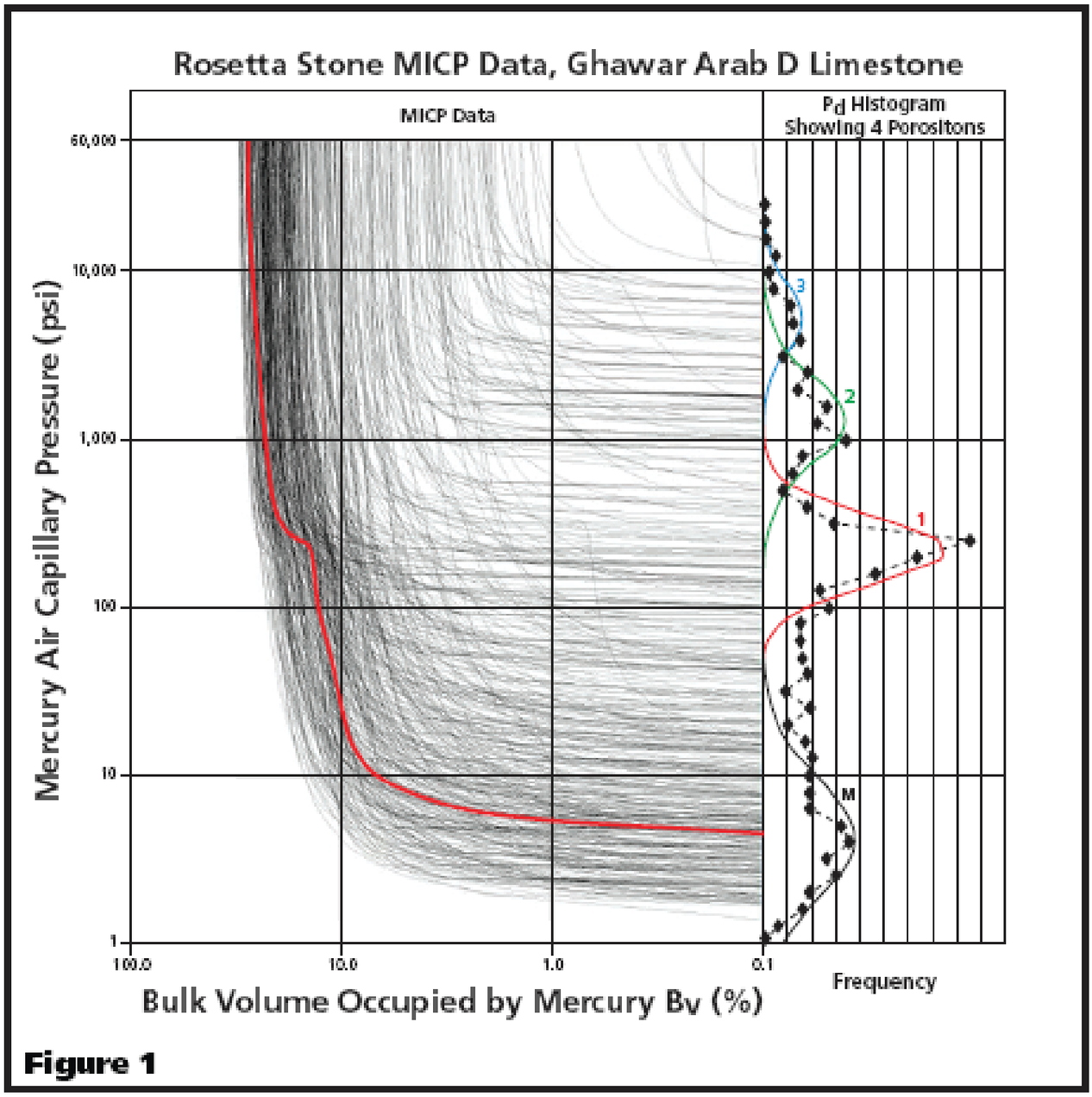

Figure 1 Rosetta Stone MICP data after closure correction and Thomeer analysis with a histogram of the extracted entry pressures shown as black diamonds. The modes in the entry pressure (maximum pore-throat diameter) spectrum can be fit by four normal (Gaussian) distributions to an r2 of 0.85. The Macro mode is in black on the right, with Type 1 microporosity in red, Type 2 microporosity in green and Type 3 microporosity in blue. Full discussion of this data is in reference 1. One of the prevalent bimodal capillary pressure curves, M_1, is highlighted in red.

Background

Thompson et al.[11] in Advances in Physics wrote a portentous review of the pore geometrical problems of sedimentary rocks noting, "Prediction of rock properties, such as the transport properties of fluids in the pore space, and the elastic properties of the grain space, requires a set of statistics that embody the relevant physics"; and "More generally, the statistical description of pore geometry awaits definition of relevant statistics. This approach could ultimately tie the geology of rock formation to their reservoir properties, a tie with important consequences for oil exploration and production."

Our pore system statistics for the M_1 Arab D limestone extracted using Thomeer[7] analysis of MICP data, extend the pore system and petrographic observations of

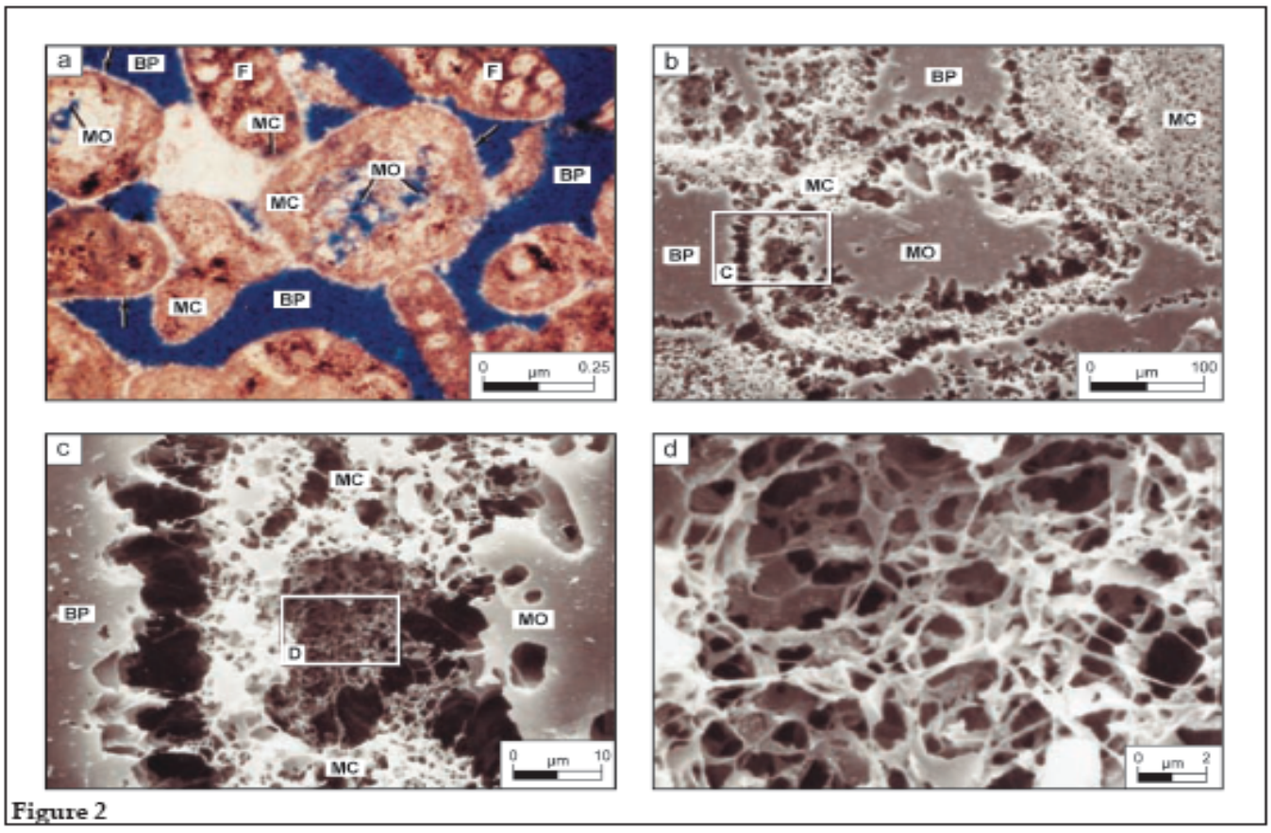

Figure 2 Petrographic image of the Arab Formation limestone M_1 pore system after Cantrell and Hagerty, 1999. Porosity is filled by blue dye in the upper left image. The succeeding SEM images are of pore casts of increasingly higher magnification focusing on the Type 1 microporosity after removal of the carbonate matrix by acid. The microporosity is well connected. (reproduced with permission of GeoArabia)

Cantrell and Hagerty[2,3] into three dimensional statistical information encompassing petrophysical and dynamic reservoir properties.

Our data gathering methods emphasized high quality control in the assignment of geological facies[1] to the core plugs. Non-Thomeer behavior was only observed in core plugs that were mechanical composites of two distinct geological facies[1].

The statistics of the maximum pore-throat diameters (which can be represented as mercury injection entry pressures, P_d's) were neither random nor uniform but instead presented a spectrum that could be modeled by four distinct porositons[6] (Figure 1). The data and the porositon Gaussian mode fitting parameters are published in Clerke et al.[1]

Other three dimensional image quantification techniques such as micro-CT can only resolve information about the macropore system. The current micro-CT resolution limit of about 0.5 microns precludes the capture of microporosity network details.[12,13] The petrographic investigations of Cantrell and Hagerty demonstrated the well connected nature of the Type 1 micropores (Figure 2). Type 1 micropores are tubular intraparticle micropores[2,3] that are very uniform in maximum pore-throat diameter (see narrow Type 1 red peak in Figure 1) and very well sorted (low Thomeer G). The Type 1 pore-throat diameters and reservoir saturations indicate that they also contain reservoir oil at most reservoir elevations.

Previous workers using MICP data have identified internal substructures in the behavior of the filling of a pore system by mercury and coined terminology to describe those modes.

Melrose[14] indentified a particular mode in the mercury filling, called "rheon". Morrow[15] introduced the mode term "ison" and Yuan[16] subdivided the ison into "rison" and sub-ison". In our work, we observe structures in the statistics of the Thomeer parameters. Four modes, modeled with Gaussian distributions in the Log (Pd, max) frequency spectrum, are observed in the maximum pore-

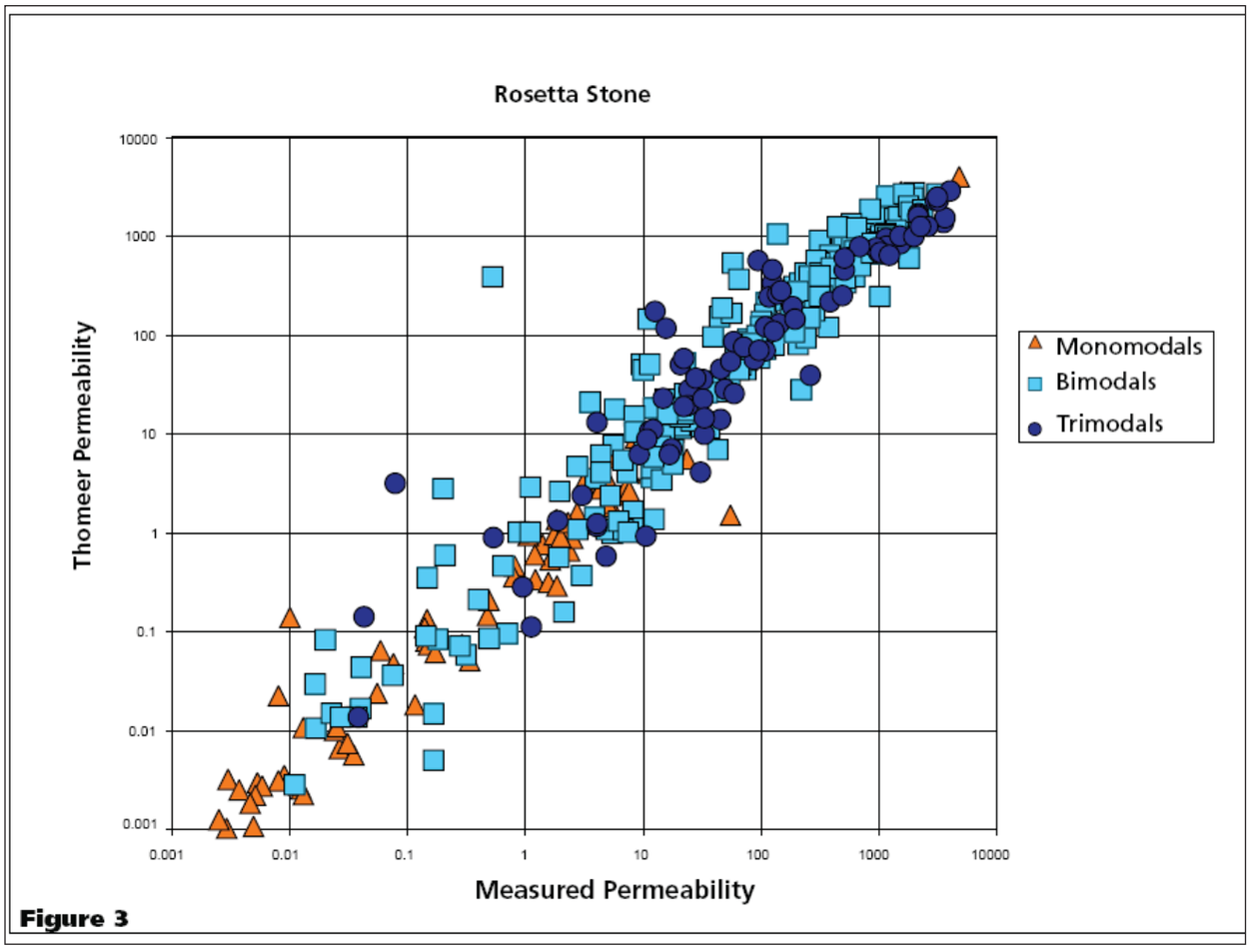

Figure 3 Permeability computed by the Thomeer algorithm using the parameters from only the first pore system in multimodal samples versus measured permeability for 484 limestone samples within the Rosetta Stone data set. Monomodals (orange triangles), bimodals (light blue squares) and trimodals (dark blue squares) are shown.

throat diameter statistics. This is interesting and practical because as the pore-throat diameter increases towards its' maximum pore-throat diameter value, it approaches the magnitude and perhaps the behavior of the pore bodies. Hence maximum pore-throat diameter behavior and pore body behavior may be closely related.[1] Pore body information is inferred by NMR measurements. More observations on the maximum pore-throat diameter (MICP) to pore body relationships (NMR) in these samples are presented in Clerke et al.[1] and are a subject of active investigation.

Thompson et al.[11] emphasized the importance of properly characterizing the statistics of the pore system attributes. He also noted that "within the many studies of pore networks composed of pipes of widely varying sizes, which are distributed randomly along the links of the network, … there are no experimental data to contradict the assumption of random distribution of pores." Our data[1] is likely the first and the most comprehensive data to show a deeper and nonrandom structure in the pore network parameters of the Arab D limestone. Our studies also indicate that a major portion of the depositional facies: Cladocoropsis, Stromatoporoid-Red Algae-Coral and Skeletal-Oolitic and a large portion of the reservoir pore volume can be identified with one particular Macro-micro Type 1 (M_1) porositon combination (Figure 1).

The static and dynamic properties of the prevalent bimodal M_1 pore systems are very important for forecasting Arab-D limestone reservoir performance.

Permeability of Multimodal Pore Systems in Arab-D Limestone

Multimodal pore systems are common in our Ghawar Arab D limestone MICP data[1]. Multimodality refers to the number of Thomeer Hyperbolas required to fit the MICP data of one core plug sample; each of which had been thoroughly inspected to be a member of only one geologic facies[1]. Up to three Thomeer Hyperbolas per sample were required, hence the sample modality no-

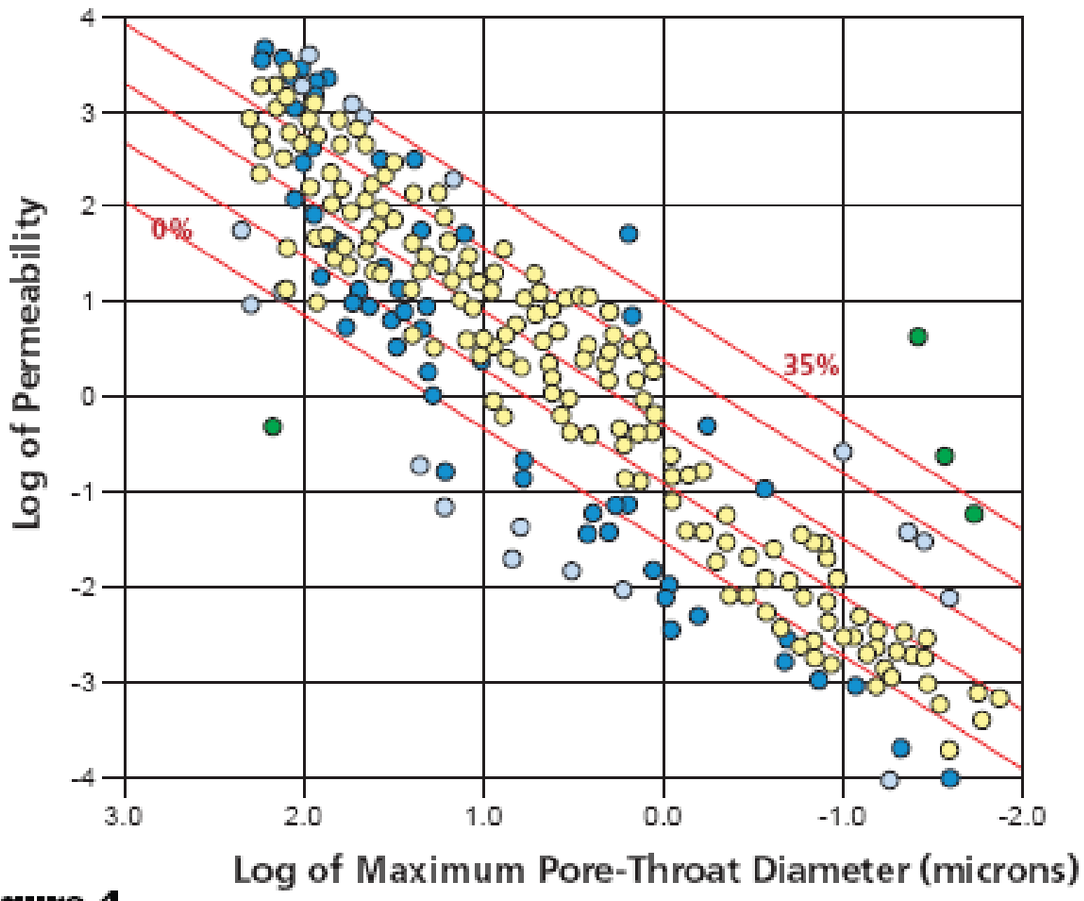

Figure 4

Figure 4 Permeability versus Maximum Pore-throat diameter data are shown on a log- log scale with a red background implicit porosity grid for porosities from 0 to 35%. Correlation with Maximum Pore-throat diameter is good but neither parameter by itself is sufficient to establish a very high quality prediction for permeability. Yellow color points are within one standard deviation of a two dimensional surface fit shown in figure 5. Dark blue are within 2 standard deviations. Light blue are outside 2 standard deviations. (reproduced with permission of GeoArabia)

menclature: monomodal – one Thomeer Hyperbola, bimodal – two Thomeer Hyperbolas, and trimodal – three Thomeer Hyperbolas. Only the porositon containing the largest pore-throat diameters (in this case the M porositon in the M_1 bimodal) in these multimodal pore systems contributes to the measurable total sample permeability. Use of the Thomeer permeability algorithm[17], demonstrates that the first pore system contains all of the information regarding measureable permeability. Thomeer published an algorithm for the air permeability using the three Thomeer parameters derived from matching MICP data to a Thomeer hyperbola[7,17]

$$Ka\ [md] = 3.8068\ G - 1.3334\ (\ B_v, \infty\ /\ P_d\ )\ 2\ .$$

The calculated Thomeer permeability value is compared to the measured value for over 400 samples[1] of which 18% are trimodal, 53% are bimodal and 29% are monomodal, using only the Thomeer parameters from the first pore system (Figure 3). The results show excellent comparison to data from 0.1 md to nearly 10 Darcy using logarithmic axes. (Multimodal samples are very common in rocks with permeability over 10 md[1]) The agreement with the measured permeability is well within the claimed uncertainty[17] (1.82x) of the Thomeer algorithm, and far exceeds conventional porosity-permeability approaches which may have two and one half orders of magnitude uncertainty.

Now, focusing on the Thomeer parameters of only the M pore system, the explicit dependence of the permeability upon each individual Thomeer parameter is inves-

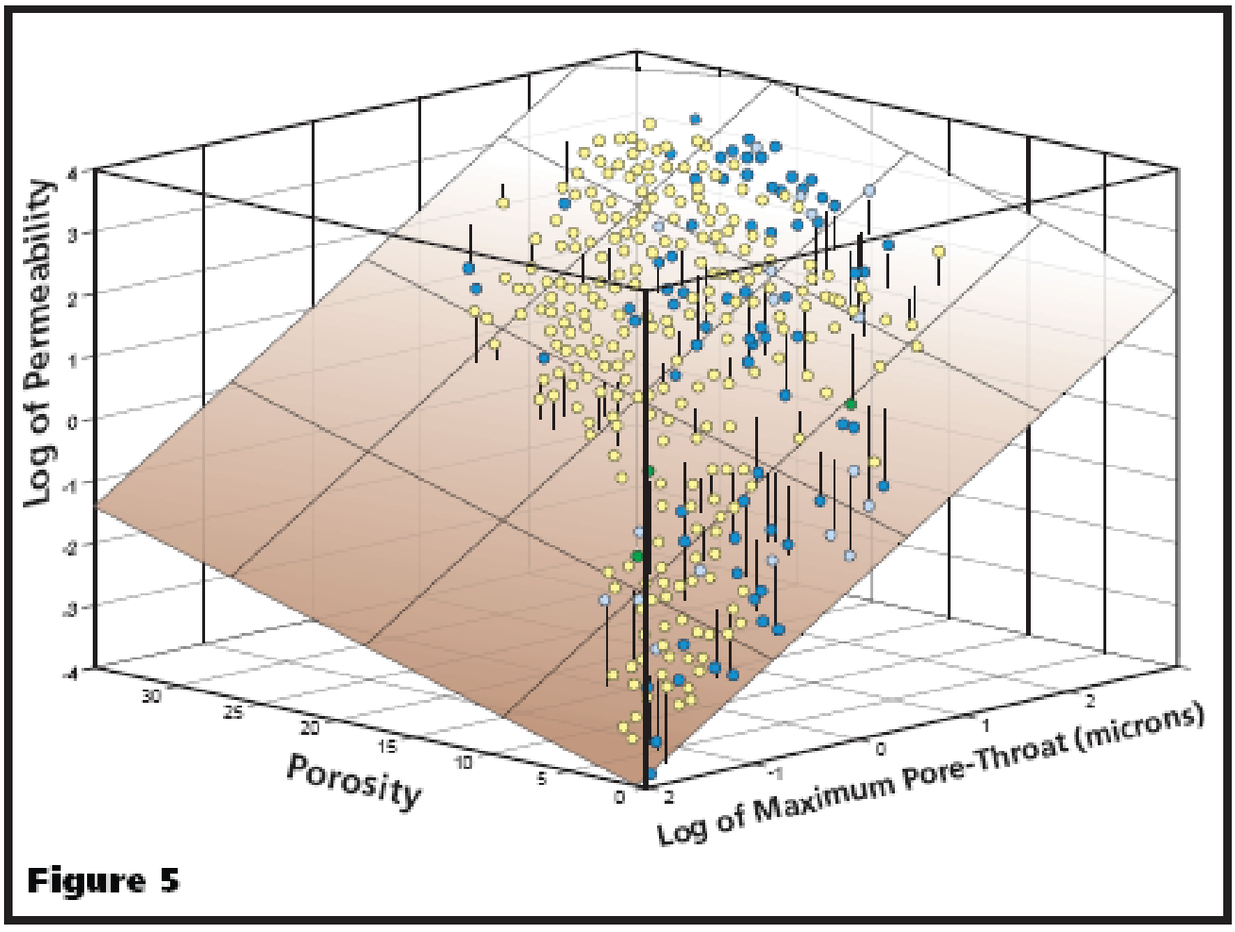

Figure 5 Three dimensional view of the two dimensional surface fit to compute permeability from Maximum Pore-throat diameter and porosity in TableCurve3D™. Yellow color points are within one standard deviation of the two dimensional surface fit. Dark blue are within 2 standard deviations. Light blue are outside 2 standard deviations. (reproduced with permission of GeoArabia)

tigated. The three Thomeer parameters are7: P_d, G and B_v, ∞ , which parameterize: the minimum entry pressure directly related to the maximum pore-throat diameter, c; the uniformity (low G) or non-uniformity (high G) of the pore-throat diameters; and the pore volume in that particular Thomeer hyperbola, B_v, ∞, respectively. In our data, the major control on permeability is exhibited by the Thomeer parameter, $P_{d,f}$, which is indicative of the diameter of the maximum pore-throat in the first (lowest entry pressure, f = M for the M_1) pore system (Figure 4). For reference, the conversion from pressure to pore-throat diameter is given by the Young-Laplace equation[18]:

$$P_c = \frac{0.58\sigma\cos\theta}{d}; \quad \text{for a mercury/air system,}$$

θ =140 degrees and σ = 480 dynes/cm, d, pore-throat diameter is in microns and P_c is in psia, yielding for the largest pore throat, $d_{throat,\ max}$, and the initial entry pressure, $P_{d,f}$:

$d_{throat,\ max}$ [microns] = 214/ $P_{d,f}$ [Hg/air psi].

The strongest correlation r^2 is between permeability and $P_{d,f}$, 0.65. Another good correlation r^2 is between permeability and the total porosity, 0.55. Neither parameter by itself is sufficient to establish a very high quality prediction for permeability.

Two Term Permeability Equation for M_1 Bimodal Pore Systems in Arab-D Limestone

The Rosetta Stone MICP data[1] was then used to investigate simple two term permeability equations. TableCurve 3D™ software allows a rapid investigation of many equations in terms of the correlation quality. For ease of general implementation, I only discuss the use of the maximum porethroat diameter and the total porosity. This high quality and simple two term permeability

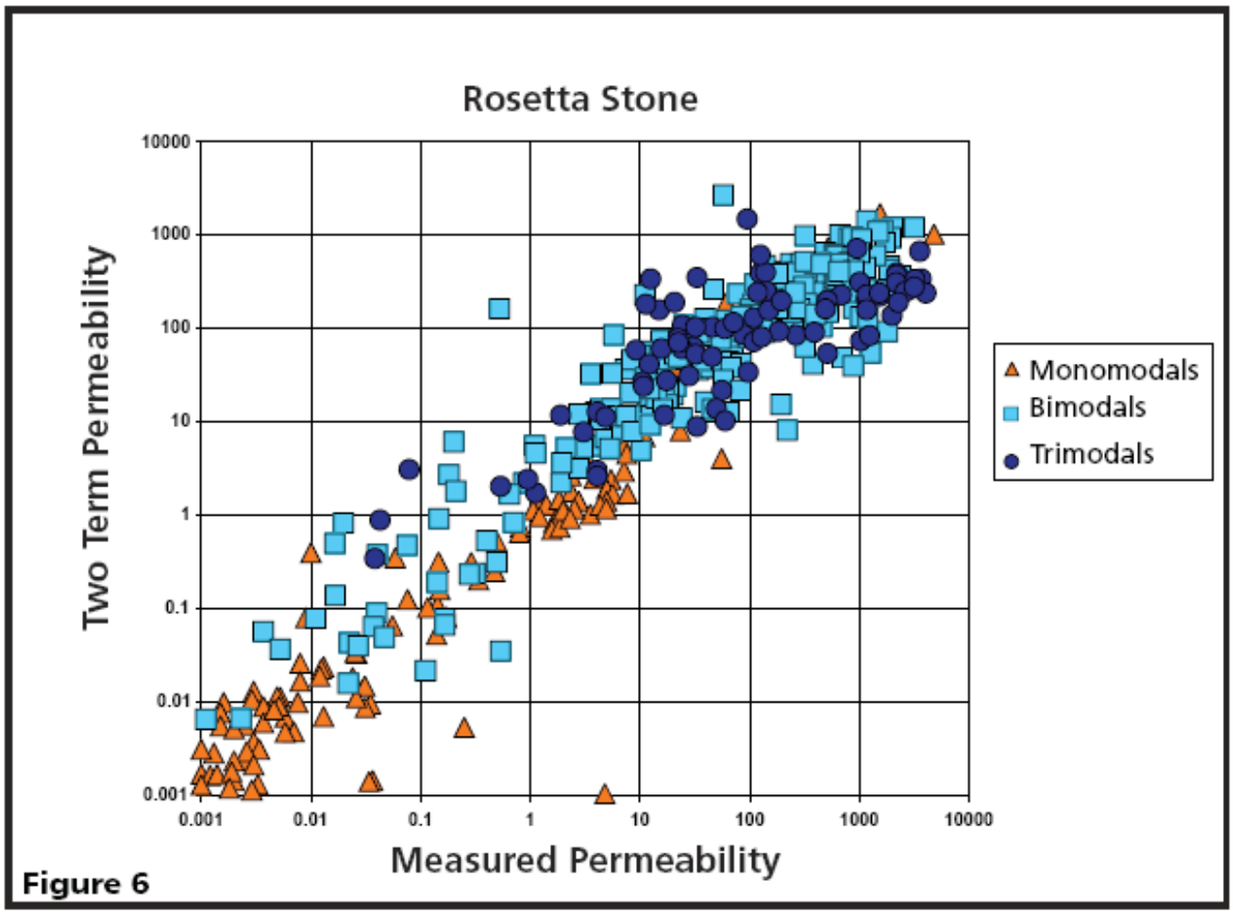

Figure 6 The permeability computed using the new two term permeability equation versus measured permeability for 436 samples from the Rosetta Stone data set. Monomodals (orange triangles), bimodals (light blue squares) and trimodals (dark blue squares) are shown.

model is (Figure 5)

$Z = a + bX + cY;$

with a = -1.54, b = 1.20, c= 0.073

using the variables:

X: Log_{10} (maximum pore-throat diameter in microns = $214/P_{d,f}$),
Y: Porosity in percent,
Z: Log_{10} (measured permeability);

and the overall correlation r^2 is 89%. The result is shown in Figure 5, the yellow color points are within one standard deviation of the fit surface, dark blue are within two standard deviations.

The measured versus predicted plot for this simple two term permeability model gives an excellent result over seven orders of magnitude (Figure 6). A two term algorithm is similar to the approach of Lucia[19] who proposed a two variable pore space-permeability model using: the particle size and the interparticle porosity for non-vuggy rocks. Instead of the particle size, we use the maximum pore-throat diameter. The two input parameters, total porosity and maximum pore-throat diameter of the first pore system, are under investigation for determination from conventional porosity well logs along with spectral porosity data from NMR and Electromagnetic Imaging well logs.[8,9,10]

Imbibition Oil Relative Permeability and Microscopic Displacement Efficiency of M_1 Bimodal Pore Systems in Arab-D Limestone

The previous section discusses that the M porositon carries more than 99% of the permeability information in these M_1 rocks[1]. The contribution of the microporosity to the overall pore system permeability is very small and below the reproducibility of the permeameter measurement. If it is true that the M porositon is the major control on measured permeability then it must also

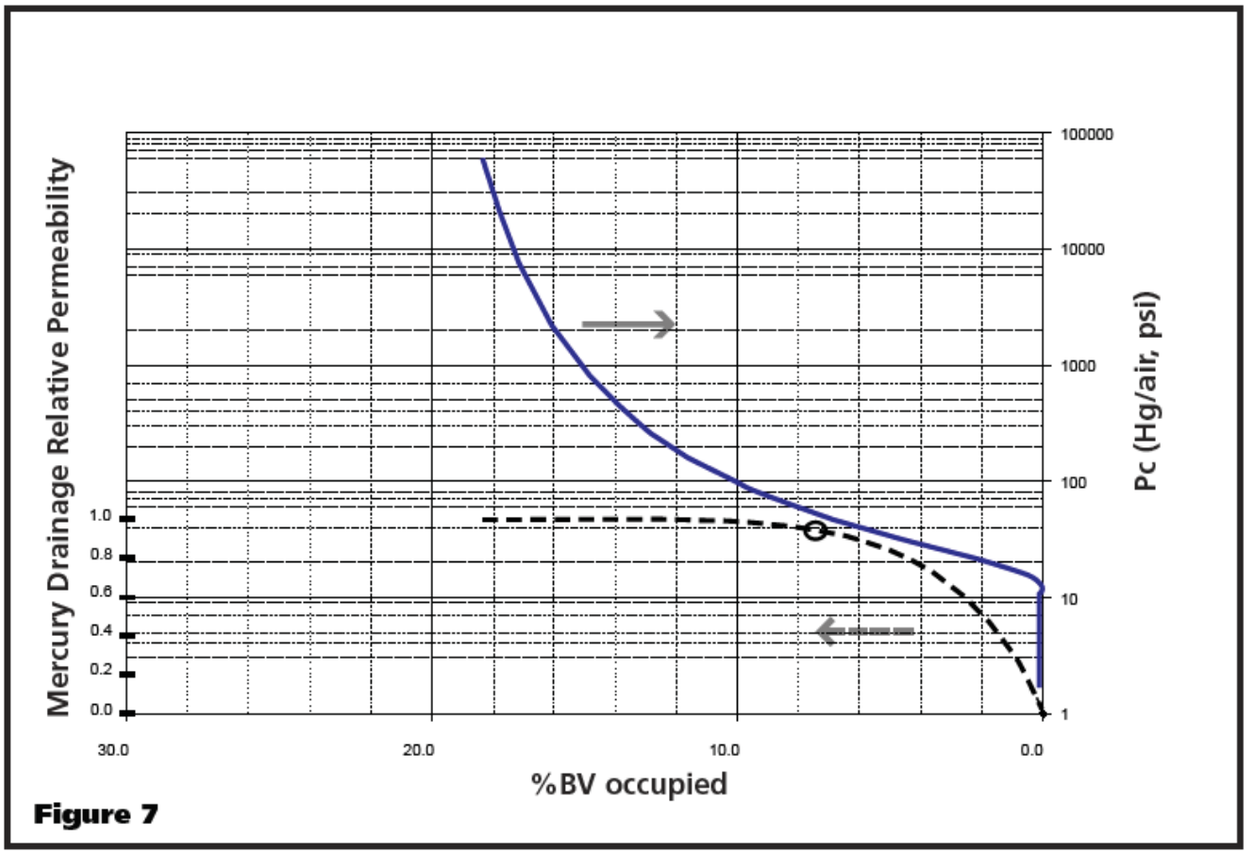

Figure 7 The mercury injection capillary pressure curve (solid) and a Purcell MDRP permeability calculation (dash) for a monomodal M pore system. The circled point indicates the 90% build up of permeability occurs at about 8%, [%BV occupied] and the sample has an ultimate % BV occupied of about 19%. Hence, the 90% permeability buildup occurs below 50% M saturation.

be the major control on the relative permeability curve among samples with a common wettability. Conversely, the Type 1 microporosity saturations must contribute to the relative permeability data in some alternate fashion. In drainage, the large capillary diameter differences between the M and Type 1 pore systems will result in significant partitioning of the two liquid saturations (oil – water). When a pressure gradient is applied as in forced imbibition, the bulk of Darcy type flow (99%) will occur within the M part of the pore system. In contrast, the small diameter Type 1 micropores will provide significant capillary forces to the system along with an imperceptible contribution to flow. The small pore throats and tubular weblike nature of the Type 1 network (Figure 2) suggest that these micropore systems are much more likely to be water wet than macropores at equivalent reservoir elevations. The low curvature (large diameter) surfaces of the M pore systems are likely to have significant areas that are oil wetted. Hence, bimodality is related to mixed wettability. It can be shown that the partitioning of the pore space by the entry pressure (drainage) classification (porositons) is also related to partitioning behavior in the imbibition properties.

To investigate two phase flow in our bimodal pore system in the absence of wettability effects, I modify a mathematical device by Purcell. Purcell[20] proposed a simple model of a pore system as consisting of a bundle of tubes of varying radii and volumes. He proceeded to calculate the contribution to the permeability that each tube makes as a function of its radius (~$1/P_c$) and volume when filling is by the (strongly nonwetting) intrusion of mercury. His model leads to a straightforward calculation of the contribution to permeability of each tube in the tubular bundle to the total permeability.

Purcell[20] states:

$$K \propto \int_{S_{nonwet}=0}^{S_{nonwet}=100\%} \frac{dS_{nonwet}}{P_c^2}.$$

I apply a series of these Purcell integrals[20] to our MICP data (P_c, S_{nonwet}) with a steadily increasing upper limit

of integration. For my series of Purcell integrations, I steadily increase the upper limit of integration, S_{nonwet}, from zero to 100%, to produce a series of mathematical calculations for the Mercury (to air) Drainage (strongly non wetting) Relative Permeability, K_{MDRP}. As the upper limit approaches S_{nonwet} = 100%, then K_{MDRP} must reach the Purcell permeability value, K. In symbols, we have that

$$\text{as } S_{nonwet} \rightarrow 100\%$$

$$\text{for } K_{MDRP} = \int_{S_{nonwet}=0}^{S_{nonwet}} \frac{dS_{nonwet}}{P_c^2}$$

More importantly, the calculation of my series of Purcell integrals results in a graph of the strongly non-wetting K_{MDRP} curve arising from the the accumulating MDRP permeability as mercury (non-wetting) saturation increases by successively accessing tubes starting with the largest diameter.

Results from this MDRP curve calculation on both monomodal and bimodal capillary pressure data are compared.

For a group of monomodal M samples represented by one particular sample of 18% porosity and 28md permeability, the MDRP permeability accumulation is essentially complete at approximately 50% of the total M porosity (Figure 7).

Similarly, the MDRP permeability accumulation for the bimodal M_1 in Figure 8 (22 % porosity, 34md permeability) is complete at about 8% porosity which is about 50% of the M porosity (the high pressure extrapolation of the lower pressure first Thomeer hyperbola of about 18%). The MDRP permeability accumulations demonstrate that permeability is dominated by the Macroporosity (large tubes) and less than the largest 50% of the M porosity as ranked by decreasing M pore-throat diameters.

The Type 1 microporosity contributes in a different way. This is examined using sets of special twin plugs from another MICP data set (Hagerty-Cantrell, unpublished). These special twin pore systems have nearly the same porosity and permeability but differ in the presence/absence of microporosity. In Figures 9 and 10, the capillary pressure curves for the M_1 -307 and M -309 special twin samples are displayed along with the calcu-

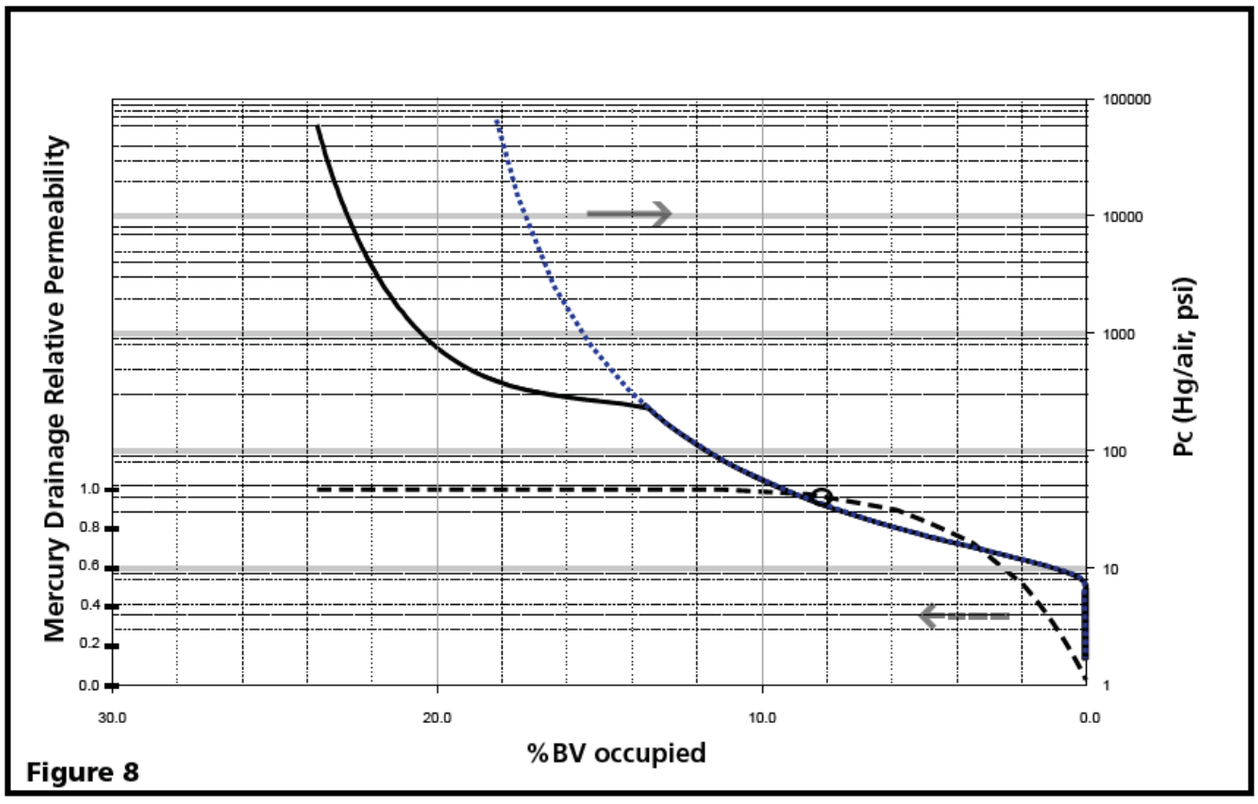

Figure 8 The mercury injection capillary pressure curve (black solid and short dash, blue dash showing the extension of the Macro pore system) and a Purcell MDRP permeability calculation (long dash) for a bimodal M_1 pore system. The 90% build up of permeability occurs at about 8%, [%BV occupied] and the sample has an ultimate % BV occupied for M of about 18%. Hence, the 90% permeability buildup also occurs near 50% M saturation in the M_1 system.

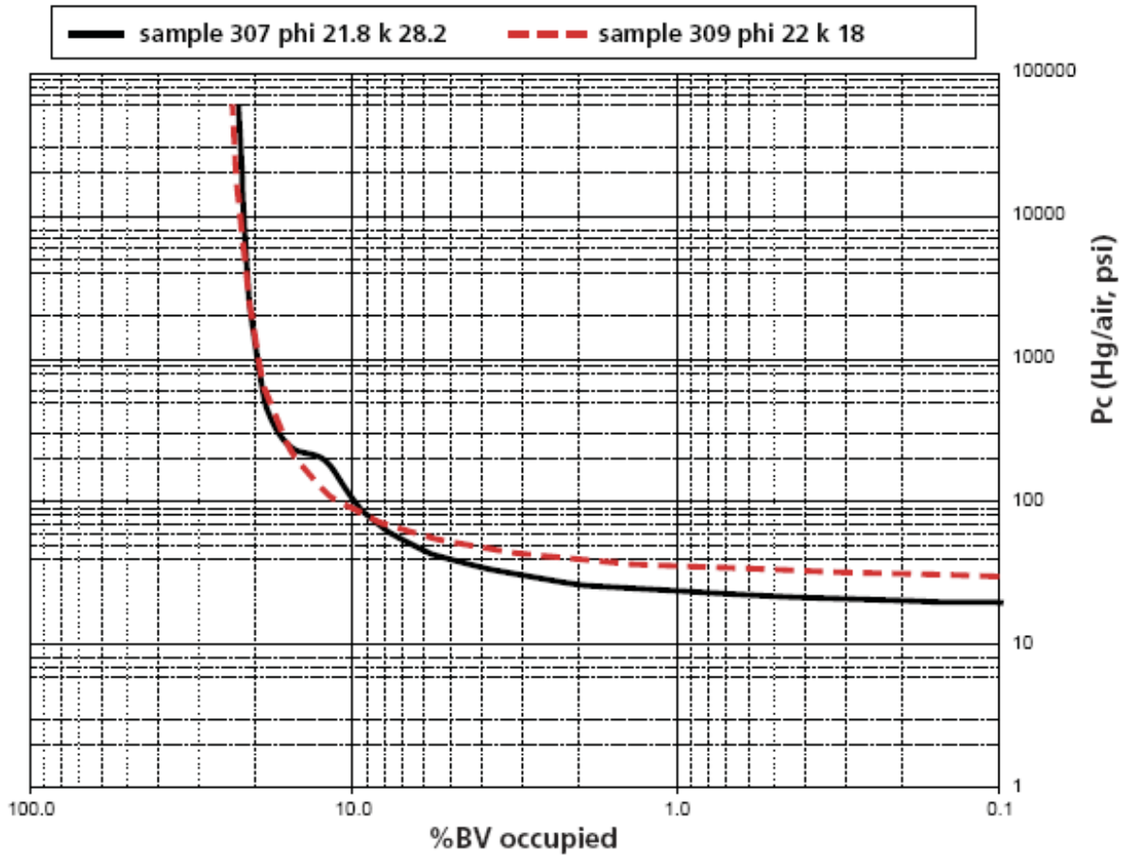

Figure 9

Figure 9 Samples 307 (bimodal – solid) and 309 (monomodal – red dash) MICP data with similar porosities (22) and permeabilities (28 and 18, respectively) but with and without Type 1 microporosity. Sample 307 has a micropore system into which mercury starts to enter at about 200 psi Hg/air.

lated MDRP permeability accumulation curves. Sample 307 has microporosity and sample 309 does not. The MDRP permeability accumulation shows that the major difference in the two MDRP curves is in the value of the saturation at which K_{MDRP} reaches 1.0. The saturation at which K_{MDRP} reaches 1.0 for the microporous sample (M_1-307) is shifted to the right or to increased wetting phase saturation as compared to the monomodal (M-309). The relative increase of the wetting phase saturation or saturation-offset is caused by the "permeability -ineffective" saturation of the capillary dominated Type 1 micropores.

New Pore Geometrical Model of Imbibition Relative Permeability Data for Multimodal Pore Systems in Arab-D Limestone

Actual oil-water imbibition (brine saturation increasing) relative permeability experiments using M_1 rock types were acquired using the steady state method in 1994 and were re-examined to investigate this saturation offset and the relationship to the presence of Type 1 microporosity. That study (unpublished Aramco internal report) performed high quality relative permeability measurements on eight composite M_1 cores from two Arab-D cored wells. The steady-state experiments used live reservoir fluids (recombined Abqaiq crude and live synthetic brine) and restored core conditions at reservoir temperature (210°F) and pressure (fluid 3300 psig and net confining stress 3100 psi). The cores were also under reservoir stress approximating that of the reservoir.[21, 22, 23]

Matched core plugs were used in each composite.[24] These floods were followed by centrifuge imbibition oil relative permeability and imbibition capillary pressure tests on the individual preserved core plugs from four of the eight composites. Centrifuge tests were made at 160°F and 3100 psig net overburden. The steady state

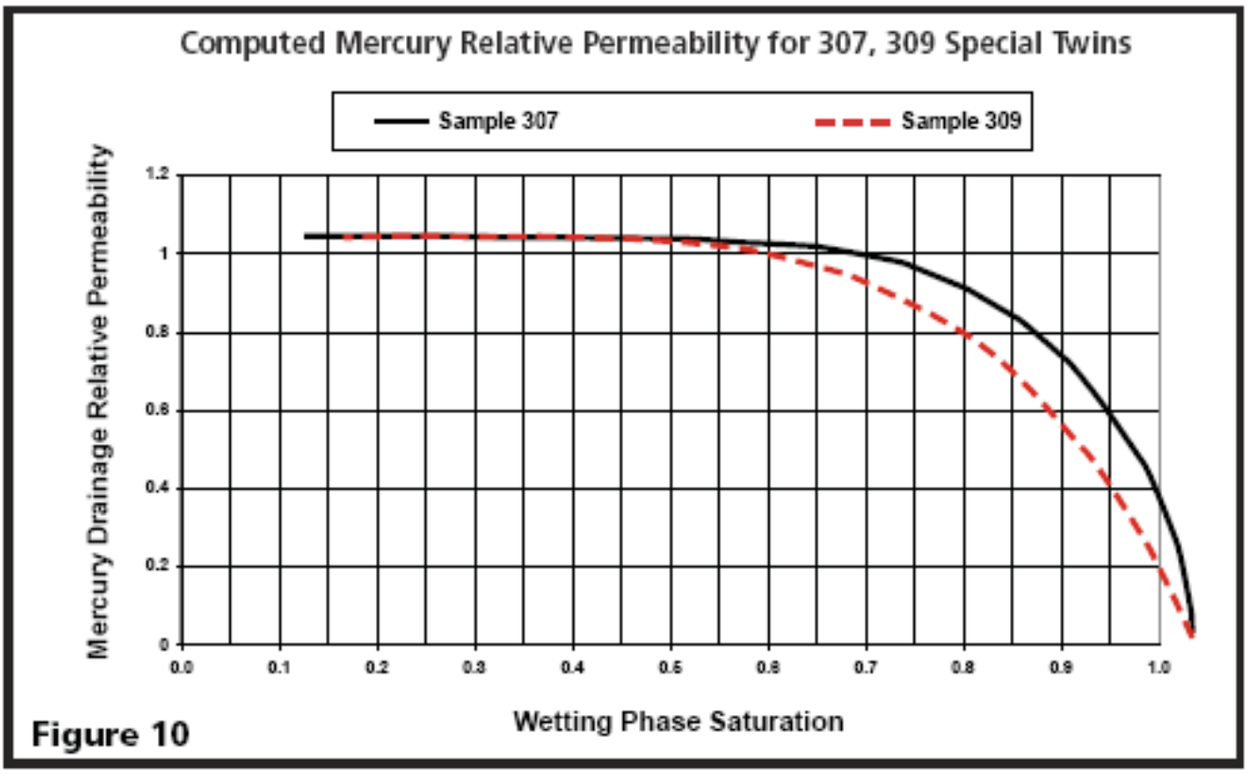

Figure 10 Computed MDRP permeability curves for the two samples: 307,M_1 bimodal (black) and 309, M, monomodal (red), show a systematic shift to the right of the MDRP permeability curve in the presence of Type 1 microporosity (307) relative to the monomodal (309).

imbibition oil relative permeability data were refined and extended by D. H. Jones in 2002 using both the centrifuge data and the steady state data (Figure 11) and is used here. The resulting K_{ro} curves all have very similar shapes and a cursory inspection seems to indicate a left-right translation or saturation-offset behavior. This saturation-offset behavior was previously shown to occur in the special twin samples as the amount of microporosity varied and affected the MDRP permeability accumulation.

To examine the data more closely, the extended and refined composite data were offset to a common origin, K_{ro} of 1 at S_w - S_w, max (K_{ro} = 1), and the saturation-offset values tabulated; this was done to separate the differences related to saturation offset and slope-curvatures. Once offset to a common origin (Figure 12), the imbibition relative permeability data are easily observed to steepen with increasing absolute permeability. To parameterize this behavior, these offset data (single point normalization) were fit over their whole range to high accuracy using the function

$$\ln(K_{ro}) = a(^{e-y} -1) + b(y/\ln y)$$

with

$y = S_{w,\ offset}$ (Figure 12)

where the data were offset using the intercepts shown on Figure 11.

$$S_{w,\ offset} = S_w - S_{w,\ max}(K_{ro} = 1)$$

The fit coefficients: "a" and "b" (Figure 13) were observed to steadily increase with the permeability of the composites which is the fit parameter manifestation of the steepening behavior shown in Figure 12. Using the "a" and "b" regressions and the permeability value at $S_{w,\ ir}$ we reconstruct the oil relative permeability data versus $S_{w,\ offset}$ (Figure 14).

The new function using the "a" and "b" regression equations agree with the data very well over three orders of magnitude in oil relative permeability with the exception of composite waterflood [6].

For a complete (denormalized) reconstruction of the restored state imbibition oil-water relative permeability

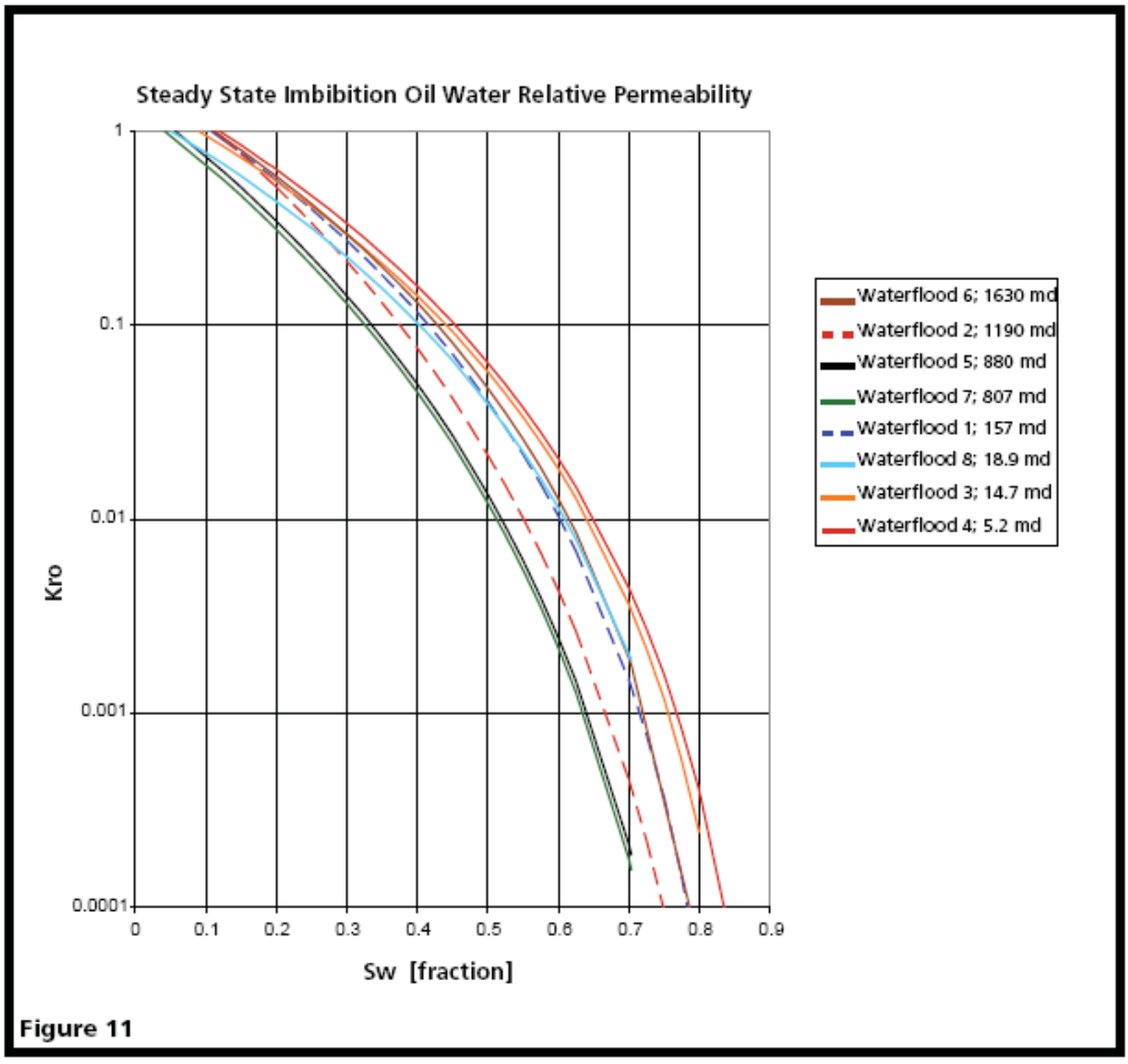

Figure 11 Imbibition oil relative permeability curves for 8 M_1 composite core waterfloods, 1994 study, refined and extended by D. H. Jones. The intercepts at Kro = 1 define the values of Sw,max (Kro = 1).

data, it remains to understand and parameterize the S_w offsets, i.e., the $S_{w,max}$ (K_{ro} = 1) intercept values that were used for the single point normalization. Within the 1994 relative permeability study on M_1 pore systems, one of the imbibition oil relative permeability composites provided the key. The waterflood composite 3, like all of the composites, consisted of five matched core plugs with very similar porosities (~26 pu) and permeabilities (~10 md). Yet the individual core plug centrifuge data obtained showed a very wide variation in the position of the oil relative permeability curve (Figure 15). The significant offset differences in the individual centrifuge behavior of these five core plugs are not likely to be a result of the well matched porosity and permeability properties.

The MDRP permeability calculation exercise suggests that the offset in the relative permeability data arises from varying amounts of Type 1 microporosity in these core plugs. To test this, we investigate the correlation of the $S_{w,\,max}$(K_{ro} = 1) intercept value to the quantitative presence of Type 1 microporosity. The plugs had MICP data from each plug end which was analyzed for pore system Thomeer parameters[1, 7].

The comparison of the $S_{w,\,max}$(K_{ro} = 1) intercept values with the Type 1 microporosity volumes is shown in Figure 16 for the five core plugs from composite three. The data is fit with a quadratic equation. The correlation is high and is in agreement with the results of the MDRP permeability calculation. The presence of an increasing

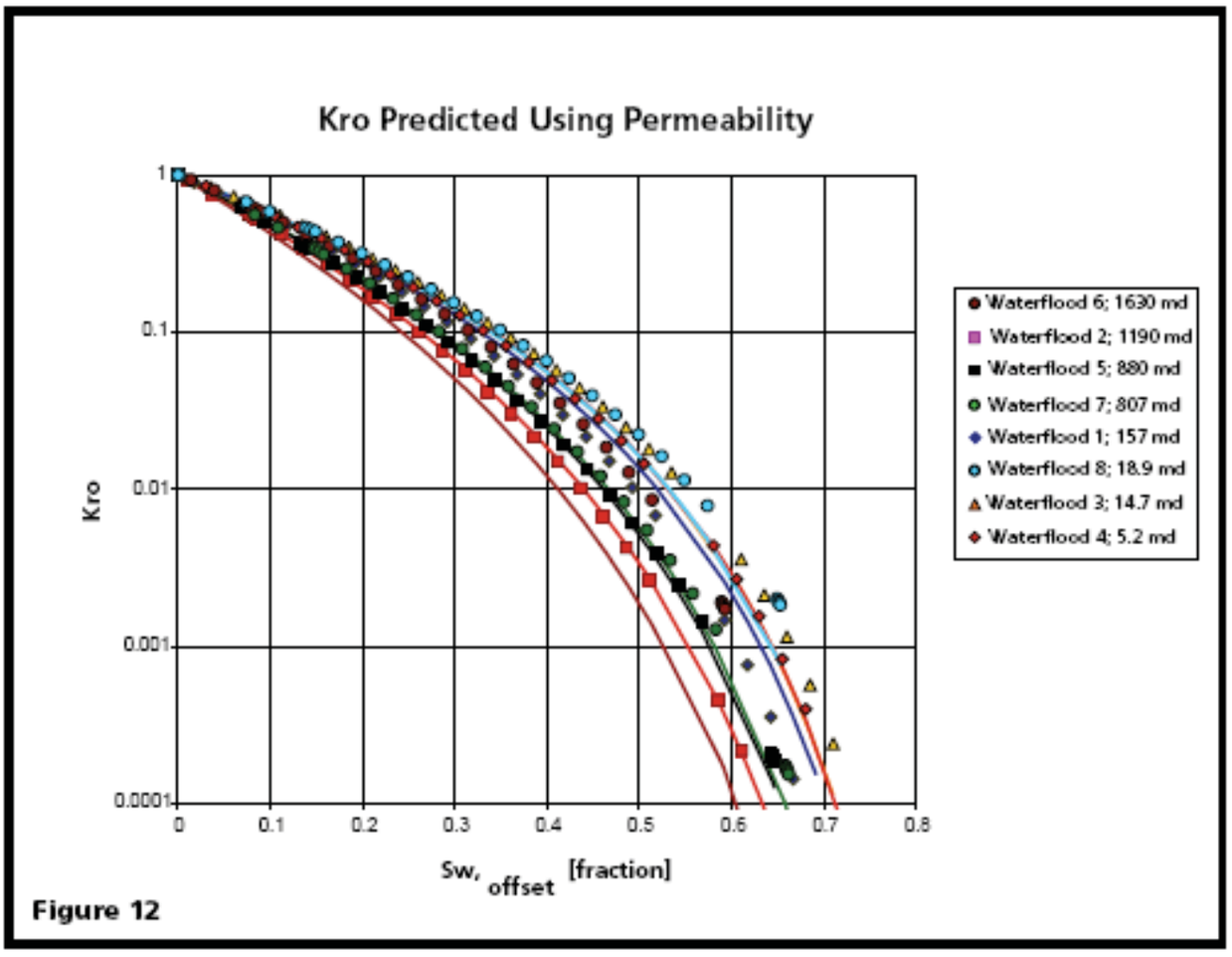

Figure 12 Imbibition oil relative permeability data for 8 M_1 waterfloods with fits to the data as lines. The imbibition oil relative permeability curves are offset to a common origin and are observed to steepen with increasing permeability.

volume of Type 1 micropores correlates with the steadily increasing water saturation offset of the actual reservoir fluids and the concomitant reduction of the residual oil saturation. The low initial water saturations for these plugs ensured that oil was in the Type 1 microporosity. The Type 1 microporosity is suggested to contribute to oil production through the spontaneous imbibition of water from and expulsion of oil to the adjacent M macropores. Additional data is being acquired to further investigate this behavior.

Conclusions

The permeability of the Ghawar Arab D limestones is largely governed by the large pore-throat diameters of the M macroporositon which commonly occurs along with some Type 1 microporosity to form the M_1 ultimate recovery petrophysical rock type. The M porositon is observed to carry substantially all of the measurable permeability while the contribution of the microporosity to permeability is imperceptible. This explains the poor results that arise from the total porosity-permeability methods for this carbonate. For this carbonate, the porosity-permeability crossplot and its inherent scatter is recognized to result from not addressing two important pore system properties related and not related to permeability: the largest pore-throat diameter and the presence of permeability "ineffective" microporosity, respectively.

A new two term permeability model is constructed with the dominant term being, $P_{d,f,}$ or the maximum pore-throat diameter of the M pore system and the total porosity. Though other parameters could have been used as the second input besides total porosity, these two parameters are targets for determination using appropriately acquired and processed modern spectral porosity well log data.

Detailed analysis of the permeability accumulation for the M_1 bimodal reservoir rocks uses a series of Pur-

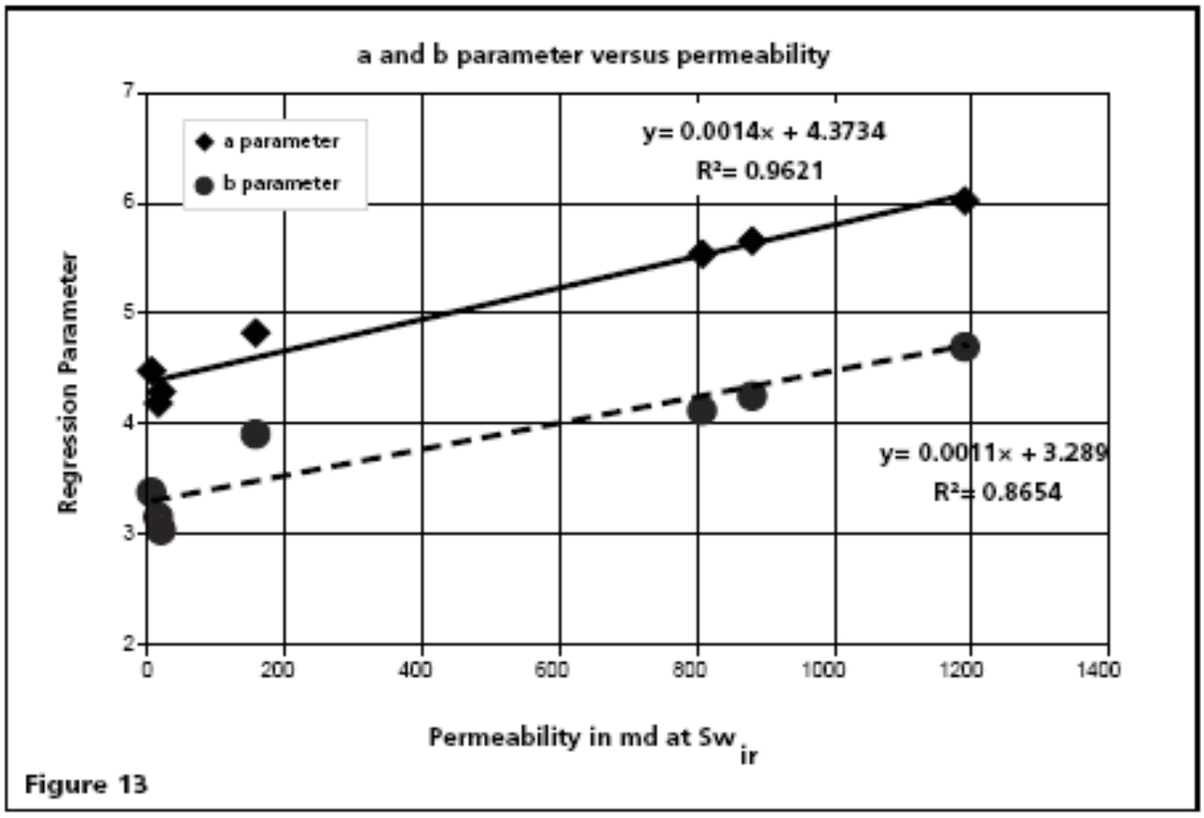

Figure 13 The "a" (solid) and "b" (dash) parameters in the imbibition oil relative permeability regression plotted versus composite core permeability at Sw, ir. The values steadily increase with permeability.

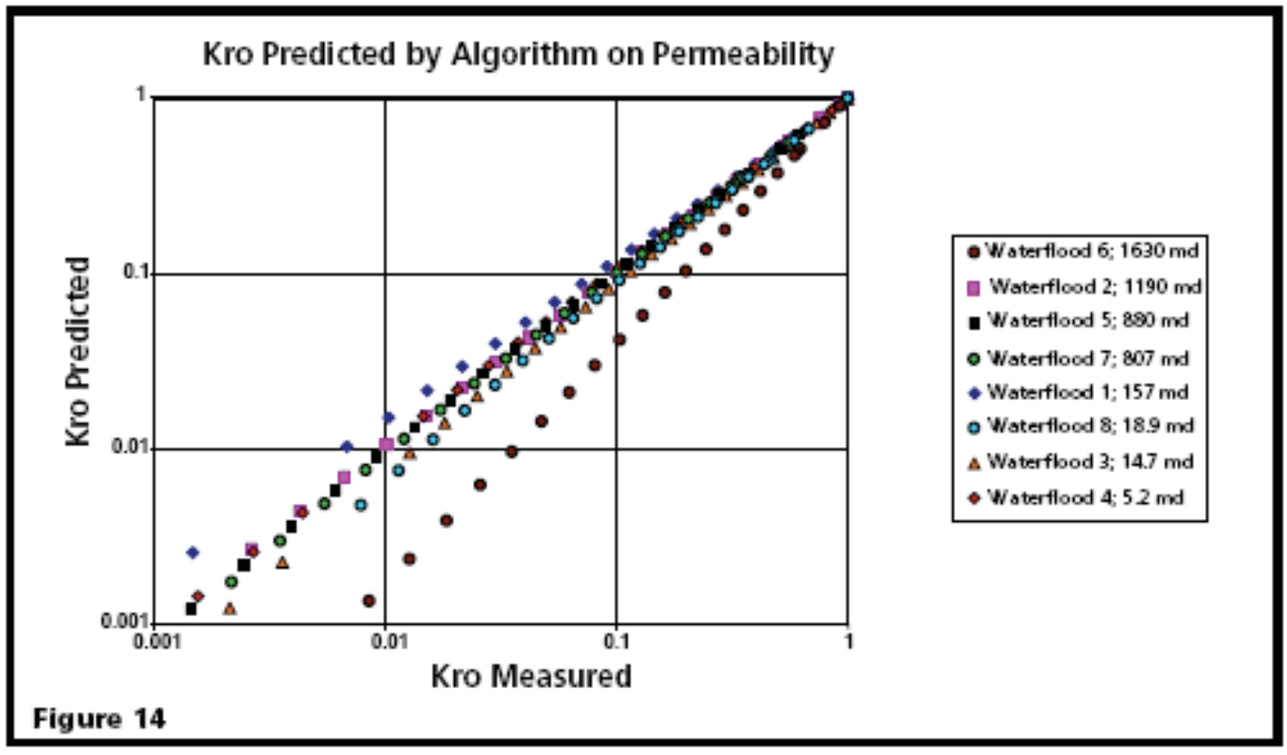

Figure 14 Regression predicted offset imbibition oil relative permeability using only the independent parameter- permeability at Sw, ir against the measured, refined and offset values of Figure 12. The regressions reproduce the data extremely well in all cases except for waterflood 6.

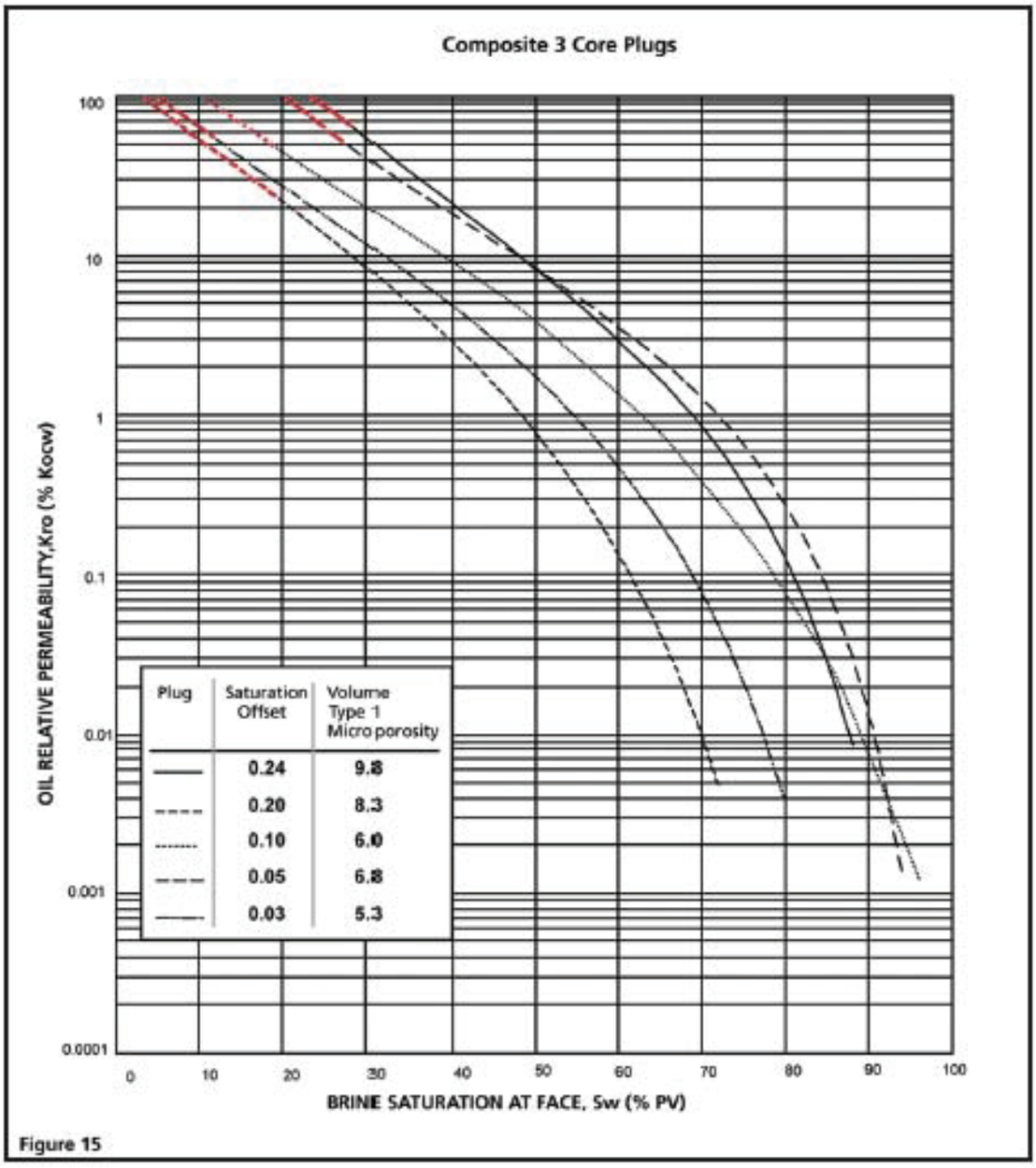

Figure 15 The individual core plugs from composite 3 showed variable water saturation offset behavior in their individual centrifuge oil relative permeability despite being matched for porosity and permeability. Investigation of the MICP data by Thomeer analysis on the plug end trims shows a varying amount of Type 1 microporosity among the plug set. Note that the relative permeability curve shapes are similar for the plugs. The legend shows the water saturation offset shown by the red extension of the data and the type 1 microporosity volumes for each plug.

cell integrals to calculate the Mercury Drainage Relative Permeability curve and demonstrates that essentially all of the permeability and the shape of the relative permeability curve is controlled by the largest pore throats and volumes which occur in about half of the M pore volume. The shape (single point normalization) of the imbibition relative permeability curves for eight waterflood composites can be modeled using this same permeability for samples of a wide range of permeability and prepared using the same wettability restoration process. The relative permeability curve shows steepening with permeability.

The pore volume classified as Type 1 microporosity does not perceptibly contribute to the permeability as measured in current laboratory practice (~ 3 significant digits). It follows that if the micropores do not measurably contribute to the absolute permeability, their contribution is also not perceptible with two phase permeameters. The micropore volumes then do not contribute to

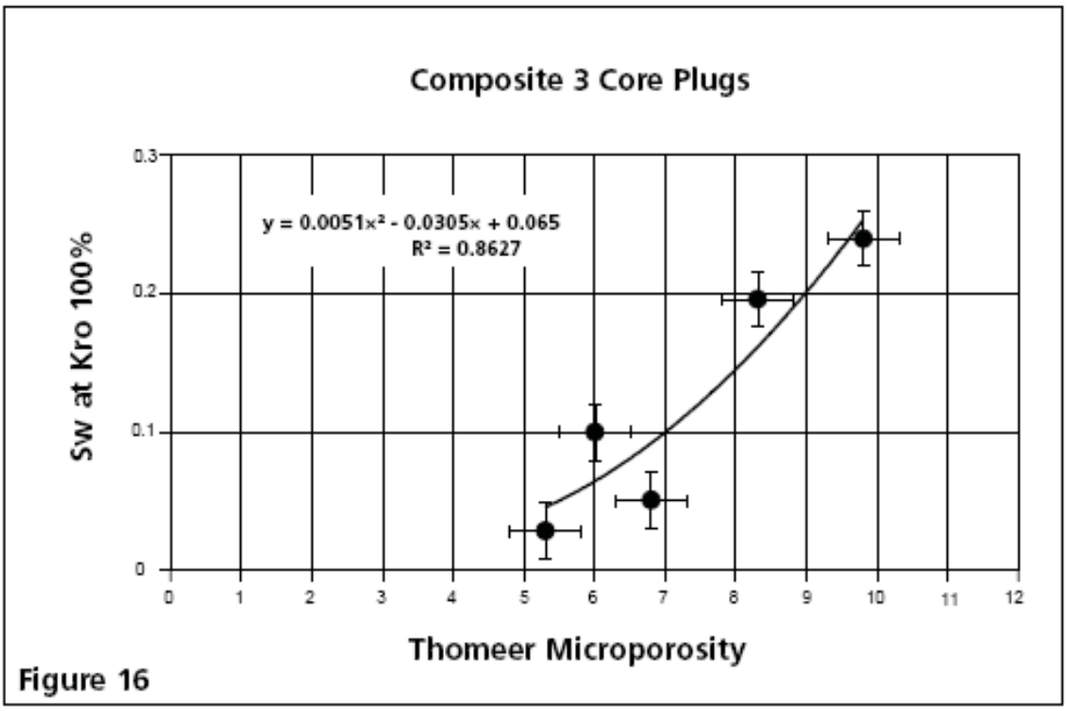

Figure 16 The Sw, max(Kro = 100 %) offset value for each core plug in composite 3 centrifuge oil relative permeability (Figure 15) plotted against the amount of Type 1 microporosity as determined by the Thomeer analysis of the plug end MICP data.

the shape of the relative permeability curve. Instead, the increasing volumes of Type 1 microporosity in these experiments manifest themselves as an increasing intrinsic water saturation offset when imbibition is initiated and as a concomitant reduction of the residual oil saturation. Relative permeability data curves must be handled considering this microporosity effect before discussions about the wettability effects are meaningful for this petrophysical rock type. These conclusions about M_1 pore system behavior imply that:

• Flow test and flowmeter data from the Ghawar Arab D are dominated by the behavior of the first half of the very permeable M pore subsystem and therefore flow is not necessarily indicative of the ultimate hydrocarbon recovery of the composite M_1 pore system. The flow response of the Type 1 microporosity is too small to be detectable in the presence of the large M permeability

• Ultimate recovery forecasts based on fractional flow and relative permeability equations require specific knowledge of both the macro (M) and Type 1 micro pore systems. This important knowledge could be supported by obtaining information from appropriately processed NMR and Electromagnetic Imaging spectral porosity well logs in conjunction with conventional well logs

• Reservoir monitoring must include detailed saturation determinations along with petrophysical rock type information which include the detailed characteristics of the M_1 bimodal pore systems

• Ultimate recovery (dynamic) petrophysical rock types have been demonstrated for the limestones in this reservoir

This work on the dynamic reservoir properties of the M_1 pore system when combined with previous work[1] demonstrate that these ultimate recovery petrophysical rock types can be linked to the geological rock types for

integrated reservoir characterization of the Arab D reservoir. These results will greatly improve reservoir simulation studies for improving ultimate recovery.

Nomenclature

B_V	percent of the bulk volume occupied by mercury
$B_{v,\infty}$	Thomeer parameter arising from the fit of a Thomeer hyperbola to MICP data, the asymptote of bulk volume occupied at infinite pressure
d	pore-throat diameter, [microns]
$d_{throat,max}$	maximum pore-throat diameter arising from $P_{d,f,}$ [microns]
G	Thomeer pore geometrical factor, [dimensionless]
K_a	air permeability, [md]
K_{MDRP}	calculated mercury to air drainage relative permeability, i.e., a permeability versus saturation curve from a series of Purcell integrals operating on the MICP data and using a steadily increasing upper integration limit, [dimensionless]
K_{ro}	relative permeability to oil, [dimensionless]
M	porositon with the largest maximum pore throat diameters, macroporositon
M_1	porositon combination of M (macro) and type 1 (micro) pore systems
P_d	initial displacement pressure in which mercury starts to enter the pore system; a parameter arising from the fit of a Thomeer hyperbola to MICP data, [psia, mercury to air]
$P_{d,f}$	initial displacement pressure of the first pore system, [psia, mercury to air]
S_{nonwet}	saturation of the nonwetting phase, [dimensionless]
S_w	water saturation, [dimensionless]
$S_{w,ir}$	irreducible water saturation, [dimensionless]
$S_{w,offset}$	water saturation offset by S w, max (K_{ro} = 1) to bring the centrifuge K_{ro} curves to a common origin, [dimen sionless]
$S_{w,max}$ (K_{ro} = 1)	value of the maximum S_w for which K_{ro} is still equal to one, [dimensionless]
$\sigma\cos\theta$	surface tension times the cosine of the contact Angle, [dynes/cm]

Acknowledgements

The author wishes to acknowledge the support and guidance of D. H. Jones, the GIANT team leader and Dr. Nansen Saleri under whom the bulk of this work was performed and whose support was greatly appreciated. Special thanks to the rest of the GIANT team and the multi-organizational management support received for this work from Saudi Aramco.

References

1) Clerke, E. A., Mueller III, H. W., Phillips, E. C., Eyvazzadeh, R. Y., Jones, D. H., Ramamoorthy, R., Srivastava, A., (2008) "Application of Thomeer Hyperbolas to decode the pore systems, facies and reservoir properties of the the Upper Jurassic Arab D Limestone, Ghawar field, Saudi Arabia: A Rosetta Stone approach", GeoArabia, Vol. 13, No. 4, p. 113-160, October.

2) Cantrell, D. M., Hagerty, R. M., (1999), "Microporosity in Arab D Carbonates, Saudi Arabia," GeoArabia, Vol. 4, No. 2, p. 129-154.

3) Cantrell, D. M., Hagerty, R.M., (2003), "Reservoir Rock Classification, Arab-D reservoir, Ghawar Field, Saudi Arabia," GeoArabia, Vol. 8, No. 3, p.453-462.

4) Clerke, E. A., (2003), "Beyond Porosity-Permeability Relationships: Determining Pore Network Parameters for the Ghawar Arab-D Using the Thomeer Method," GeoFrontier, Vol. 1, Issue 3, September.

5) Clerke E. A. , (2004), "Beyond Porosity-Permeability Relationships—Determining Pore Network Parameters for the Ghawar Arab-D Using the Thomeer Method," 2004 Middle East Geoscience Conference and Exhibition, Manama, Bahrain, March 7–10.

6) Ahr, W. M. , Allen, D., Boyd, A., Bachman, H. N., Smithson, T., Clerke, E. A., Gzara, K. B. M. , Hassall, J. K., Murty, C. R. K., Zubari, H., and Ramamoorthy, R., (2005): "Confronting the Carbonate Conundrum," Oilfield Review 17, No. 1 (Spring): p. 18–29.

7) Thomeer, J.H.M., (1960), "Introduction of a Pore Geometrical Factor Defined by a Capillary Pressure Curve," Petroleum Transactions, AIME, Vol. 219, T.N. 2057, p. 354-358.

8) Allen, D. F., Boyd, A., Massey,J., Fordham, E. J., Amabeoku, M.O., Kenyon,W. E.,Ward, W. B., (2001): "The Practical Application of NMR Logging in Carbonates: 3 Case Studies" Trans. SPWLA 42nd Ann. Logging Symp., Paper K.

9) Newberry, W.M., Grace, L.M., and Stief, D.D., (1996): "Analysis of Carbonate Dual Porosity Systems from Borehole Electrical Images", SPE 35158, presented at the Permian Basin Oil & Gas Recovery Conference in Midland, Texas, March.

10) Russell, S.D., Sadler, R.K., Weihua, W., Richter, P., Eyvazzadeh, R., and Clerke, E. A., (2004): "Applications of image log analyses to reservoir characterization, Ghawar and Shaybah fields, Saudi Arabia". 6th Middle East Geosciences Conference, GEO 2004. GeoArabia, Abstract, Vol. 9, No. 1, p. 125.

11) Thompson, A.H., Katz, A.J., Krohn, C.E., (1987), "The Microgeometry and Transport Properties of Sedimentary Rock, " Advances in Physics, Vol. 36, No. 5, p. 625-694.

12) Arns, C. H., (2005), "Pore Scale Characterization of Carbonates using X-Ray Microtomography," SPE Journal, Vol. 10, No. 4, p.475-484.

13) Knackstedt, M. A., (2004), personal communication

14) Melrose, J. C., (1965), "Interfacial Phenomena as Related to Oil Recovery Mechanisms," Can. J. Chem. Eng., v. 48, p 638-644.

15) Morrow, N. R., (1970), "Physics and Thermodynamics of Capillary Action in Porous Media, "Industrial and Engineering Chemistry, Vol. 63, p. 32-56.

16) Yuan, H. H., (1991), " Pore-Scale Heterogeneity From Mercury Porosimetry Data, " SPE Formation Evaluation, Vol. 6, No. 2, p. 233-240.

17) Thomeer, J. H. M., 1983, "Air Permeability as a Function of Three Pore-Network Parameters," Journal of Petroleum Technology, April, p. 809-814

18) Adamson, A. W., Physical Chemistry of Surfaces, (Wiley – Interscience, New York, 1990) 5th ed., p. 4-45.

19) Lucia, F. J., (1995), "Rock fabric/petrophysical classification of carbonate pore space for reservoir characterization," AAPG Bulletin, Vol. 79, No. 9, p. 1275-1300.

20) Purcell, W. R., (1949), "Capillary Pressure – Their Measurement using Mercury and the Calculation of Permeabilty Therefrom," Petroleum Trans, AIME, p 39-48, February.

21) Shafer, J. L., Braun, E. M., Wood, A. C., Wooten, J. M., (1990), "Obtaining Relative Permeability Data Using a Combination of Steady-State and Unsteady-State Waterfloods," Paper SCA 9009, Fourth Annual Technical Conference of the Society of Core Analysts, Dallas, TX., August 14-16.

22) Braun, E. M., Blackwell, R. J., (1981), "A Steady-State Technique for Measuring Oil-Water Relative Permeability Curves at Reservoir Conditions," SPE 10155, 56th ATCE San Antonio, TX., October 5-7.

23) Johnson, E. F., Bossler, D. P., Naumann, V. O., (1959), "Calculation of Relative Permeability from Displacement Experiments," Trans. AIME, 216, p. 370.

24) Huppler, J. D., (1969), "Waterflood Relative Permeabilities in Composite Cores," J. Pet Tech, p. 539, May.

Electrofacies and Geological Facies for Petrophysical Rock Typing: Khuff C

By Edward A Clerke, Ph.D. SPE /Saudi Aramco

This paper was prepared for presentation at the 2009 SPE Saudi Arabia Section Technical Symposium and Exhibition held in AlKhobar, Saudi Arabia, 09–11 May 2009.

Abstract

For integrated reservoir characterization a translation scheme must be established to link subsurface data across the disciplines, from the seismic and geological through the petrophysical to the reservoir dynamic properties. This translation process requires data sets that cross discipline boundaries and that establish robust mathematical and statistical relationships. Such information does not readily arise from single discipline based workflows, especially considering the various discipline specifics in the treatment of uncertainty. A process has been started to establish these cross disciplinary data sets for the Khuff gas reservoir and to develop the cross disciplinary translation process. In this work, we show important first results from the first well studied and establish some important links between well log electrofacies and the geological facies of Dukhayil for this well described by Tawil.

In this well, Khuff C cores have been described geologically by Dr. Aus Al Tawil. A fairly complete set of conventional well logs was acquired. In addition, the cores had a thin slice taken along their entire length (veneer) and this material was carefully ground and homogenized on a foot by foot basis. This powdered veneer material was submitted for X-Ray Diffraction analysis. The veneer mineralogy data represents a very complete analysis of the bulk mineralogy of the interval.

Today, new well logging technology makes similar mineralogy data available from well logs albeit with reduced accuracy and precision and for a reduced suite of minerals. In this sense, this core-log integration study explores the additional capabilities that mineralogy data enables in integrated characterization at a level more accurate than our current best well logs. An early important result from the mineralogy data is the distinguishing of exposed aerial influenced sediments from purely aqueous sediments.

With this well log and mineralogy data, electrofacies are developed in good agreement with a combination of the Tawil descriptions and the Dukhayil depositional facies and the Grain Type and Grain Size data. All of these results are being used to guide selective core resampling for petrophysical rock types. Key findings regarding the important data types are the result of this work and are reported here with preliminary electrofacies – geological facies results.

• Determination of the amount of anhydrite and the amount of total aluminosilicate (QIFM – Quartz, Illite, Feldspars, Mica) are paramount.
• The calculated water saturation which is quite proba-

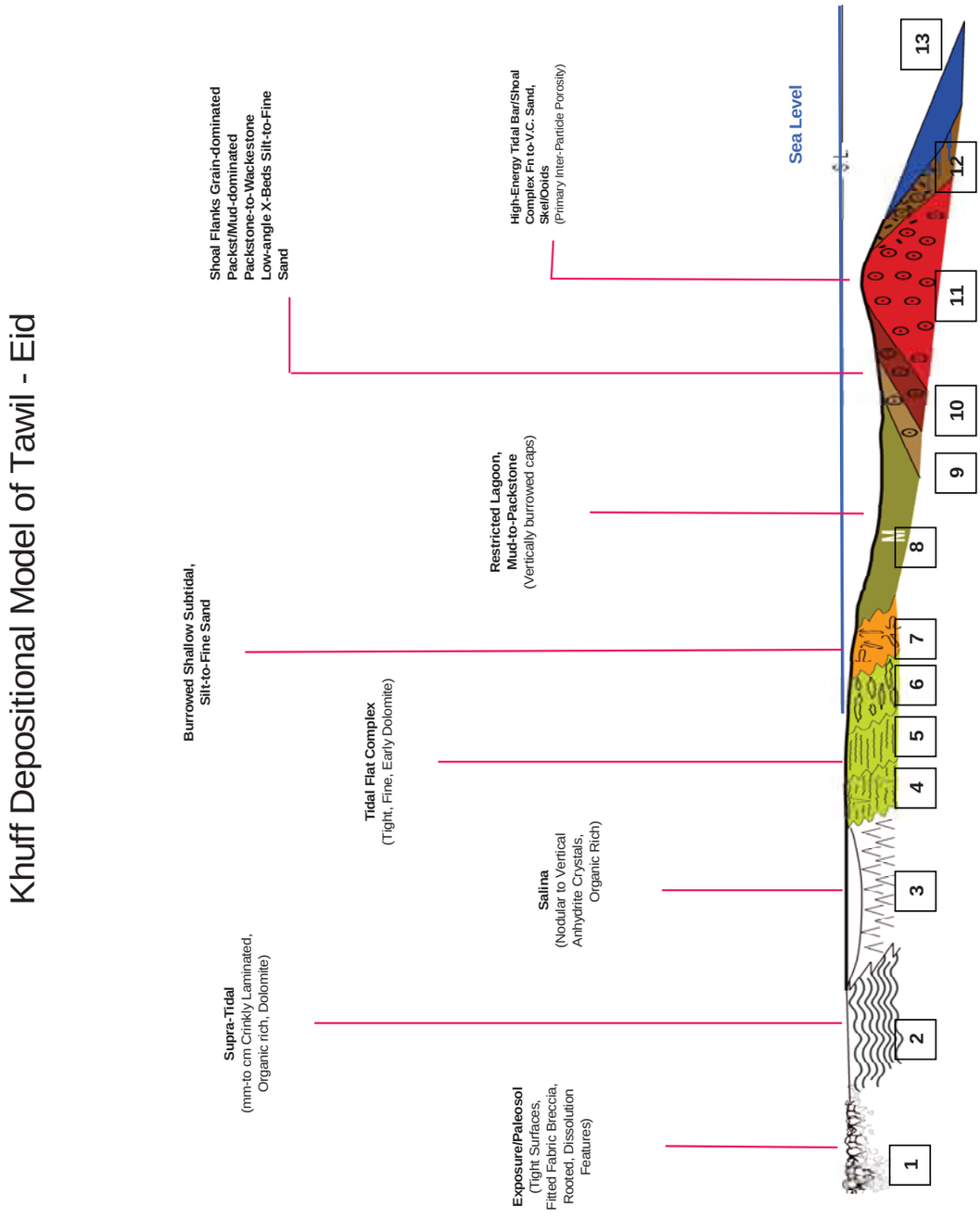

Figure 1 Depositional facies model used for Khuff C core description by Tawil after Dukhayil.

bly the irreducible water saturation is strongly correlated to the total amount of QIFM material.

- Mineralogy is highly variable and if poorly defined limits the ability to accurately define the porosity.
- The compressional sonic velocity, when used in conjunction with an accurate, mineralogy independent well log porosity, can greatly aid characterization of carbonate texture variations, facies and permeability modeling.
- Pore system variations of facies represent themselves in the flushed to deep zone saturation behavior in this well which is above a water contact and where gas is present.
- Core material described with the Archie rock typing scheme showed rapid variation and thin bedding styles throughout the core and high vertical resolution data acquisition is required.
- Appropriate petrographic data was developed for support of the petrophysical rock typing.

Introduction

The F29 well was cored and logged and described through the Khuff C interval. A fairly complete set of conventional well logs was acquired. In addition, the cores had a thin slice along their entire length removed (veneered) and this material was carefully ground and homogenized on a foot by foot basis. This powdered veneer material was submitted for X-Ray Diffraction analysis through ResLab and XRAL. The veneer mineralogy data represents a very complete analysis of the bulk mineralogy of the interval. Today, new well logging technology makes much of this mineralogy data available from well logs though with reduced accuracy and precision and for a reduced suite of minerals. The simultaneous occurrence of these multiple data types in one well make this well an excellent candidate for the establishment of multidisciplinary translation methods.

The core material was described using the Archie rock typing scheme and photographs were taken at core scale, 10x and 60x scale using a camera and a digital microscope. Additional descriptive text described attributes (Archie Rock Type, etc.) important to the petrophysical response, to tie that response to the geological facies or to support the high resolution depth shifting this well required. Routine core analysis data were collected along with the geological descriptive data. The slab veneer Bulk XRD data acquired by Clerke in 20011 was also collected. An integration panel was prepared where all of the data has been carefully depth shifted to very high accuracy. This integration panel was used to select 96 new core plug locations for additional petrographic work and MICP data to support the definition of petrophysical rock types in the Khuff.

Well logs "see" rock properties and geologic properties through the prism of the individual tool's physics and details of the tool resolution. Many users of these data types are familiar with the limited vertical resolution of well logging tools. It is necessary to bring the core descriptive data and the well log data to some common intermediate basis where they can be honestly compared. For core plugs measurements of porosity and permeability, the resolution matching process is well known. Less well known but not less important is the logging tool physical-response filter to apply to core descriptive text.

This response filter depends on the well logs used and the depositional environment and is not easily codified. The author has been performing petrophysical core description for decades on core from basins around the world.

Modifications to Tawil-Dukhayil Depofacies

The Khuff C core was described by Tawil and used facies defined by Dukhayil.[2] Certain modifications of the Tawil-Dukhayil (T-D) depofacies (Figure 1, Table 1) are used here to bring these descriptions to a common basis for use by well logs:

1. Thin facies (facies on the order of one foot thickness or less) were removed and assigned facies value of the major adjacent facies.

2. Facies boundaries were adjusted by +/- 0.5' to align with log bed boundaries.

3. High Energy Tidal Bar/ Shoal Complex facies was split for petrophysical reasons (clasts have a distinct well log response) into
a. Tidal Bar /Shoal Complex.
b. Tidal Bar/Shoal Complex with Clasts.

The Dukhayil facies diagram is reproduced in Figure 1 followed by the facies description table (Table 1). All of the processed well log data (FAL) used and shown here are associated with reprocessing of the data in 2008.

Electrofacies Investigations

Exploratory work was performed with this large data set to see if electrofacies could be determined with any relationship to the T-D geological facies. This effort met with some success which can most likely be advanced using similar concepts if not identical procedures in FacimageTM software.

Facies Subject to Aerial Exposure

Modern geochemical well logs have the capability to detect the primarily clastic minerals: Quartz, Illite, Feldspar and Mica (QIFM), especially in a dominantly carbonate matrix. X-ray diffraction (XRD) measurements can determine the quantitative presence of these minerals in the laboratory in very dilute amounts. The veneer powders were thoroughly analyzed using XRD. Within the facies described by Tawil were facies expected to have been periodically exposed and subject to influx of wind blown dust, which transports QIFM minerals from afar. T-D geological and petrophysical core description identified cored intervals that had been altered by post sedimentary processes. These intervals consist of breccias, regoliths, possible cave collapse sections with possible geopetal structures (R. Lindsay, personal communication), intraclasts and local resedimentation. In particular, the T-D facies that could have experienced aerial exposure are: 1– Exposure/Paleosol, 2 – Supra-Tidal, 3 – Salina, 4, 5, 6 – Tidal Flat Complex and possibly 7

Lithofacies Code	1	2	3	4	5	6	7	8	9	10	11	12	13
Mineralogy	Limestone to Dolomite	Dolomite, organic rich with anhydrite	Anhydrite interbedded with organic rich dolomite	Dolomite	Dolomite	Dolomite	Dolomite	Dolomite with anhydrite	Dolomite and Limestone	Dolomite and Limestone	Limestone/partially dolomitized	Limestone	Limestone
Texture (Dunham + grain type)	Mudstone	Dolomitic Anhydrite	Anhydrite	Mudstone	Mudstone	Mudstone	Dolosiltite/Sucrosic	Mudstone to Packstone	Mudclast skeletal Peloid/Ooid Packstones to Wackestone	Mudclast skeletal Peloid/Ooid Grain-dominated Packstones	Skeletal Ooid Grainstone	Flat pebble conglomerate to intraclastic Grainstone to Packstone	Skeletal Packstone to Mudstones
Sedimentary Structure	Pedogenic and collapsed breccias, soft sediment deformation and minor rootlets	Nodular to nodular bedded to crinkly laminated anhydrite interbedded with anhydritic dolomite	nodular to bedded to vertically growing crystals	Mud cracked to crinkly laminated, anhydrite, filled roots	Crinkly laminated	Burrowed mottled	Extensive horizontal burrowing, low angle crossbeds to structureless	Vertically burrowed caps	Horizontally burrowed to none	Horizontal to subhorizontal laminations	High energy cross bedded		Horizontal burrowing
Grain Size	Clay to Silt to Pebble	Clay	Clay	Clay to Silt	Clay to Silt	Clay to Silt	Mainly Silt size	Clay to Granule	Clay to Granule	Clay to Granule	Fine to Medium to Coarse	Fine to Pebble	Clay + Coarse to Granule
Fossils								Forams, Algae, Gastropods, Molluscs, Skeletal Fragments	Forams, Gastropods, Brachiopods	Gastropods, Brachiopods, Forams	Brachiopods, Bryozoans, Gastropods	Brachiopods, Bryozoans, Gastropods	Bryozoans, Crinoids, Brachiopods, and Microbial mats and/or Thrombolites
Reservoir Quality							High between crystalline porosity and high permeability			Fair moldic and between crystalline porosities plus low to medium permeability	High moldic porosity and low permeability	Fair moldic porosity and low permeability	
Depositional Environment	Exposure	Supratidal	Salina	Upper intertidal	Middle intertidal	Lower intertidal	Shallow subtidal	Restricted lagoon	Shoal flanks, mud dominated packstones to wackestone	Shoal flanks, grain dominated packstones	Shoal core	Storm influence	Open marine
Others	Gray to dark gray color	White, very dark grey-black	off white	Light to medium gray	Light to medium gray	Light to medium gray	Tan to light brown	Gray to dark gray	Brown	Brown	Light to medium brown	Medium to dark brown	dark gray to dark brown

Table 1 Lithofacies table of Dukhayil.

– Burrowed Shallow Subtidal. It is possible that these sediments experienced aerial exposure and enrichment with QIFM relative to the normal aqueous carbonate minerals. This work finds that these two competing and disparate source of minerals can be analyzed with the ANHYDRITE versus QIFM - 3*FLOR crossplot as shown (Figure 2).

The mineral information used in this study is obtained using X-ray diffraction on the veneer powders, in the case of the QIFM abundance deductions are made for the presence of the mineral Fluorite. Fluorite is associated with very low sedimentation rates and anoxia. By iteratively working this crossplot with regions and the T-D facies, the sediments in the Khuff C are separated

based on the extent of aerial QIFM (Fluorite corrected) influence. Data within the blue region are dominantly aqueous with little QIFM but a wide range of Anhydrite abundance. The gray area indicates data with significant aerial influence. This forms a first and basic subdivision of the sediments using petrophysically accessible signals. Windblown dust has been shown to be correlated to decreasing carbonate reservoir quality and complete reservoir deterioration occurs at windblown dust bulk percentages above five percent[2].

Using the crossplot of Figure 2, the major exposure influence interval from x735 – x765 (Figure 3) is correctly classified as aerially influenced. This is shown in the Integration Panel segment (Figure 3) as the light blue (aqueous) and gray (aerial) in track 2. The aerial intervals on the FAL show moderate porosity with the pore space occupied by water (Track 4) in contrast to the other porous intervals. The T-D description of the aerial interval is breccia and regolith in part and observations of finely laminated and cracked sediments recemented and with recemented seams. The interval from x736-x744, I describe as Archie IF vitreous 'marble' and could be polished up to be good tile material. This is clearly not reservoir rock.

The Potassium curve (POTA) of the Natural Gamma Spectroscopy Tool (NGS) provides an alternate clastic influence discrimination tool. Windblown dust contains a significant component of potassium-bearing minerals3. The POTA curve statistics for the two regions (Aerial and Aqueous) are shown in Figure 4.

The Aqueous – Aerial intervals can be discriminated for this well using a POTA cutoff of 0.87. Similar results were found for Permian Leonardian Clearfork carbonate sediments by Clerke et al.4. This POTA cutoff value is both exacting and sensitive, therefore the use of this approach on a multiwell basis would require very careful log data acquisition and environmental corrections of the NGS POTA data. A practical reality is that both the NGS for POTA and the Elemental Capture Spectroscopy (ECS) for total aluminosilicates and sulfates should be used to drive both or a combination procedure. The two methods give similar results for the lower well defined Tidal Flat interval. Note that the two methods give different results in the upper intervals of the well (Figures 5 and 6). Future core-log integration studies should aid in clarifying the value of the two methods.

Aqueous Sediments' Porosity Type Indicator from Total Porosity and Acoustic Velocity

The acoustic velocity and total porosity can be used synergistically to give subtle indications of the variation in

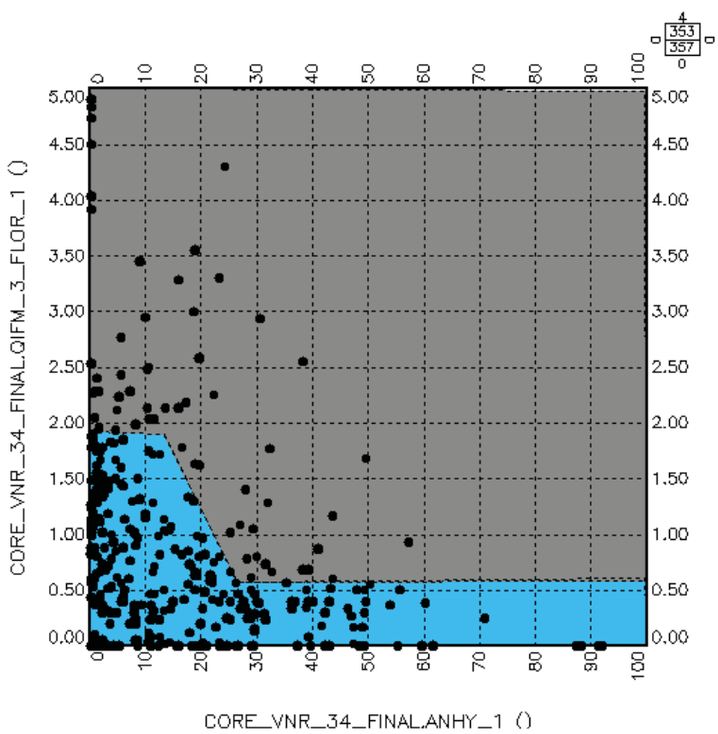

Figure 2 The crossplot of QIFM minus 3 time Fluorite (y-axis) and Anhydrite from the veneer mineralogy (x-axis) can be used to separate Aqueous intervals (blue) from the Aerial influenced (gray). The classification based on this crossplot is shown in Figure 3 Track 3. The veneer XRD mineralogy shows that the Aerial interval is enriched with QIFM - 3* Fluorite as compared to other intervals

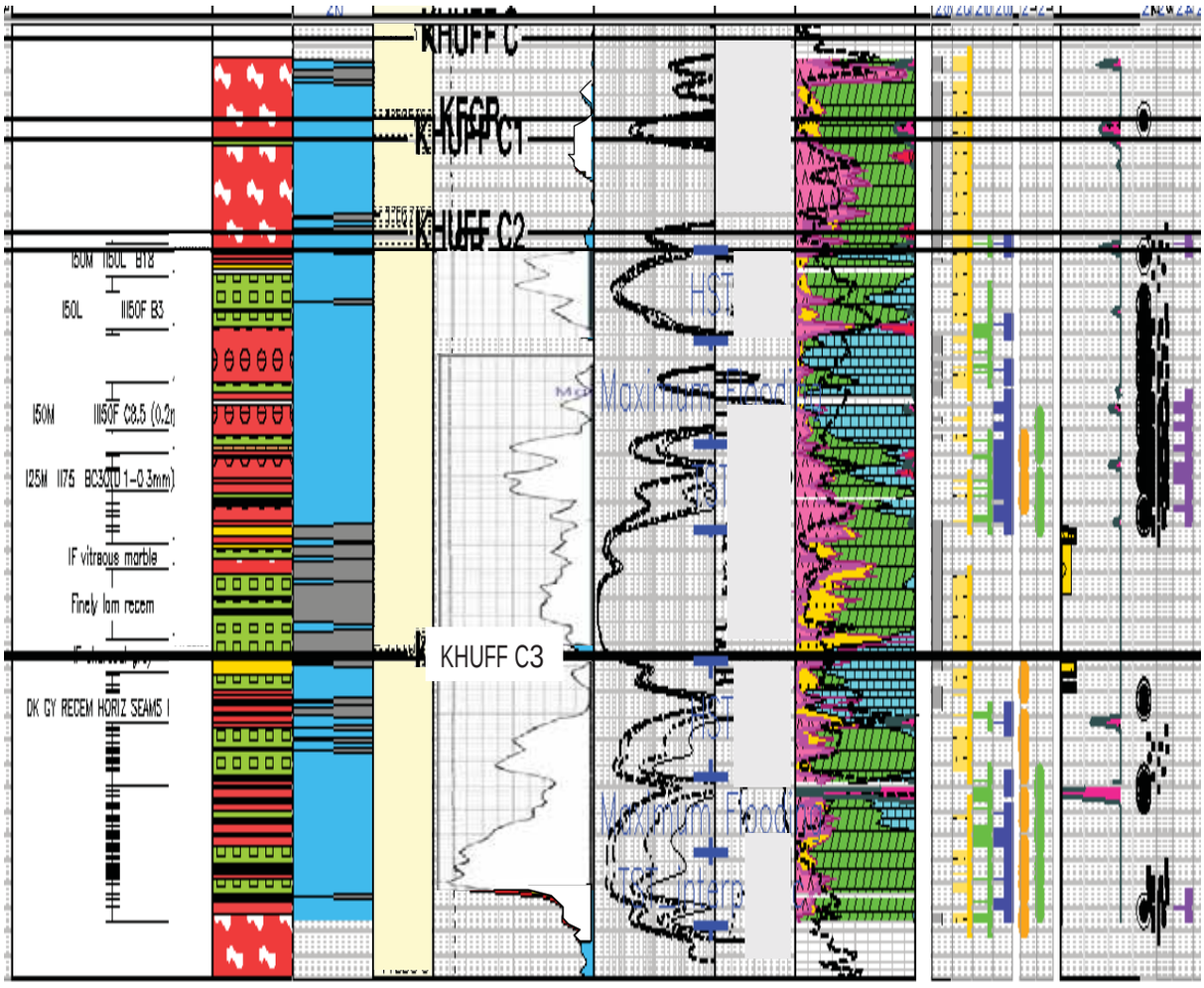

Figure 3 A section of the Integration Panel. Track 2 shows the Aqueous sections (blue) and the Aerial (gray) from the Figure 2 crossplot.

the carbonate pore system texture within the limited scope of pore system changes present here. This is readily implemented using the acoustic velocity to porosity slope parameter[5]. For the Khuff, this step is applied after the application of the Aqueous – Aerial discrimination crossplot which separates major carbonate textural changes. In the Aqueous sediments, the acoustic velocity – porosity textural change is used to differentiate two sub domains: the Aqueous upper trend and the Aqueous lower trend (Figure 7). This very basic classification is all that can be supported until more detailed pore system information is obtained.

Additional detailed pore system attributes are being gathered with additional petrographic work on this core. In practice, a form of this classification and can be used in a facimage training program. The Aqueous acoustic velocity – porosity slope is computed using the equation

Slope = (20.03 – 1000/dt)/(Dphi_vnr_matrix).

Where dt – is the compressional acoustic travel time, and Dphi_vnr_matrix is a density porosity computed using the grain densities obtained from the powdered veneer measurements. This is equivalent to a porosity determined using a robust multimineral model for the Khuff supported by adequate well logs.

The intervals defined by the two crossplot trends within the Aqueous sediments generate a remarkable relationship to the T-D porosity types of the core description which varied from intergranular (BC – between crystalline) to moldic (MO) (Figure 8).

At this juncture in the developing analysis, there are three electrofacies:

- Aerial (display code = gray).
- Aqueous (display code = red) Upper Trend.

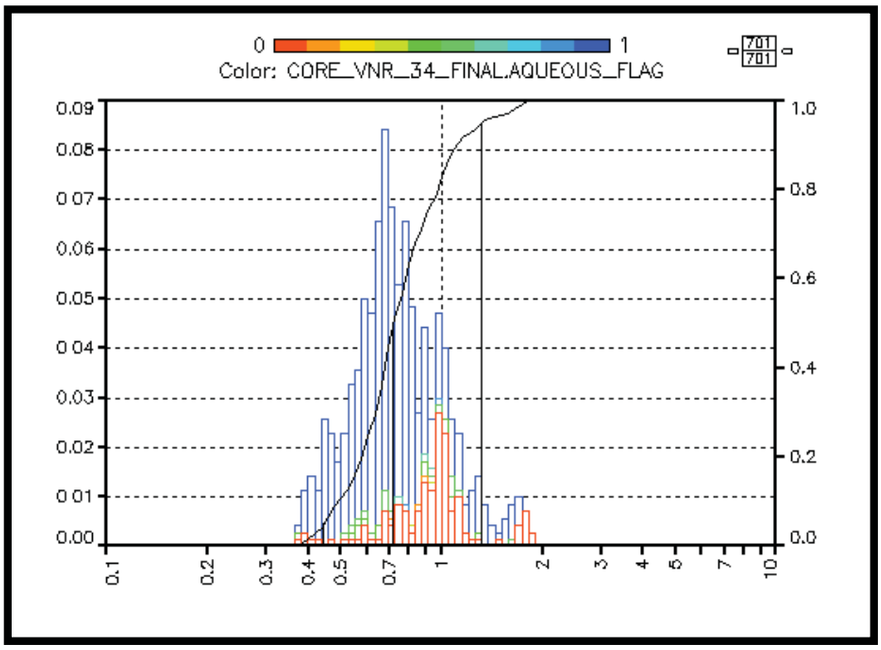

Figure 4 Spectral gamma ray potassium (POTA) statistics for the Aqueous (blue) and Aerial (red) sections in the Khuff C cored interval. The intervals can be fairly well separated using a 0.87 cutoff.

• Aqueous (display code = red) Lower Trend.

The latter two electrofacies will be further subdivided by some additional log response characteristics. For the Aqueous Upper Trend and the Aqueous Lower Trend electrofacies, respectively, an additional crossplot is defined using the flushed zone (Indicator = 1 / Sxo) and deep water saturations. The two crossplots for the upper trend (Figure 9) and the lower trend (Figure 10) are shown. So within the Aqueous Upper Trend reside the electrofacies:

• u_ch_st9 (display code = pink)
• uu_biot (display code = biot).

And for the Aqueous Lower Trend reside the three electrofacies:

• l_biot (display code = green).
• llll_st9 (display code = orange).
• llll_iron (display code = iron).

The results from this sequential multi-crossplot approach to the Khuff C electrofacies are shown in the next three figures (Figures 11, 12 and 13) using the display described in Table 2. Neither of the crossplots of Figures 9 and 10 uses an explicit porosity magnitude classification. Track 2 shows the modified description as previously discussed for thin beds and with Shoal facies subdivided for clast content. Track 3 shows the Acoustic Velocity – Porosity categorization. Track 4 shows the Electrofacies codes from the described process.

There is good to fair agreement between the electrofacies and the T-D geologic facies but significant differences. Despite not using porosity magnitude as a classifer (Figure 7 regions cover two full ranges of porosity), the resulting electrofacies contain some general conformance to porosity variation. The electrofacies agreement with the T-D geologic facies is fair and in some cases, excellent. In some intervals, the electrofacies classification subdivides an interval covered by a less variable core description (Figures 12 and 13). These are issues that should be resolved with the further planned work.

Additionally, it is observed that the amount of aluminosilicates is strongly correlated to the volume of water in the unflushed (deep resistivity) zone (UWAT) of the FAL analysis (Figures 6, 14 and 15). Aluminosilicate surface chemistry renders them more water wet than limestone, and/or the presence of these minerals is strongly associated with very fine grained Silt to Clay sizes as noted by the T-D descriptions. This observation further substantiates the value and need for precise and accurate aluminosilicate volumes for the Khuff.

Petrographic Descriptions to Support Khuff Petrophysical Rock Types

Detailed petrographic requirements tailored to the petrophysical issues identified for the Khuff will be important to the fully integrated analysis. I have delineated the specific petrographic information required and included that information here for future reference.

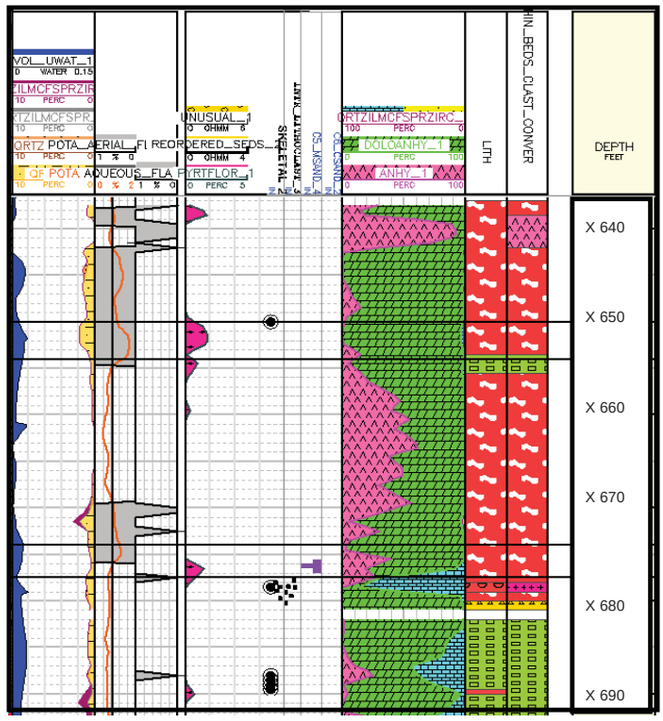

Figure 5 The upper cored section of the well. In track 2 on the left half is the POTA Aerial intervals in gray and the right half has the crossplot (Figure 2) Aerial intervals. The POTA determined intervals are thicker.

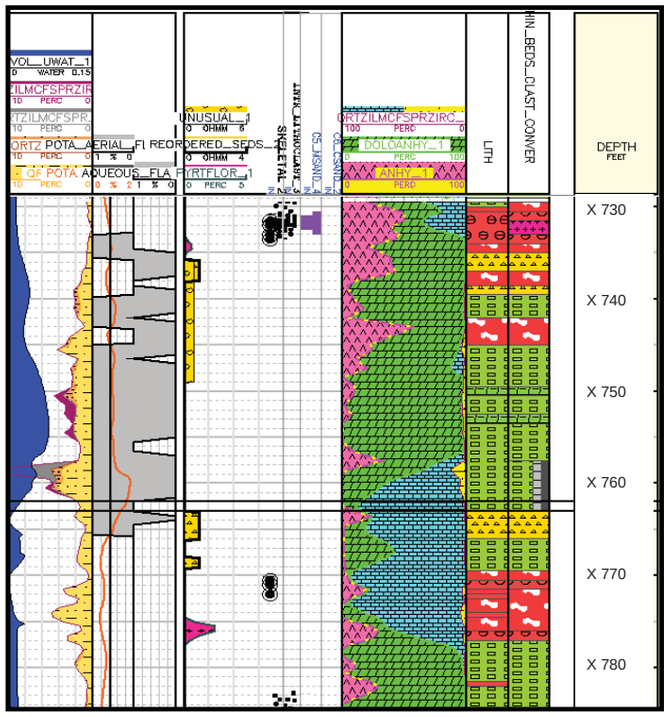

Figure 6 The lower cored section of the well. In track 2 on the left half is the POTA Aerial intervals in gray and the right half has the crossplot (Figure 2) Aerial intervals. The results are comparable.

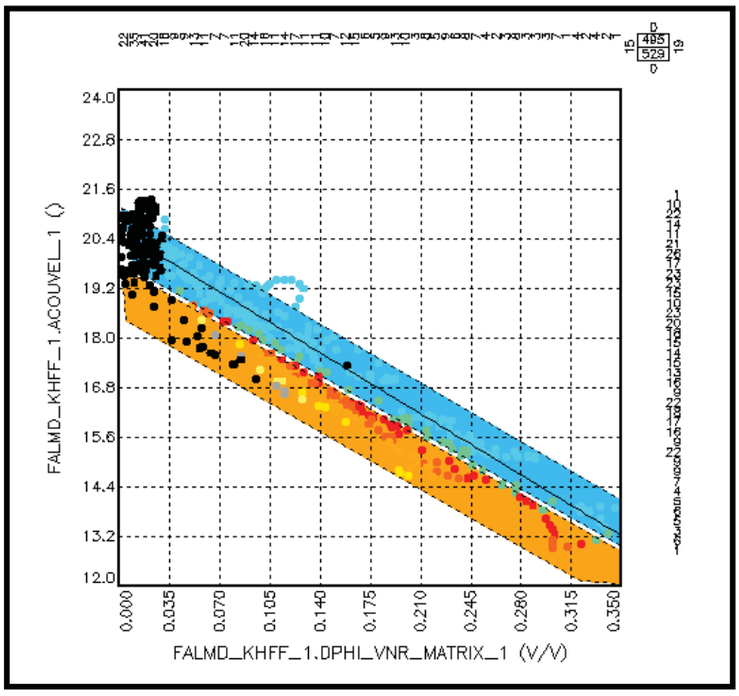

Figure 7 For the Aqueous sediments, the velocity versus porosity plot is shown. Two basic groups are shown, however more details are available for eventual use with appropriate petrographic data.

Electrically Conductive Grains even at trace levels, i.e. iron bearing minerals – Pyrite, siderite, glauconite.

Gamma Ray Contributing Grains down to trace levels: apatite, fluorite – down to trace levels.

High or Low Grain Density Grains down to trace levels: with the grain density variation being defined as normal between 2.71 (Limestone) and Dolomite (2.85).

Environment Specific and Redox Specific Grains down to trace levels: Celestite, phosphate bearing minerals, Uranium, indicative of exposure, Mg, Ca, Si.

High Neutron Absorber Grains down to trace levels: Iron bearing minerals, High atomic number (Z) minerals, Hydrous minerals, be careful to note barite as poikilotopic grain growth. Annotate minerals that are suspected to be derived from mud filtrate.

Spectral Gamma and Neutron Induced Gamma Spectroscopic Grains – Many of the above mentioned minerals are also determined from Neutron-Induced Gamma Spectroscopic and Natural Gamma Spectroscopic well logs – but in addition are: Potassium bearing minerals, Aluminosilicates as a broad class (Aluminum being the detected atom), Sulfur bearing minerals (Sulfur detection), Iron bearing minerals (Iron detected), Uranium bearing minerals, QFM (Quartz, Feldspar, Mica), coal, salt, calcium, magnesium bearing grains.

Carbonate Textures – the standard Dunham textures are requested with additions of the following:

- **Percent Spherical (nearly spherical) Grains.**

- **Percent of Spherical Grains above with eroded centers to intact centers (0 to 100).**

- **Mold Excavation Percentage** – the degree to which the eroded mold centers are totally eroded: 0-100%.

- **Grain to Grain Contacts** – the nature of the grain to grain contacts are the major control on the pore throats in an intergranular media – if grains have welded and sutured grain to grain contacts the pore throats are likely to be very small compared to the grains, likewise the nature of the cements in the vicinity of the grain to grain contacts are more important for permeability than cements in the open pore body.

Pore Space Attributes In addition to the total visible porosity, we request the following porosity subdivisions:

Microporosity – the difference between the plug porosity and the visible thin section porosity.

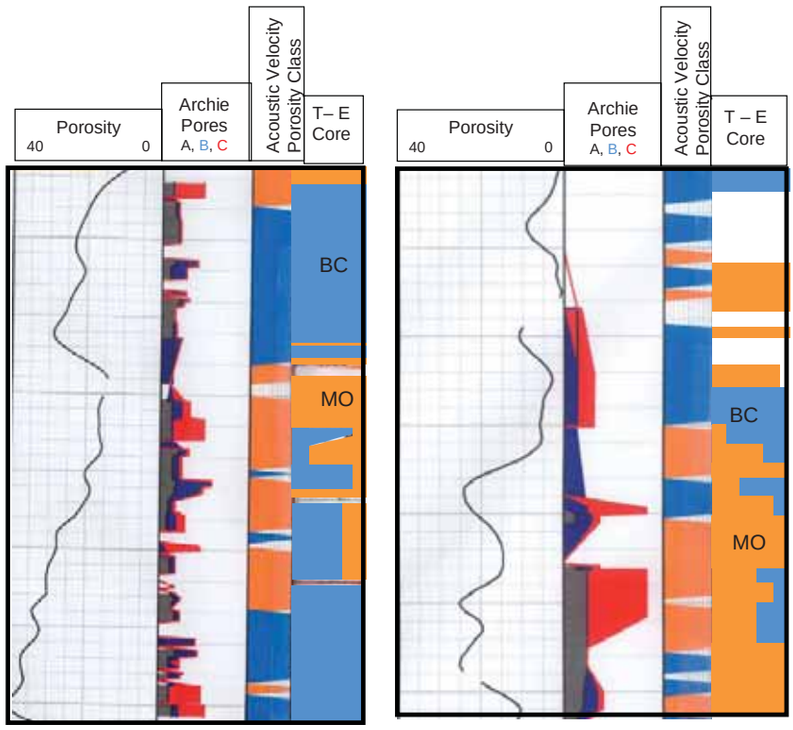

Figure 8 The two acoustic velocity – porosity trends are shown from the crossplot of Figure 7 compared to the T-D core description of between crystalline (BC, blue) and moldic porosity (MO, orange).

Poorly Connected and Moldic porosity – the amount of porosity contained within molds and not well connected – Consider the connection size ranges to be in packages of factors of 10 in pore throat diameter (100 microns and above, 100-10, 10-1).

Mold Shape Retention Percentage – percent of molds that are intact nearly spherical shape and not broken or cracked.

Intermicritic porosity – the amount of visible porosity present in the micritic regions of the thin section.

Controls on Interconnected visible porosity - what grains, types and sizes are controlling the largest pathway in the visible and connected pore space and estimates of that largest pathway cross section diameter – and what grains, types and sizes are controlling the smallest pathway in the visible and connected pore space and estimates of that smallest pathway cross section diameter.

Optimal Well Log Suite

The results from this early and preliminary study of just one Khuff well already suggest revisions to the well logging program:

- High resolution determination of QIFM (total aluminosilicates) at low concentration.
- Precise and accurate determination of Anhydrite.

(Both of these are needed to segregate Aerial non reservoir facies from Aqueous facies.)

- Acoustic velocity well logs.
- Logging program able to compute a robust grain density comparable to core plug grain density in a highly variable lithology – for accurate total porosity.
- MicroLaterolog type resistivity device – not induction type and very high vertical resolution (discussion of the support for this tool is not included here).
- Well determined multiple invasion depth resistivities.

Conclusions

This multidisciplinary data set has started to be constructed and exercised. Preliminary electrofacies concepts were developed in good agreement with the combination of the depositional facies and the Grain Type and Grain Size data. These early results are being used to guide selective core resampling for petrophysical rock types.

Preliminary electrofacies have been determined on one well for aid in selection of special petrophysical core plug data. The electrofacies seem to have combined at-

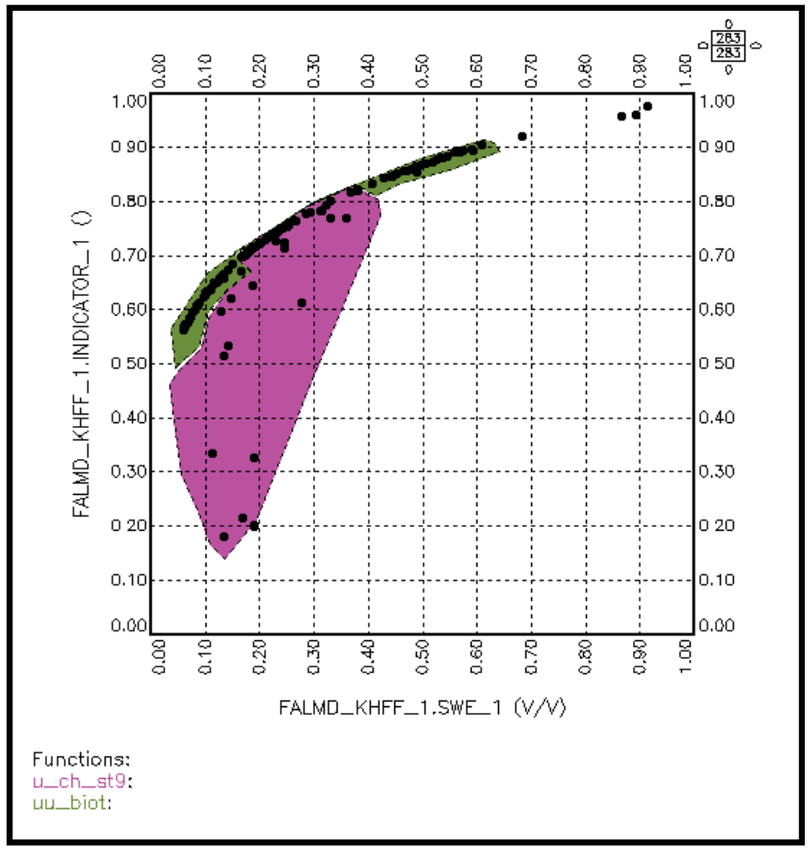

Figure 9 For Aqueous sediments whose acoustic velocity – porosity trend is in the upper band (Figure 7), an additional crossplot is shown which generates regions that compare well to the T-D geologic facies.

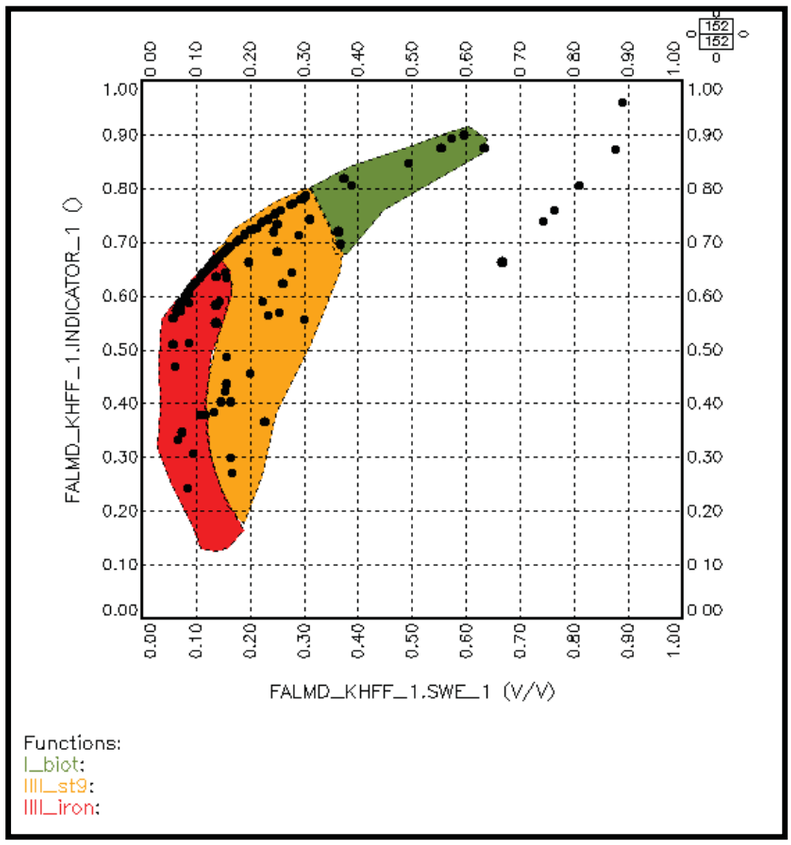

Figure 10 For Aqueous sediments whose acoustic velocity – porosity trend is in the lower band (Figure 7), an additional crossplot is shown which has regions that compare well to the T-D geologic facies.

Track 1 **Archie Text**
Track 2 **Tawil-Eid Facies with thin beds removed and Shoal facies and Shoal Facies with clasts**
Fill codes are:

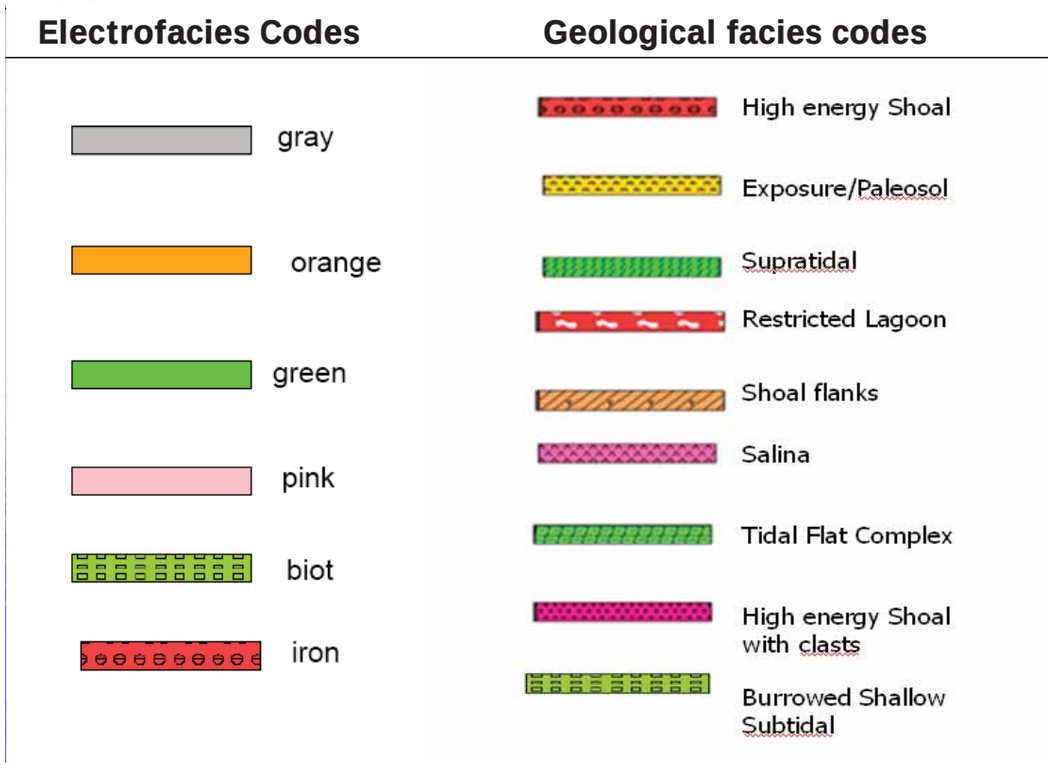

Track 3 **Acoustic Velocity – Porosity Slope Categories**
Track 4 **Electrofacies from this work**
Track 5 **Grain Sizes** from geological description up to fine sand, then pellets, peloids
Track 6 **Depth**
Track 7 **FAL** Porosity
Track 8 **FAL Induction logs**
Track 9 **Veneer Mineralogy: QIFM, Celestite, Pyrite, Fluorite exaggerated**

Table 2 Legend for figures 11, 12 and 13.

tributes of both the depofacies and grainsize. Electrofacies are determined from simple well log groups and should be transportable to other wells.

Key Findings

• Determination of the amount of anhydrite and the amount of total aluminosilicate (QIFM – Quartz, Illite, Feldspars, Mica) are paramount. The QIFM determination needs to be precise for low concentrations (0 – 5 %. +/-0.5%).

This sets a benchmark for evaluating QIFM detecting well logs.

• Mineralogy is highly variable and if poorly defined limits the ability to accurately define the porosity. A full mineralogical well log suite should be acquired in order to accurately reproduce the grain density behavior of the core.

• The compressional sonic velocity when used in conjunction with an accurate and mineralogy independent well log porosity can greatly aid characterization of carbonate texture variations, facies and permeability modeling.

• Pore system variations of facies represent themselves in the flushed to deep zone saturation behavior in this well which is above a water contact and where gas is present.

• The calculated water saturation which is quite probably the irreducible water saturation is strongly correlated to the total amount of QIFM material.

• Core material described with the Archie rock typing scheme showed rapid variation and thin bedding styles throughout the core and high vertical resolution data acquisition is required. Profile permeability data were acquired.

• An additional table of petrographic data was developed for support of the petrophysical rock typing.

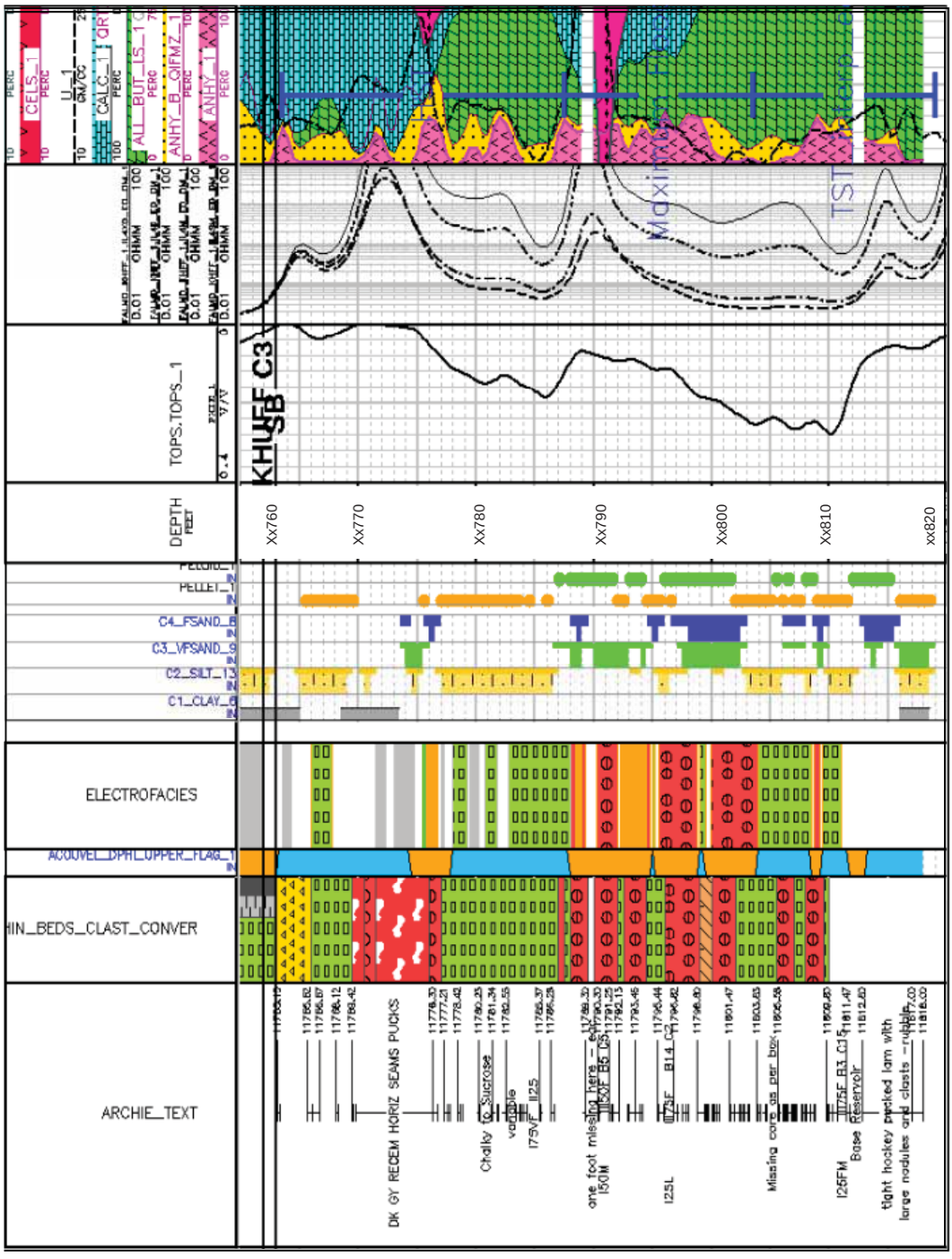

Figure 11 Lower interval of Khuff C core.

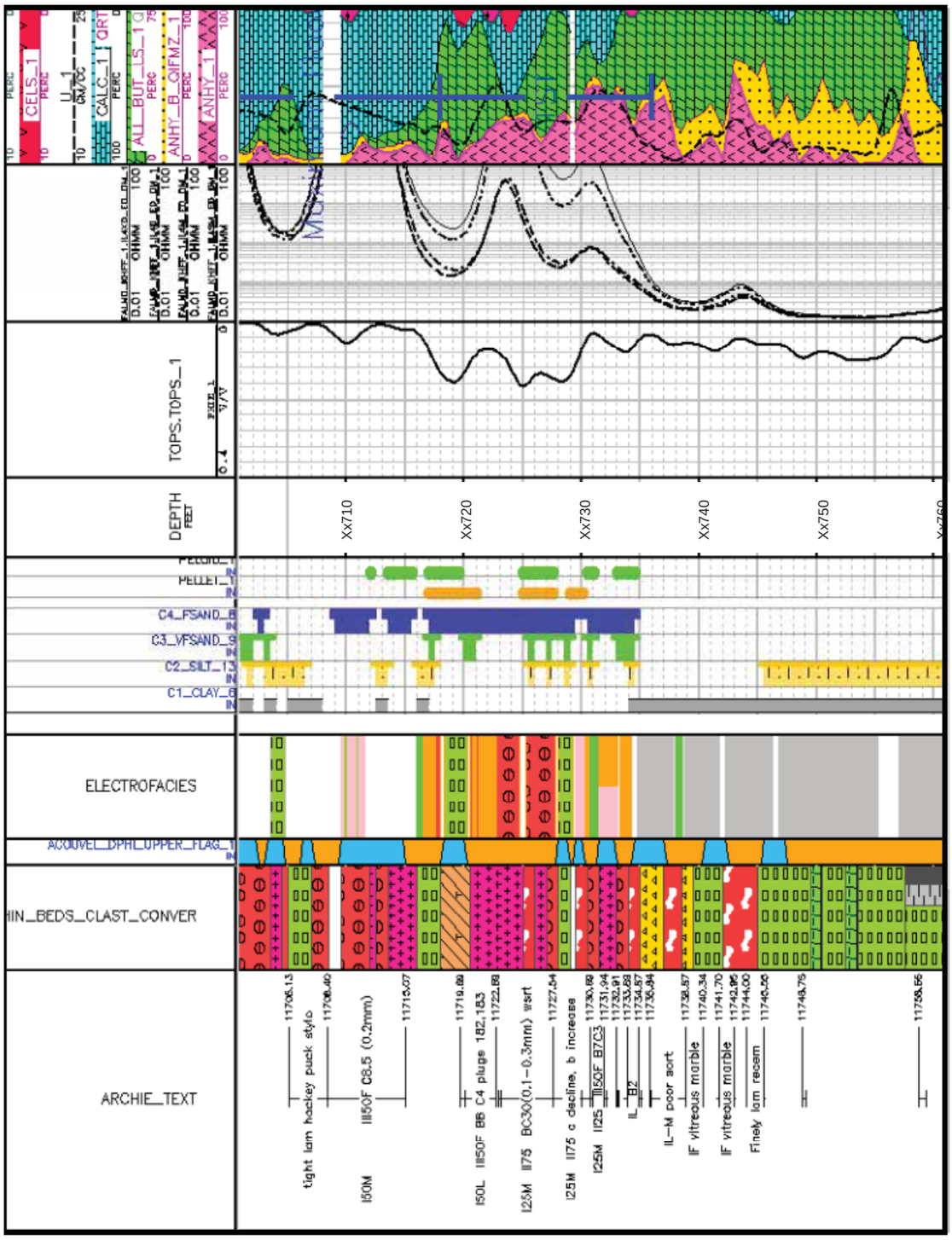

Figure 12 Middle interval of Khuff C core.

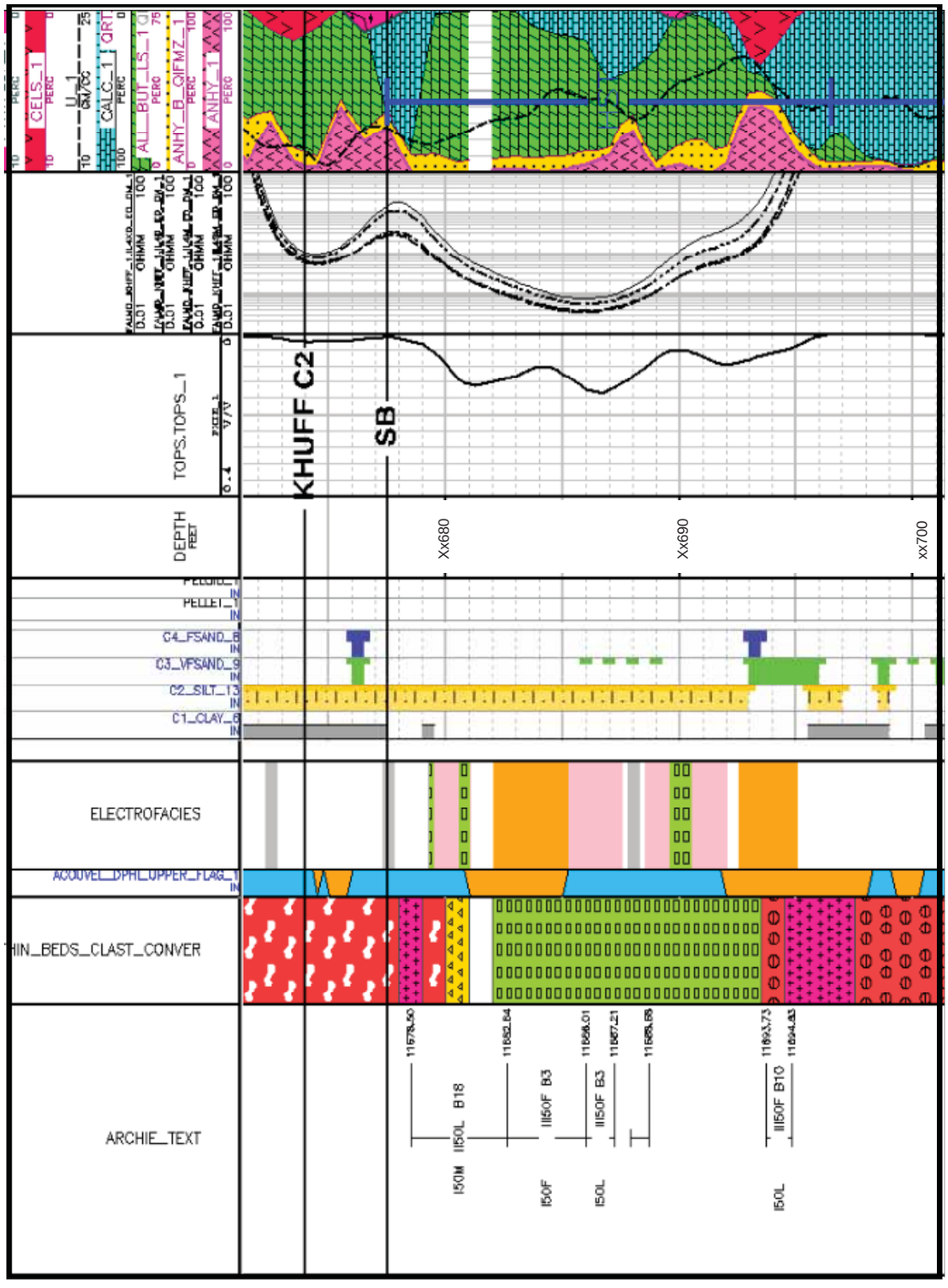

Figure 13 Upper interval of khuff C core.

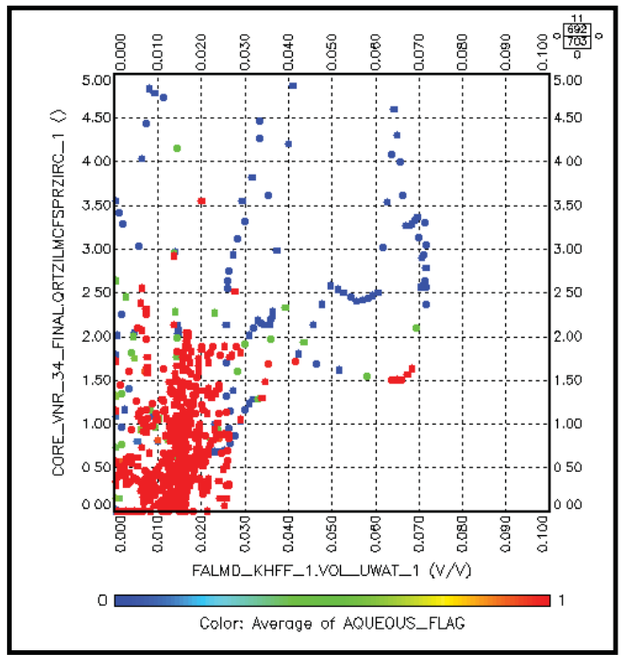

Figure 14 QIFM versus the unflushed zone water volume (UWAT). The Aqueous sediments (red) show a very good trend absent in the Aerial sediments (blue).

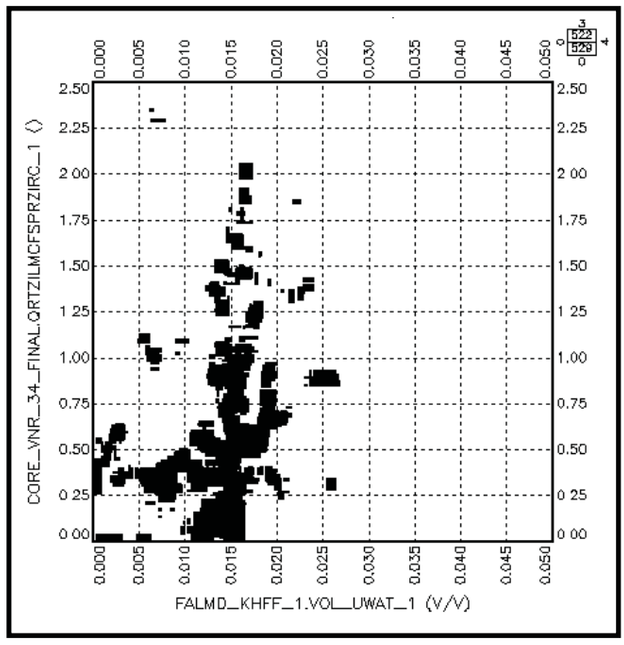

Figure 15 The Aqueous sediments of Figure 14 shown in detail. A very good trend is observed.

References

1. Clerke, E. A., The Khuff PoroLith Study, RCD Report, 2001

2. Dukhayil, Raed, M. S. Thesis.

3. Chamley, Herve, Clay Sedimentology, Springer – Verlag, 1989.

4. Clerke, E. A., Williams, K. W., Pearce, L. A. (1995), The DAK Formation Evaluation Model for the Permian Basin Clearfork, 1993 Best Paper Award of the West Texas Geological Society and published in The Log Analyst, January, p 10-27.

5. Clerke, E. A., The Linearized Sonic Velocity – Porosity Algorithm, unpublished.

Facility Offers Flexibility in Man through Collaboration in Techno

By Paul Sauser

Amin Nasser, SVP Exploration & Production, Saudi Aramco, officially opens the center in the presence of several Schlumberger and Saudi Aramco representatives.

Schlumberger and Saudi Aramco representatives during a tour of the facilities.

DAMMAM – Close collaboration between Saudi Aramco and Schlumberger has resulted in some innovative and effective tools for well completions. And now it has resulted in a new Schlumberger manufacturing plant that will bring business, jobs and expertise to Saudi Arabia.

The new Completions Manufacturing Plant was inaugurated Oct. 5, ready to manufacture three products: single wire-wrap screens with a unique shrink-fit design; inflow control devices for existing producing wells; and injection devices to control the profile of water injection wells add energy to water, gas and CO2 injection.

The devices were developed in part after the two companies came together to address challenges in Saudi Aramco's fields.

"The theme for this event, 'Manufacturing, Technology and Investment in Saudi Arabia,' is indeed an ideal fit for the milestone we are celebrating here today as it mirrors Saudi Aramco's focus on maximum reservoir contact and local content," said Zuhair A. Al-Hussain, vice president of Saudi Aramco Drilling and Workover.

Before an audience that included Amin H. Nasser, senior vice president of Exploration and Producing, and Abdulla A. Al Naim, vice president of Exploration, Al-Hussain elaborated on Saudi Aramco's role in the plant, saying it had "set the stage for advancement in this field through

ufacturing and Custom Design logy Development

L to R: Reservoir Production Group President Doug Pferdehirt, Amin Nasser, and ARM GeoMarket Manager Sherif Foda.

various tests, assessments, technical exchanges and concrete commitment in employing this technology in our fields. In turn, Schlumberger responded with a matching commitment in launching the first Inflow Control Devices manufacturing plant in the Kingdom."

He congratulated Schlumberger on its commitment to Saudi Arabia and to developing local content and talent. "This will bring us one step closer to making Saudi Arabia the home for developing technologies, designing innovative solutions and manufacturing high-tech equipment.

Sherif Foda, vice president and managing director of Arabian GeoMarket of Dhahran, agreed. "This manufacturing facility reinforces our commitment, actually our obligation, to maximize local content and Saudization." He said 2,000 of the company's 3,900 employees are Saudi and that the company is aiming for 70 percent Saudization at this new facility.

And to Saudi Aramco, he said, "A big thank you goes to you, our dear clients, for giving us the opportunity to make this a reality."

Doug Pferdehirt, president of Schlumberger's Reservoir Production Group, based in Houston, said Schlumberger was no stranger to Saudi Arabia, outlining the company's history with the Kingdom, beginning in 1941. Then, he said, "We ran our first wire-line log on Well No. 27 in Dammam Field."

Of the importance of the new manufacturing facility, the first of its kind in the Kingdom, he said, "Local manufacturing capability not only provides additional manufacturing flexibility but also allows the custom design and manufacturing of sand-control systems."

Bringing the manufacturing to the Kingdom, Pferdehirt said, "This will meet the requirements and needs of many fields. It offers, therefore a complete, made-in-Saudi-Arabia solution in a collaborative environment that we believe will be mutually beneficial to operators in the Kingdom as well as for Schlumberger."

His company has invested $25 million in the plant and plans "to be around for a long time." He thanked Nasser and his team "for their encouragement and support, without which we could not be taking part in this celebration today."

Drill Cuttings Re-Injection (CRI) Assessment for the Manifa Field: An Environmentally Safe and Cost-Effective Drilling Waste Management Strategy

By Yousef M. Al-Shobaili, Kirk M. Bartko, Philip E. Gagnard, Mickey Warlick and Ahmad Shah Baim

ABSTRACT

Over the past few decades, environmental regulations for oil and gas companies have become increasingly more stringent to protect and preserve the environment for future generations.

This is particularly true for remote areas and environmentally sensitive terrestrial and marine locations where there is a strong emphasis on protecting natural habitats and resources.

Accordingly, many regulatory agencies have adopted "zero discharge" policies requiring all generated wastes to be disposed of in a responsible manner. For drilling operations, the various waste streams that need to be handled and disposed of properly include: drill cuttings, excess drilling fluid, contaminated rainwater, produced water, scale, produced sand, and even production and cleanup waste. Old practices involve temporary box storage and hauling of the waste products to a final disposal site. Often these sites are several kilometers (km) away from the generation source, creating not only liabilities for the operating company, but also environmental risks from accidental releases and gas emissions that result in higher operating costs.

To address these concerns, waste management technologies have evolved to offer cuttings re-injection (CRI) as a safe and cost-effective alternative that permits the permanent and contained disposal of drilling cuttings in an engineering-determined subsurface formation. Cuttings re-injection provides a secure operation achieving "zero discharge" by injecting cuttings and associated fluids up to several thousand meters below the surface into hydraulically created fractures.

This disposal technique mitigates any surface environmental risks and future liabilities for operating companies.

Saudi Aramco has taken the initiative to utilize CRI as the preferred technology to manage drilling wastes that will be generated in the Manifa field development. To minimize risks associated with CRI and conduct successful injection operations, an Assurance Waste Injection Process was set in place to continuously monitor the operation and plan ahead for any eventuality. Assurance of the injection operation begins during the planning phase with a comprehensive feasibility study based on existing data. Simulations are performed for the anticipated downhole waste domain to ensure containment

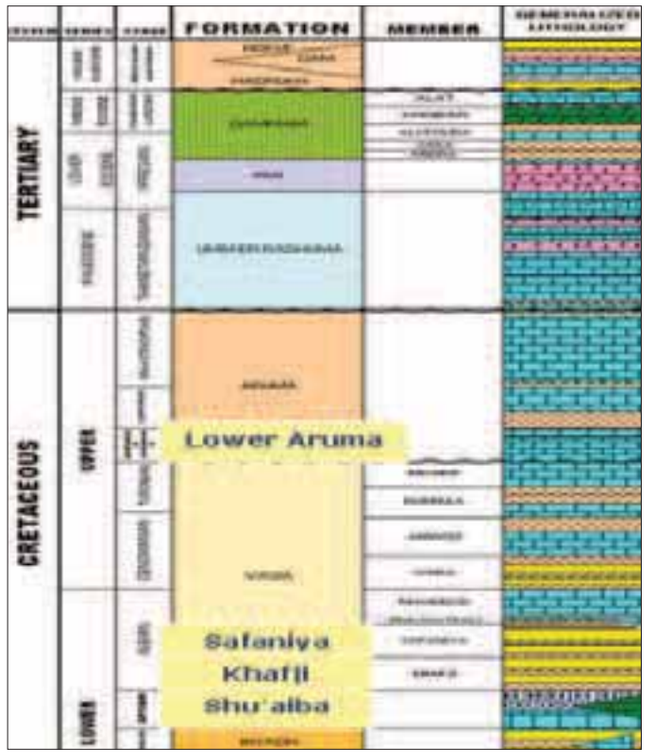

Fig.1. Stratigraphic location.

within the selected formation and permit adequate design of surface facilities for the particular project.

This article describes the various components of the first Saudi Aramco CRI pilot study. These include: reservoir/geomechanical data analysis and interpretation; preliminary geomechanical modeling; target zone selection; test well design, drilling and injectivity testing; and geomechanical model refinement using field injectivity data. The objectives of this study for the Manifa field development project were to evaluate:

• What are the most promising zones for injection based on the geomechanical model?

• Do overlying formations provide effective containment of the injected wastes?

• What are the injection rates, volumes, slurry rheology, and particle size requirements for field testing?

• What were the results of the field injectivity testing at MNIF-ABC?

• What are the long-term, predictive results from recalibration of the geomechanical model?

• What is the well design and completion strategy during the implementation phase?

INTRODUCTION

The Manifa field is an offshore field that lies mainly in shallow water, up to 40 ft in depth. The Manifa field was discovered in 1957 and production began when the Manifa reservoir came onstream in 1964.

The Manifa field is a northwest-southeast trending anticline and measures approximately 28 miles (45 km) in length and 11 miles (18 km) in width. There are six oil-bearing reservoirs in Manifa: Upper Ratawi, Lower Ratawi, Manifa, and Arab-A, B and C/D. The reservoirs for increment development are the two most prolific reservoirs, the Lower Ratawi and Manifa reservoirs, Fig. 1.

The Manifa and Lower Ratawi reservoirs are primarily limestone with occasional dolomitic intervals and generally exhibit high porosity and permeability. The reservoirs were deposited in a shallow marine carbonate platform capped by tight lime mudstones and algal bounds tone facies. A continuous tar mat underlies the oil column in both reservoirs that effectively separates the oil column from the aquifer.

RESERVOIR EVALUATION

The objective of this task was the evaluation and determination of the mechanical and petrophysical properties of the formations and lithologies present in the Manifa area. These data were used to evaluate the suitability of a subsurface formation for safe disposal of waste drilling cutting slurry. This task included detailed analysis and interpretation of available well log data. A detailed reservoir evaluation helped identify the waste containment and fracture barrier capability of a formation above the injection point that could prevent uncontrolled fracture vertical growth.

Geomechanical Model

Evaluation and analysis of appropriate logs were performed to determine elastic modulus, Poisson's Ratio (PR) properties and possible fracture gradients of the different formations. Fluid leak-off coefficients for the disposal formation and other lithologies in the overburden were characterized. The information was employed to formulate the geomechanical model used for the hydraulic fracturing simulations. The simulations are performed to provide containment assurance and predict fracture extent and behavior in the specified conditions.

While modeling the injection zones, important factors were taken into consideration:

• Containment Assurance: The identification of a good containment is crucial for the success of the cuttings re-injection (CRI) operation. The following scenarios provide good indications for the proper storage of cuttings.

• Stress Contrast: The identification of stress contrast between the injection zone and the overburden is important during the selection of tentative injection points. The stress contrast acts as a barrier to avoid uncontrolled vertical growth during the CRI operation.

Additionally, that contrast can reduce the horsepower needed to fracture the formation, and consequently, help to reduce the operational and maintenance cost.

• High Leakoff Zone: Formations with high leakoff in upper layers provide a barrier to prevent uncontrolled vertical growth during the operations. The dehydration of the slurry causes premature screen out on top, which induces the storage of the cuttings in the upper area, and prevents the propagation in a vertical direction.

Identification of the high leakoff zone is important in cases where no stress contrast is identified.

• Lithology: The selection of a candidate injection zone includes the analysis of the lithology composition of the analyzed formations. For CRI operation, it is desirable to inject in a formation that is easy to fracture, that will not have any interaction with the slurry injected, and that possesses a good storage capability that allows the injection of a considerable waste volume. In general, sandstone formations are the most suitable for cuttings disposal. The physical rock properties of sandstone allow easier fracturing compared with shale,.and it is not reactive with the slurry made for the CRI operation. Also, it is important to identify the targeted area containing a proper containment formation above the CRI site. It must have the required sealing properties that assure that the injected waste will remain in the selected area, avoiding any unwanted migration of the slurry injected. These containment zones generally are shales with very low permeability and very high stress levels.

• Reservoir Depth: The location of the interest zone/pay zone needs to be taken into consideration. It is not desirable to have interferences between the "Target" injection zone and the production zone. The feasibility study analyzes and ensures that the waste injection domain will remain away from the reservoir area, to protect the future production of the field.

MECHANICAL PROPERTY LOG

The vertical stress was estimated by integrating the available bulk density with respect to depth. A pore pressure gradient of 0.497 psi/ft was used from 6,000 ft; above 6,000 ft it was assumed a normal pore pressure gradient of 0.433 psi/ft. The minimum horizontal stress was estimated based on the elastic theory, assuming an isotropic environment and no external stresses in the area.

Dynamic measurements of elastic moduli are derived from measuring acoustic velocities and the bulk density of the material. It is important to calibrate the computed dynamic elastic properties of the rock against the static rock properties taken from the actual measurements of the core material being stressed in the laboratory.

Poisson's Ratio

Poisson's Ratio is the ratio of the lateral strain to the longitudinal strain. It represents the amount the sides of a cube are compressed.

Young's Modulus

Young's Modulus (YM) is the ratio of the applied stress to the longitudinal strain or the rock "stiffness." This variable is an important variable as it impacts the fracture geometry.

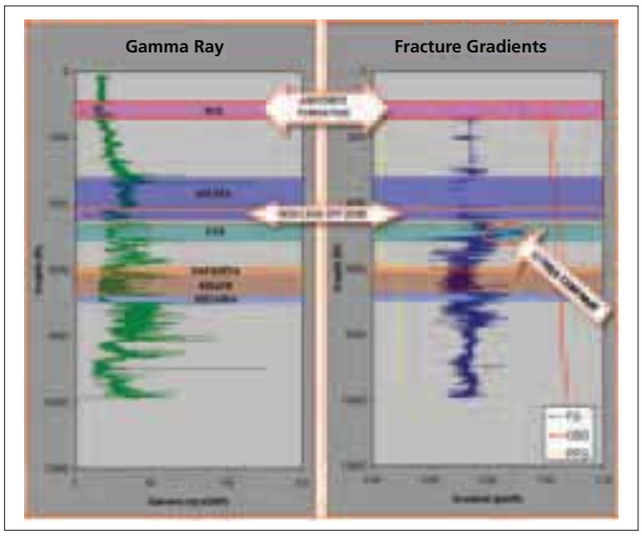

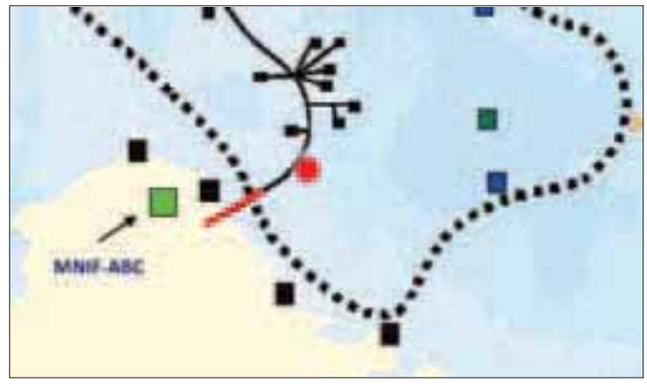

Fig 2 (left). Containment assurance.

Fig 3 (above): MNIF-ABC location.

Dynamic elastic moduli correlations were calibrated against static moduli obtained for the core analysis. As a result of this analysis, the following corrections were made:

Shuaiba Formation:
YMstatic = 0.542*YM-dynamic + 586
PRstatic = 0.665*PR-static + 0.16

Khafji Formation:
YMstatic = 0.8278*YM-dynamic - 667
PRstatic = 0.5348*PR-static + 0.171

Safaniya Formation:
YMstatic = 10.721*YM-dynamic + 300
PRstatic = -1.463*PR-static + 0.549

The MNIF-XYZ compressional and shear sonic log data was used to develop a mechanical property log for estimating fracture height growth and net pressure in the three potential injection intervals: Safaniya, Khafji and Shuaiba formations.

The minimum stress calculated from the sonic data indicates little stress contrast within the formation of interest. This is expected in a high permeability environment having clean, low modulus rock throughout the interval. Because of this little stress contrast, the fracture geometry will be dependent on the Young's Modulus contrast of the formation.

The lithologic characteristics of the lower Aruma shale and Wasia formations suggest these zones are suitable for CRI. A high leakoff area is known to exist, and was identified in the lower part of Aruma where natural fissures occur in the limestone at 4,000 ft. This increase in permeability makes an excellent barrier for preventing uncontrolled fracture height growth. High stress contrast on top of the Lower Aruma Shale (LAS) formation also provides a good containment barrier for the underlying injection zone.

Additionally, a cap rock of anhydrite in the Rus formation ensures the waste would not reach the surface. All these features are presented in Fig. 2.

Based on the analysis discussed, four possible injection points were identified. The bottom of the LAS formation constitutes one of those selected injection zones. This point is located at 5,180 ft under the high stress contrast presented in that area.

This condition would provide fracture height control.

The Safaniya and Khafji members of the Wasia formation also constitute suitable zones for injection purposes. Both formations consist of shaly-sand lithology, and the low fracture gradient (FG) of this type of lithology makes for suitable operations. Two injection points were recognized in the Khafji member at 6,320 ft and 6,730 ft, respectively; however, to take advantage of the entire thickness of the Khafji, injection at 6,730 ft was selected as the main injection point. The injection point at 6,320 ft could provide another suitable place for cuttings disposal in case of any contingency event.

FLUID PROPERTIES

Fluid properties used for the injection model were based on an Aberdeen and North Sea[1] fluid slurry mixture. This fluid is similar in nature to what several other operators

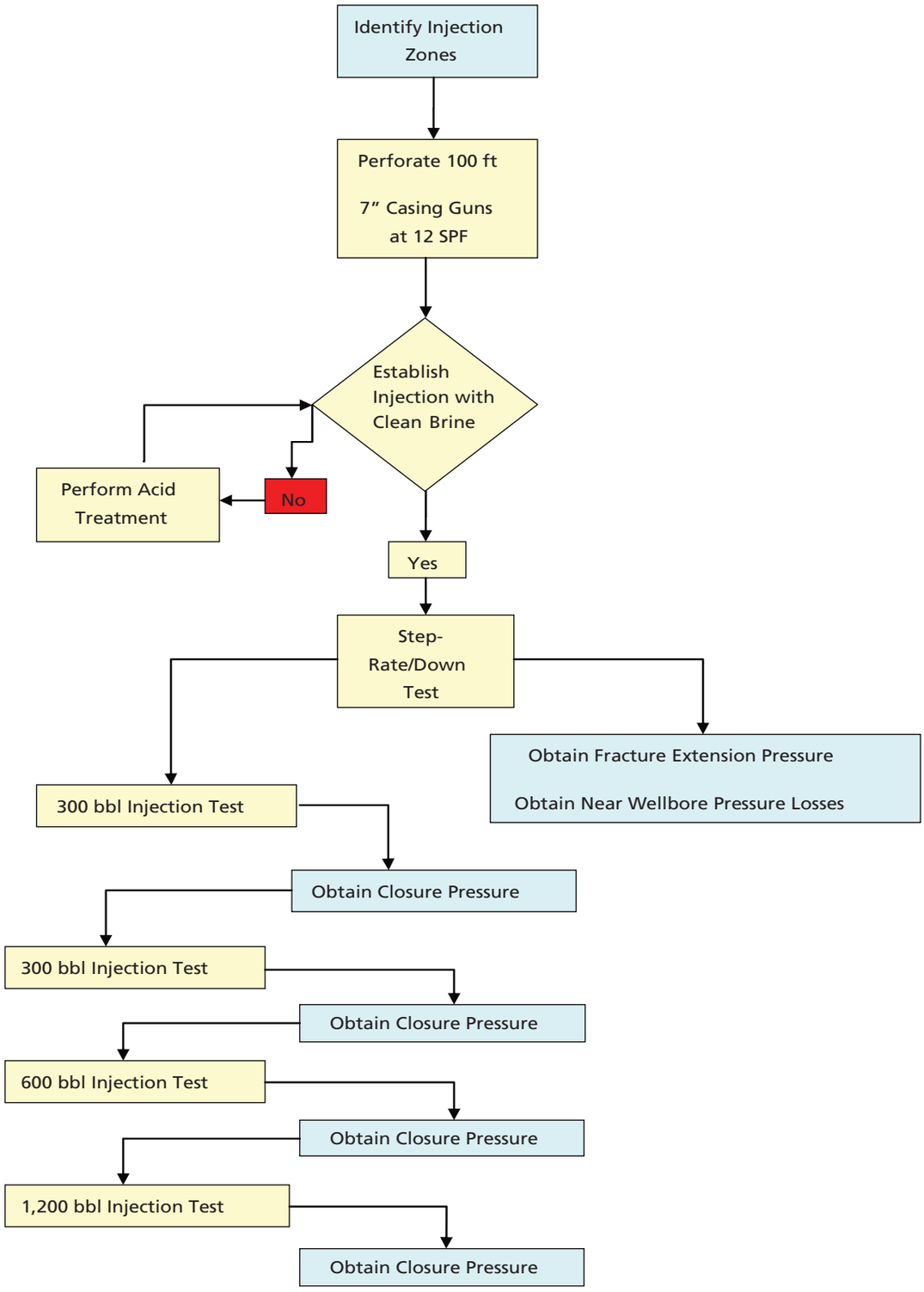

Fig 4. CRI injection test process.

have used in published SPE papers. The requirement of an injection fluid is to have sufficient viscosity to carry the solid cuttings. Table 1 provides the fluid rheology used for this study along with others for comparison.

All fracture models require a fluid with filter cake capabilities that are governed by fluid loss. This number can be calculated in the field based on the fluid efficiency of the total fracture system after the minifrac. This number

would be an average number of the fines concentration in the fracture.

Leakoff tests in the laboratory were performed with actual cuttings. The slurry was xanthum-based polymer with 20% cuttings. Results from the laboratory leakoff tests for the three intervals are shown in Table 2. For the high leakoff zones (i.e., Safaniya and Khafji), the laboratory based leakoff ranged from 0.0005 ft/sq-min to 0.0009 ft/sq-min while the tighter Shuaiba indicated laboratory leakoffs ranging from 0.0003 ft/sq-min to 0.0005 ft/sq-min. Other studies have suggested that slurry leakoff tests for high permeability sands, in both field and laboratory measurements, have leakoff values from 0.004 ft/sq- min to 0.005 ft/sq-min[2, 3]. For low permeability formations, such as shales, the leakoff coefficients range from 0.0005 ft/sq- min to 0.0006 ft/sq-min[4, 5] measured from field slurry tests.

FIELD TEST

MNIF-ABC, a land based well, Fig. 3, was selected to evaluate the feasibility of CRI into selected target zones to determine the most promising zones for injection of drill cuttings from the proposed offshore platform wells. The CRI injection test process, Fig. 4, was applied to the four injection intervals to determine fluid leakoff, minimum stress and fracture extension pressures. The multiple injection tests evaluated short- and long-term injection cycles. These multiple tests provided an understanding of the fluid leakoff characteristic over time, and the injection pressure based on an increase in slurry volume injected into the formation. The multiple injection tests also established an injection rate and pressure history that will be used later to determine the completion strategy: annular vs. tubing injection.

All four formations, with the exception of the Safaniya formation, clearly showed fracture extension and closure pressure based on the step-rate and pressure falloff. Figure 5 shows a typical injection test that was performed. This particular test was in the Aruma formation where three injection tests were performed pumping 300 bbl, 600 bbl and 1,200 bbl at three barrels per minute (bpm).

The injection test in the Safaniya formation was curtailed due to the excessive breakdown pressure and the formation sand flowback into the wellbore. The Shuaiba formation fracture extension pressure and predicted closure pressure was correctly predicted. The Khafji closure pressure prediction was higher than the actual closure pressure, which was probably due to the Khafji being highly permeable and friable. The Aruma calculated clo-

i ield	Sec i ic Gav ity	n	k'	Viscos ity c
Aberdeen Fluid	1.04	0.7	0.0051	71.5
Ekofisk Fluid	1.04	0.22	0.641	1280
Linear #30 HPG	1.04	0.55	0.007	54.3

Table 1. Fluid rheology data.

iorat ion	Ro os ity	Re mab ility md	Le ako Co e icient t /min²	Sut Lo ss g al/100 gal
Safaniya	34	9,500	9.06E-4	7.8
Khafji (Plug 1)	24	2,240	5.62E-4	3.6
Khafji (Plug 2)	24	2,240	8.19E-4	2.5
Shuaiba (Plug 1)	16	0.5	3.21E-4	1.6
Shuaiba (Plug 2)	16	0.5	5.52E-4	0

Table 2. Laboratory based fluid leakoff and spurt loss

Table 2. Laboratory based fluid leakoff and spurt loss.

Formation	Maximum Surface Pressure (psi)	Extension Pressure (psi)	Fracture Extension Pressure Gradient (psi/ft)	Fracture Closure Pressure (psi)	Fracture Closure Pressure Gradient (psi/ft)	Predicted* Fracture Closure Pressure (psi)	Predicted* Fracture Closure Pressure Gradient
Aruma	2,000	4,125	0.86	4,083	0.83	2,757	.71
Khafji	2,800	4,557	0.69	3,828	0.58	4,578	0.71
Shuaiba	2,800	5,610	0.79	NA**	NA**	5,391	0.79

Table 3. Pressure analysis results
*** MNIF XYZ MI study prediction**
**** Pressure falloff time was not sufficient**
***** All pressures are bottom-hole unless identified as surface**

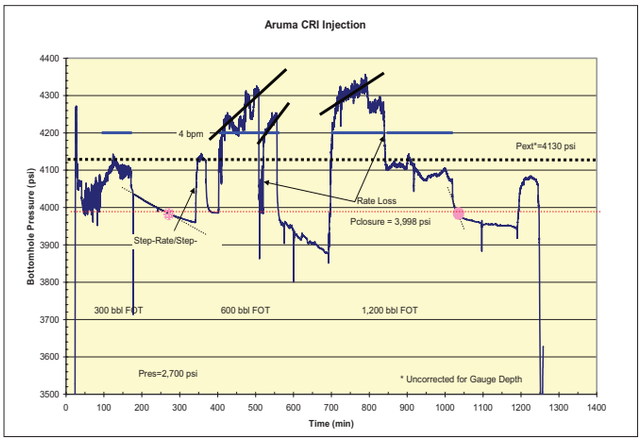

Fig 5. Aruma CRI injection test.

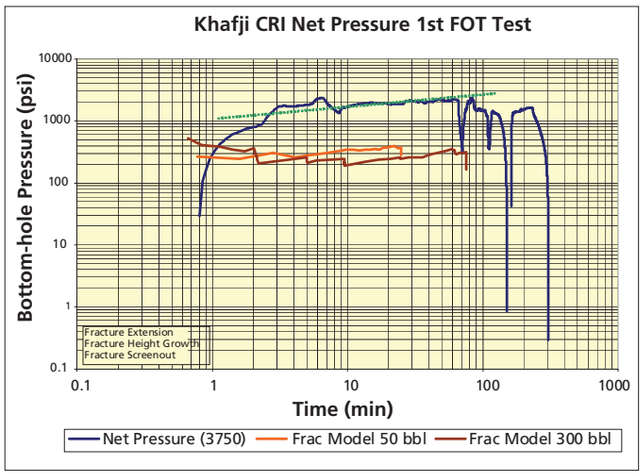

Fig 6. Khafji net pressure match – Lower net pressure is related to fracturing soft unconsolidated sandstone formation.

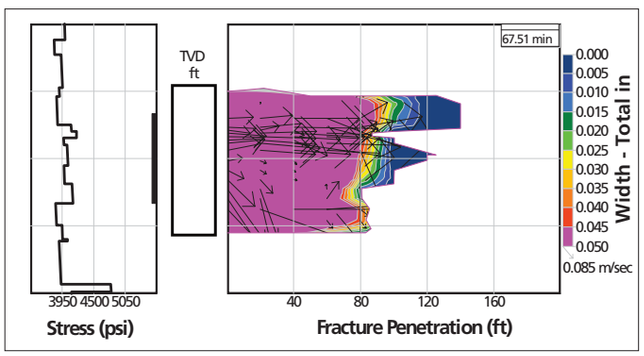

Fig 7. Fracture geometry prediction after 300 bbl slurry injected in MNIF-XYZ.

sure pressure was higher than predicted. The complete results of the pressure analysis based on the injection tests are tabulated in Table 3.

FRACTURE MODEL PRESSURE MATCHING DISCUSSION

The modeling effort to determine the fracture geometry of the cuttings was performed with a fully three dimensional fracture model. The model is a fully numerical solution for two dimensional fluid-flow/proppant-transport calculations and a rigorous Finite Element Method (FEM) solution for fracture width/propagation in a layered formation with varying moduli. Net pressure matching was performed on all three successful injection zones. The Aruma and Shuaiba formation resulted in the best pressure match, requiring minimal change to the geomechanical model developed for these two formations. The Khafji net pressure match was the most difficult and resulted in only capturing the trend and not the absolute value, Fig. 6. Further work needs to be done in the fracture model to compensate for the soft rock fracturing and possible filtration of the slurry within the porous media.

Formation	Fracture Height Containment (100 ft perforated interval)	Fracture Length (ft)
Aruma	Yes	250 - 300
Khafji	Yes	50 - 100
Shuaiba	Yes	30 - 50

Table 4. Fracture model geometry prediction – 300 bbl injection period.

Figure 7 shows the resulting fracture geometry based on this match. The fracture stayed contained within the perforated interval and resulted in a fracture length of 50 ft to 100 ft. No post diagnostics were performed after the slurry injections to confirm the fracture height; however, the net pressure plot indicates the fracture stayed contained, and grew laterally based on the positive pressure gain throughout the slurry injection.

Table 4 is a compilation of the predicted geometries for the three injection zones. All three zones showed containment within the perforated interval and fracture lengths that ranged from 30 ft to 300 ft. The Aruma was a much harder formation and showed the greatest length of 350 ft.

COMPLETION STATEGY

The offshore Manifa wells will require the wellbore to be at a high angle (< 30°) through the proposed injection zone target to reach the well's primary objective in the Manifa and Lower Ratawi formation. The well will be drilled in a spider pattern, resulting in a quantity of the wells oriented in the wrong direction to the maximum stress. Incorrect well orientation would result in excessive treating pressures and multiple fracture generations. To reduce these impacts, plus the possibility of the cuttings falling out on the low side of the pipe, it

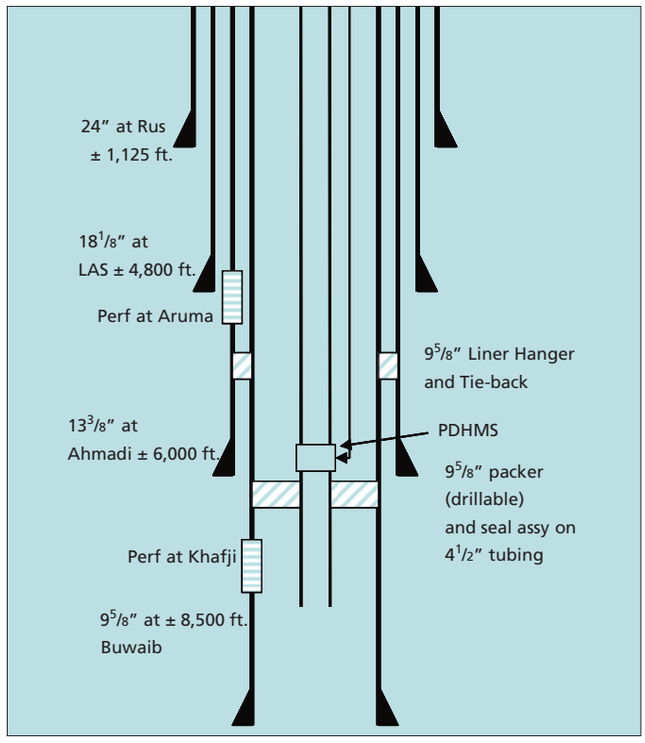

Fig 8. Planned MNIF CRI well completion.

was recommended that the slurry be pumped down the tubing string vs. annular injection. The tubing injection reduced the risk of not being able to inject in this interval over time. This provides the opportunity to clean out the pipe with coiled tubing and add additional perforations if the formation will not accept slurry.

The final proposed well design provides a well where the slurry can be injected down into the 4½" tubing, and then down the backside into the Aruma formation, if the Khafji fails to accept all the slurry material, Fig. 8. The injection wells will be at an inclination of not more than 30° across the injection zone with a minimum separation of 800 ft from nearby wells at the injection zones, and it will be possible to resume drilling to the downhole target upon completion of the planned wells on the platform. The cuttings injection at this time will be injected through the annular into the Aruma formation. In addition, the completion includes a real time downhole pressure gauge for the Khafji formation, to observe pressure changes during the injection cycles.

CONCLUSIONS

1. Three possible injection zones were identified based on integrating log data, core data and geomechanical data: the LAS formation, and the Safaniya and Khafji, both members of the Wasia formation.

2. CRI pilot field testing at MNIF-ABC was successful, and all the three selected injection zones can provide suitable capacity for drill cutting disposal.

3. Tubing injection can be performed in all CRI zones with no problems about containment and uncontrolled fracture growth.

4. The presence of high leakoff zones in the lower part of Aruma provides assurance to control the risk of uncontrolled height growth.

5. The cap rock in the Rus formation and the high stress contrast in the LAS formation offer additional containment assurance.

6. The geomechanical model is based on inferred parameters and correlations. The validation of the model is applicable only in a certain region where it is assumed uniform properties exist.

7. It is recommended the calibration of the geomechani-

cal model, with the proper injectivity test, be completed before the beginning of the CRI operations, especially if the injector well is far away from the wells analyzed in this report.

8. CRI well design must consider fracture pressures and injectivity potential.

ACKNOWLEDGMENTS

The authors wish to thank Saudi Aramco management for their support and permission to present the information contained in this article. We also would like to acknowledge contributions from the Manifa CRI Team Members for their valuable input in making this a successful test, and to Drilling and Workover for executing the slurry injection testing program.

REFERENCES

1. Nagel, N.B. and Strachan, K.J.: "Implementation of Cuttings Reinjection at the Ekofisk Field," ISRM/SRM paper 47218, presented at the ISRM/SRM Eurock, Trondheim, Norway, July 8-10, 1996.

2. Sassen, A., Tran, T.N., Joranson, H., Meyer, E., Gabrielsen, G. and Tronstad, A.E.: "Subsea Re-Injection of Drilled Cuttings – Operational Experience," SPE paper 67733, presented at the SPE/IADC Drilling Conference, Amsterdam, The Netherlands, February 27 - March 1, 2001.

3. Guo, Q., Geehan, T. and Ulyott, K.W.: "Formation Damage and its Impact on Cuttings Injection-Well Performance: A Risk-Based Approach on Waste Containment Assurance," SPE paper 98202, presented at the SPE International Symposium and Exhibition on Formation Damage Control, Lafayette, Louisiana, February 15-17, 2005.

4. Guo, Q., Dutel, L.J., Wheatley, G.B. and McLennen, J.D.: "Assurance Increased for Drilling Cuttings Re-Injection in the Panuke Field Canada: Case Study of Improved Design," IADC/SPE paper 59118, presented at the IADC/SPE Drilling Conference, New Orleans, Louisiana, February 23-25, 2000.

5. Wilson, S.A., Rylance, M. and Last, N.C.: "Fracture Mechanics Issues Relating to Cuttings Re-Injection at Shallow Depth," SPE paper 25756, presented at the SPE/IADC Drillling Conference, Amsterdam, The Netherlands, February 23-25, 1993.

Biographies

Yousef M. Al-Shobaili is currently the Northern Onshore Fields Group Leader at the Reservoir Characterization Department. He joined Saudi Aramco in 1994 after receiving his B.S. degree in Petroleum Geology and Sedimentology from King AbdulAziz University, Jiddah, Saudi Arabia. During his career he has worked in several disciplines of the Exploration and Petroleum Engineering organizations. Yousef's experience covers several reservoir aspects, including reservoir evaluation and assessment, reservoir management and engineering assessment, petrophysical integration, reserves estimation and assessment, identifying new hydrocarbon from old fields, drilling operations and well planning, reservoir description, geomechanics and wellbore stability, log analysis and interpretation, and core description and integration. He has also trained several summer students, geologists, geophysicists, and reservoir engineers, and he developed an in-house log interpretation and petroleum geology training course. Yousef has authored and co-authored 18 technical papers in reservoir evaluation, reservoir description, geosteering, rock mechanics, reservoir management and dynamics and log/core petrophysics. He is the founder and the first president of the Saudi Petrophysical Society (SPS). Yousef attended and passed an intensive six month petrophysical and log evaluation Schlumberger program. He was the first worldwide non-Schlumberger employee to ever join this program.

Kirk M. Bartkois a Senior Petroleum Engineering Consultant with Saudi Aramco's Petroleum Engineering Support Division. He received his B.S. degree in Petroleum Engineering from the University of Wyoming, Laramie, WY. Kirk joined Saudi Aramco in 2000 and he supports stimulation and completion technologies across Saudi Arabia. His experience includes 19 years with ARCO with various global assignments including Texas, Alaska, Algeria, and the Research Technology Center supporting U.S. and international operations. Kirk has authored and co-authored more than 36 technical papers on well stimulation, holds a patent on monitoring fracture pressures, and has been actively involved in the Society of Petroleum Engineers (SPE) since 1977.

Philip E. Gagnard is a Petroleum Engineering Specialist with the Drilling & Workover Services Department (D&WOSD). Currently, he is the team leader for the Manifa Cuttings Re- Injection (CRI) Project and an active member in the Manifa onshore waste management efforts. In 1970, Philip received his B.S. degree in Mathematics and in 1972 his M.S. degree in Ground Water Hydrology from the University of Illinois, Chicago, IL. Earlier in his career, 1982-1986, he worked with the Saudi Aramco Hydrology Department. In 2000, Philip re- joined Saudi Aramco working with the Environmental Protection Department. He has 30+ years of diversified environmental and waste management experience across the oil production, solid and hazardous waste, transportation and consulting industries. Philip's career has focused on groundwater resource impact evaluation, contaminant assessment, site remediation, terrestrial and marine hydrocarbon impacts, solid/hazardous waste management, waste treatment technologies, oil and gas industry waste issues, and regulatory compliance.

Mickey Warlickis a Petroleum Engineering Specialist with the Manifa Reservoir Management Division and has been with Saudi Aramco for 7 years. In 1981, he received his B.S. in Petroleum Engineering from the New Mexico Institute of Mining and Technology at Socorro, NM. Mickey joined Chevron USA Inc., and began work as a Reservoir Engineer in the Permian Basin located in west Texas and eastern New Mexico. There, he worked on diverse reservoirs ranging from shallow 2,000 ft oil reservoirs to 30,000 ft deep gas reservoirs. Mickey gained experience in working on primary, secondary and even CO2tertiary processes. He then moved to the Over Thrust area of Wyoming where he gained firsthand experience in dealing with 20% H2S gas reservoirs that required utmost safety in drilling and workover operations. Later Mickey moved on to La Habra, CA where he worked in Chevron's international operations developing and deploying new field technologies Just before his move to Saudi Arabia, Mickey transferred to Houston, TX where he worked as a Reservoir Simulation Engineer in Chevron's International Reservoir Simulation department. While in Houston, he earned his M.S. degree in Petroleum Engineering from the University of Houston, Houston, TX in 2001. Mickey joined Saudi Aramco in 2002, working as a Reservoir Engineer in the Zuluf field. When Saudi Aramco decided to bring the Manifa field on as one of its major increments, he was transferred there and is currently Team Leader for the Manifa reservoir of the Manifa field development.

Ahmad Shah Baim is a Senior Drilling Engineer in Saudi Aramco and was fully involved in the planning of the Manifa Offshore Drilling program. He joined Saudi Aramco in 2005 and has 19 years of experience in the oil and gas industry. In 1988, Ahmad received his B.S. degree in Mechanical Engineering from Gannon University, Erie, PA.

Enhanced Oil Recovery Techniques and CO_2 Flooding

By Mojsin Al-Jarba, Drilling Supervisor Assistant LUKOIL Saudi Arabia Energy, and Bandar Duraya Al-Anazi, Research Assistant ,King Abdulaziz City for Science & Technology

Introduction

Over the years, interest in enhanced oil recovery (EOR) has been tempered by the increase in oil reserves and production. Many techniques have been investigated in the laboratory and the field for improving oil recovery. The discovery of major oil fields in the world added large volumes of oil to the worldwide market. In addition, estimates of reserves from reservoirs in the Middle East increased significantly, leading to the expectation that the oil supply will be plentiful. Although large volumes of oil remain in mature reservoirs, the oil will not be produced in large quantities by EOR processes unless these processes can compete economically with the cost of oil production from conventional sources. Thus, as reservoirs age, a dichotomy exists between the desire to preserve wells for potential EOR processes and the lack of economic incentive because of the existence of large reserves of oil in the world. During the life of a well, oil recovery has three stages or categories which are:

1-Primary Oil Recovery
2-Secondary Oil Recovery
3-Tertiary Oil Recovery

Crude oil development and production from oil reservoirs can include up to three distinct phases: primary, secondary, and tertiary (or enhanced) recovery. During primary recovery, the oil is recovered by the natural pressure of the reservoir or gravity drive oil into the wellbore, combined with artificial lift techniques (such as pumps) which bring the oil to the surface. But only about 10 percent of a reservoir's original oil in place is typically produced during primary recovery. Secondary recovery techniques to the field's productive life are generally include injecting water or gas to displace oil and drive it to a production wellbore, resulting in the recovery of 20 to 40 percent of the original oil in place. However, with much of the easy-to-produce oil already recovered from oil fields, producers have attempted several tertiary, or enhanced oil recovery (EOR), techniques that offer prospects for ultimately producing 30 to 60 percent, or more, of the reservoir's original oil in place. Three major categories of Enhanced Oil Recovery have been found to be commercially successful to varying degrees:

• Thermal recovery, which involves the introduction of heat such as the injection of steam to lower the viscosity of the heavy viscous oil, and improve its ability to flow through the reservoir.

• Gas injection, which uses gases such as natural gas, nitrogen, or carbon dioxide that expand in a reservoir to push additional oil to a production wellbore, or other gases that dissolve in the oil to lower its viscosity and improves its flow rate. Gas injection accounts for nearly 50 percent of EOR production.

• Chemical injection, which can involve the use of long-chained molecules called polymers to increase the effectiveness of waterfloods, or the use of detergent-like surfactants to help lower the surface tension that often prevents oil droplets from moving through a reservoir (Gozalpour, 2005).

CO_2 FLOODING

CO_2 flooding is an effective enhanced oil recovery process. It appeared in the 1930s and had a great development in the 1970s. Over 30 years' production practice, CO_2 flooding has become the leading enhanced oil recovery technique for light and medium oils. It can prolong the production lives of light or medium oil fields nearing depletion under waterflood by 15 to 20 years, and may recover 15–25% of the original oil in place (Hao, 2004).

The phase behavior of CO_2 / crude- oil systems has been investigated extensively since the 1960s. This attention was at its peak in the late '70s and early '80s, at the onset of many CO_2 miscible flooding projects and higher

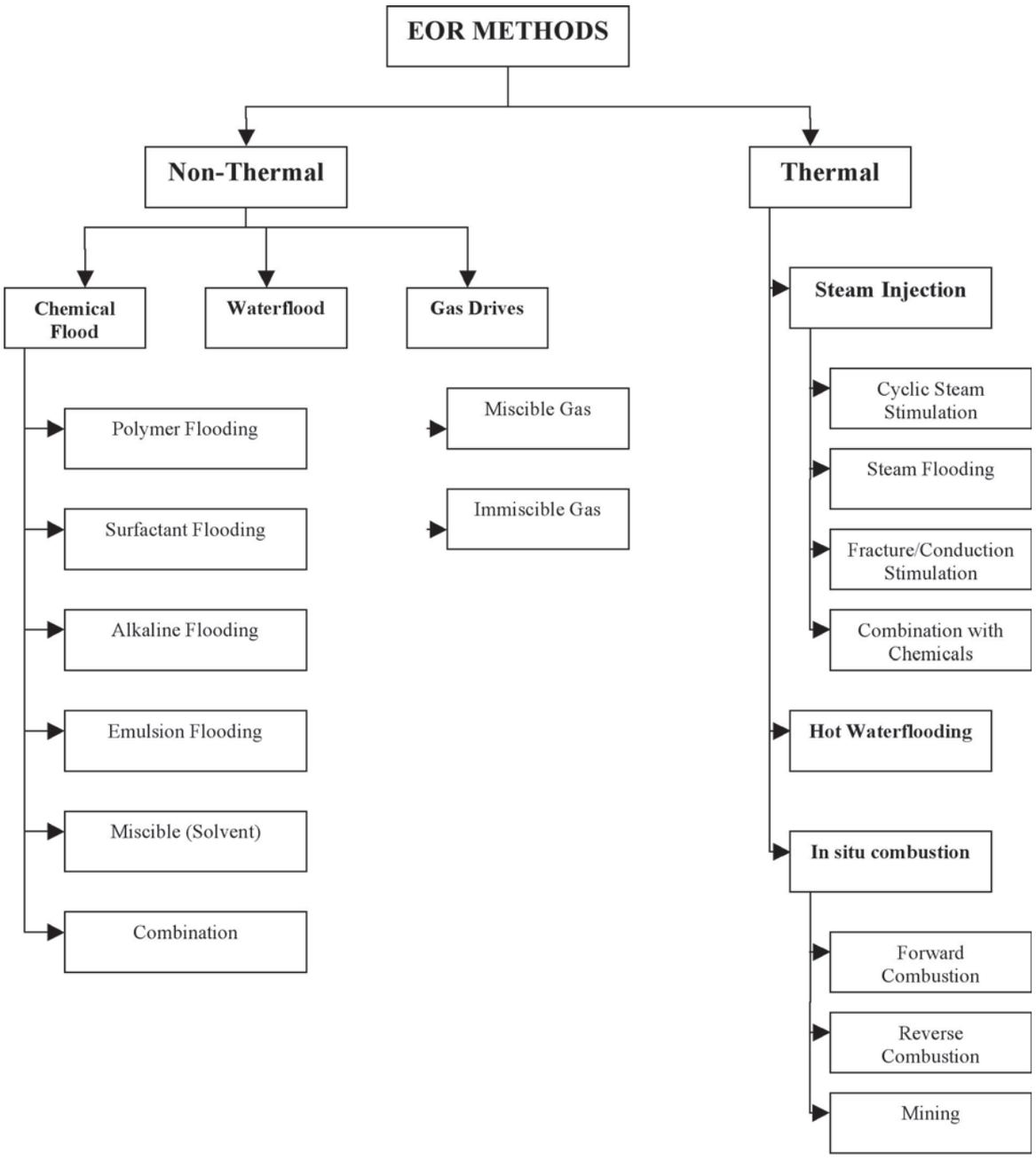

EOR Methods (After Sarma, 1999)

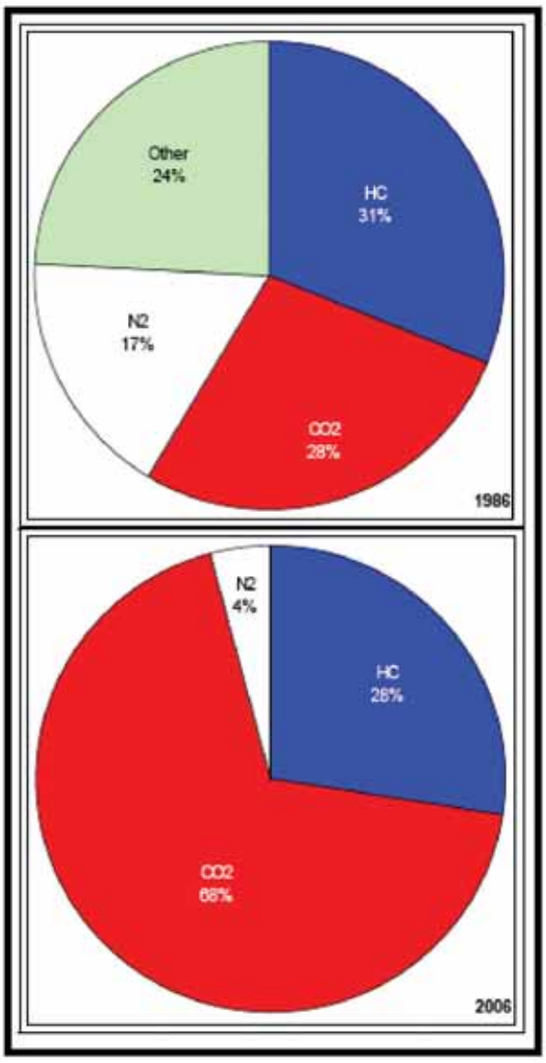

Fig.1. The changing Mix of Gas Injection EOR (Moritis, 2006).

oil prices. Interest continues as new projects come on stream and earlier projects mature. Studies to understanding the development, and prediction of the MMP for both pure and impure CO_2 injection have been ongoing for over thirty years. (Quinones et al, 1991)

Various attempts with the target of developing methods for measuring and calculating the MMP exist in the literature. Many of these are based on simplifications such as the ternary representation of the compositional space. This has later proven not to honor the existence of a combined mechanism controlling the development of miscibility in real reservoir fluids. Zick (1986) and subsequently Stalkup (1987) described the existence of a vaporizing/condensing mechanism. They showed that the development of miscibility (MMP) in multicomponent gas displacement processes could, independent of the mechanism controlling the development of miscibility, be predicted correctly by 1 dimensional (1D) compositional simulations. A semi-analytical method for predicting the MMP was later presented by Wang and Orr (1997) who played an important role in the development and application of the analytical theory of gas injection processes (Jessen et al, 2005).

Carbon Dioxide as a displacement fluid

Carbon dioxide is one of the most plentiful and useful compounds found on the earth. In 1952, Whorton et al., by using CO_2 they received the first patent for oil recovery (Klins, 1984).

Advances in CO_2 Flooding technology during the 1960s and 1970s added considerably to our knowledge of CO_2 displacement mechanisms. A 1982 survey revealed a 65% increase in the number of CO_2 projects over 1980. (Holm, 1982)

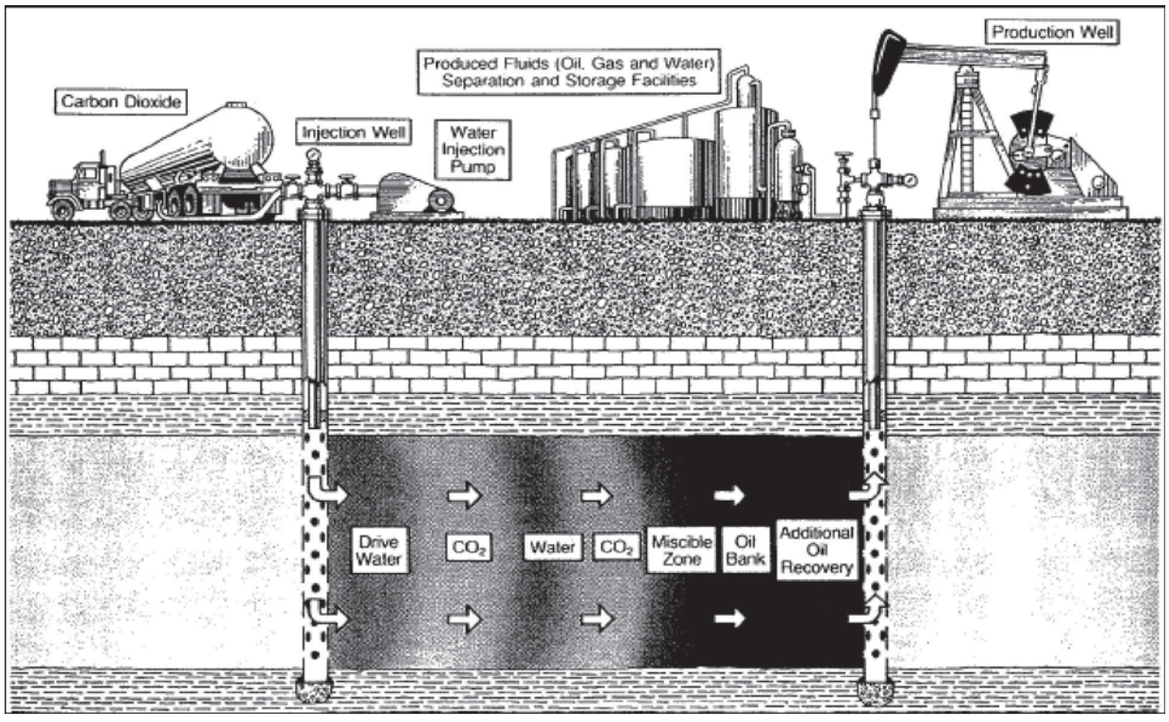

CO_2 miscible process (Green and willhite,1998).

For CO_2-miscible flooding	
Oil gravity °API	Depth must be greater than: Feet
>40	2500
32-39.9	2800
28-31.9	3300
22-27.9	4000
<22	Fails miscible, screen for immiscible
For immiscible CO_2 flooding	
13-21.9	1800
<13	All oil reservoirs fail at any depth

Table 1. Depth vs. Oil gravity screening criteria for CO_2 flooding (Jiahang, 2003).

As of the latest (2006) EOR survey published biannually is the Oil and Gas Journal, gas injection has become the largest EOR process in the U.S., displacing the long reigning thermal processes. Enhanced oil Recovery (EOR) activities in the United States account for nearly 13% of the U.S. domestic production (Petroleum navigator, 2006) .

The change in the U.S. EOR application and distribution scenario from 1986 to 2006 are shown in Figure 1, which shows the dynamics of the various gas injection EOR processes; the current U.S. dominant EOR method in the U.S., and this figure clearly indicate that with the exception of CO_2 and HC processes, the share of all the other EOR processes, has significantly decreased or reduced to zero in the last two decades. The share of CO_2 and hydrocarbon gas processes has nearly doubled in two decades. Further scrutiny of the gas injection EOR performance shows that within the last twenty years the miscible CO_2 projects have increased from 28 in 1984 to 80 in 2006 and their production during the same time period has grown by more than 7 folds from 31,300 BPD to 234,420 BPD in 1984 to 124,500 BPD in 2000 in spite of their decreasing numbers. However,

Carbon dioxide injection process	Reservoir criteria	Oil recovery mechanisms
Low pressure applications	Pressures less than 1000 psia Shallow and viscous oil fields where water or thermal methods are inefficient	Oil swelling and viscosity reduction
Intermediate pressure, high temperature applications	1000<p<2000 to 3000 psia up to reservoir temperature	Oil swelling, viscosity reduction and crude vaporization
Intermediate Pressure, Low Temperature (<122°F) Applications	1000<p<2000 to 3000 psia 00<p Temperature <122°F	Oil swelling, viscosity reduction and blow down recovery
High Pressure Miscible Applications	Pressure greater than 2000 to 3000 psia	Miscible displacement

Table 2. Dominated displacement characteristics for carbon dioxide displacement process. (Klins, 1984)

this trend has been reversed since 2002, and the EOR production from hydrocarbon gas floods has currently decreased to 95,800 BPD, perhaps due to the increasing price of natural gas (Moritis, 2006)

Advantages and disadvantages of carbon dioxide injection

When oil and water contain a significant amount of dissolved carbon dioxide their viscosities, densitiesand compressibilities are modified in a direction which helps increase the oil recovery efficiency. Therefore, the use of carbon dioxide in oil recovery should be considered where carbon dioxide is available in sufficient quantities and is economically priced. (Gozalpour et al, 2005)

Advantages, which gathered with carbon dioxide flooding, are:

- Miscibility can be attained at low pressures
- Displacement efficiency is high in miscible cases
- This process aids recovery by solution gas drive
- It is useful over a wider range of crude oils than hydrocarbon injection methods
- Miscibility can be regenerated if lost. (Amarnath, 1999)

The miscible carbon dioxide process is primarily used for medium and light crude oils. In the case of immiscible carbon dioxide displacement, advantage is taken of the swelling of the crude oil and the reduction in the crude oil viscosity upon carbonation. Because of high solubility of the carbon dioxide in the crude oil, for reservoirs containing highly under saturated crude oils or heavy oils, the benefits of immiscible carbon dioxide flooding are also significant. (Taber et al, 1996)

Disadvantages, which restrict this method, can be categorized as follows:

- Availability of carbon dioxide resources
- Transportation costs
- Under certain conditions, poor sweep and gravity segregation can be obtained
- Corrosion
- Necessity of produced gas recycling. (Amarnath, 1999)

Reservoir screening criteria for carbon dioxide injection

There are several publications for screening reservoirs with potential of CO_2 flooding. These screening guidelines are very broad and are intended only to help iden-

tify candidate reservoirs that might warrant more thorough evaluation to assess their CO_2 miscible flooding suitability. These guidelines can be summarized in Table1. (Taber et al,1996)

For a reservoir to be a CO_2-miscible flooding candidate, miscibility pressure must be attainable over a significant volume of the reservoir. Miscibility pressure for CO_2 often is significantly lower than the pressure required for miscibility with natural gas, flue gas, or nitrogen. The high pressure required for dynamic miscibility limits opportunities for miscible flooding with these gases. (Klins, 1984) However, this often is not the case with CO_2 and its miscibility can be attained at shallower depths for a much wider spectrum of oils.

Miscibility pressure usually increases with decreasing oil gravity. Reservoirs containing oils with gravities lower than about 22°API generally can't be CO_2-miscible flood candidates. Reservoirs shallower than about 2,500 ft can't usually be a candidate because at this shallow depth even a relatively low miscibility pressure cannot be attained without fracturing the reservoir (Klins, 1984).

Reservoir heterogeneity is also another parameter, which determines the suitability of a reservoir for CO_2 flooding. Water-flood history, geology, logs, and well transient tests can be indications of reservoir heterogeneity.

Oil displacement strongly depends on factors, which are related to the phase behavior of CO_2-crude oil mixtures. Reservoir's temperature and pressure and crude oil composition are the main agents in this respect. Dominated displacement characteristics for a given CO_2-displacement falls into one of the four regions as shown in the Table 2 (Klins, 1984).

Because of carbon dioxide low viscosity, the viscosity ratio with reservoir oils invariably will be unfavorable. Therefore the mobility ratio of the displacement will be unfavorable unless the CO_2 relative permeability is sufficiently reduced by alternate water injection, semisolid or heavy-liquid precipitation, or other factors to keep the mobility ratio favorable. Unfavorable mobility ratio adversely affects sweep-out and can hasten CO_2 slug destruction in the gas-driven slug process by viscous fingering. For these reasons, reservoirs containing oils of relatively high viscosity are not suitable candidates for CO_2-miscible flooding (OTA, Jan., 1978).

As in the case of hydrocarbon-miscible flooding, severe reservoir heterogeneity causing excessive production of CO_2 is to be avoided. Although some CO_2 production is to be expected even in the best-performing floods and although compression and re-injection of produced CO_2 may be economically sound in specific projects, severe channeling caused by extreme stratification or fracturing can reduce the ratio of oil recovered per gross cubic foot of CO_2 injected to an uneconomical value, and reservoirs with these characteristics should be avoided. As the hydrocarbon-miscible processes, economic factors determine the minimum oil saturation, which accepted for CO_2 flooding. However, as a rough guideline, oil saturation should not be less than about 20%. (Oskouie and Nezhad, 2004)

Future Development

Enhanced oil recovery from CO_2 flooding is expected to continue to increase in future years under most world oil price scenarios. As part of the U.S. Department of Energy's Oil and Gas supply Model, which forecast future oil and gas production in the United States, Advanced Resources developed and enhanced oil recovery sub module that specifically assesses the economics of CO_2 – EOR projects in the United States. The field-based economic model evaluates the production costs of existing CO_2 – EOR project in the U.S., as well as the development costs for expanding CO_2 flooding into new depleted oil fields, providing the ability to systematically forecast future EOR production. Alaskan CO_2 – EOR production, which is not simulated in this model, was assumed to remain constant at the current level of about 2,400 m^3 /day (15,000 BOPD) (Stevens and Kuskra, 1997).

References

Alston, R.B., Kokolis, G.P. and James, C.F., CO_2 Minimum Miscibility Pressure; A correlation for Impure CO_2 Streams and Live Oil Systems; SPEJ, pp 268-274, April, 1985

Dake, L.P., Fundamentals of Reservoirs Engineering, Elsevier Science B.V. 1978

Emera, M.K., Sarma, H.K. Genetic Algorithm (GA) – based Correlations offer More Reliable Prediction of (MMP), Canadian International Petroleum Conference, Calgary, Alberta, Canada, June 7 – 9, 2005

Emera, M.K., Sarma, H.K. Genetic Algorithm (GA)-based Correlations offer More Reliable Prediction of CO_2 Oil Physical Properties, Canadian International Petroleum Conference, Calgary, Alberta, Canada, June 13 – 15, 2006

Gozalpour, F., Ren, S.R and Tohidi, B. CO_2 EOR and Storage in Oil Reservoirs Oil & Gas Science and Technology; Rev. IFP, Vol. 60, No.3, pp. 537 546, 2005

Holm, L.W. and Josendal, V.A., Mechanisms of oil displacement by carbon dioxide; JPT, 1427-1438, 1974

Kuo, S.S, ARCO Resources Technology Predication of Miscibility for the Enriched – Gas – paper SPE 14152 – September 22-25, 1985

Ahmed, Tarek. A generalized Methodology for Minimum Miscibility pressure, SPE 39034, Sao Paulo, Brazil, 1997

Chung, F.H., Jones, R.A., and Burchfield, T.E., Recovery of viscous oil under high pressure by CO_2 displacement: A laboratory study; SPE paper 17588 presented at the SPE International Meeting on Petroleum Engineering, held in Tianjin, China, November 1-4, 1988

Stalkup Jr., F.I., Miscible Displacement; SPE Monograph Series, 139, 1984

Lee, J.L, Effectiveness of Carbon Dioxide Displacement under Miscible and Immiscible Conditions; Report RR-40, Petroleum Recovery Inst., Calgary, March 1979

Puttagunta, V.R., Miadonye, A., Dyer, S.B., and Huang, S.S., Correlation and prediction of heavy oil and bitumens containing dissolved gases, Part II: Saskatchewan heavy oils saturated with gas mixtures; AOSTRA Journal of research, Vol. 7, 251-258, 1991

Jessen. K, Standord U., and E.H. Stenby. Fluid Characterization for Miscible Eor projects and CO_2 sequestration. SPE paper 97192, SPE Annual Technical Conference and Exhibition, 9 – 12 October, Dallas, Texas, 2005

Kokal, S.L. and Sayegh, S.G., Phase behavior and physical properties of CO_2-saturated heavy oil and its constitutive fractions: Experimental data and correlations; Journal of Petroleum Science and Engineering, Vol. 9, 4, 289-302, 1993

Srivastava, R.K., Huang, S.S., Dyer, S.B., and Mourits, F.M., Measurement and prediction of PVT properties of heavy and medium oils with carbon dioxide; paper presented at the 6th UNITAR International conference on heavy crude and tar sands, Houston, Feb. 12-17, 1995

Grigg, R.B., Dynamic phase composition, density, and viscosity measurements during CO_2 displacement of reservoir oil; SPE paper 28974 presented at the SPE International Symposium on oil field chemistry held in San Antonio, TX, USA, Feb. 14-17, 1995

Taber, J.H., Martin, F.D. and Seright, R.S. EOR Screening Criteria Revised – Part 1 : Introduction to Screening Criteria and Enhanced Recovery Field Projects. SPE Reservoir Engineering, 12, 3, 189-198, 1997

About the Authors

Mojsin Al-Jarba graduated with a BSc Degree from King Saud University in Petroleum and Natural Gas Engineering Dept 2008. He works now with LUKOIL Saudi Arabia Energy Ltd (LUKSAR) as a Drilling Supervisor Assistant. He is a member of the Society of Petroleum Engineers (SPE)

Bandar Duraya Al-Anazi graduated with a BSc Degree from King Saud University in Petroleum and Natural Gas Engineering Dept in 2008 and he now works with the Petroleum & Natural Gas Research Institute at King Abdulaziz City for Science & Technology (KACST). He is a member of the Society of Petroleum Engineers (SPE), the American Association of Petroleum Geologists (AAPG), the Society of Exploration Geophysicists (SEG), Dhahran Geosciences Society (DGS), Candidate Fellowship of the Geological Society of London, Society of Petrophysicists and Well Log Analysts (SPWLA), European Association of Geoscientists & Engineers (EAGE),Canadian Society of Exploration Geophysicists (CSEG), The Edinburgh Geological Society (EGS), The Petroleum Exploration Society of Australia (PESA), Canadian Well Logging Society (CWLS), Aberdeen Formation Evaluation Society (AFES). He was a secretary of SPE-KSU chapter from 2004-2006 and was elected as President for the chapter from 2006-2007 .

World Oil and Gas Production

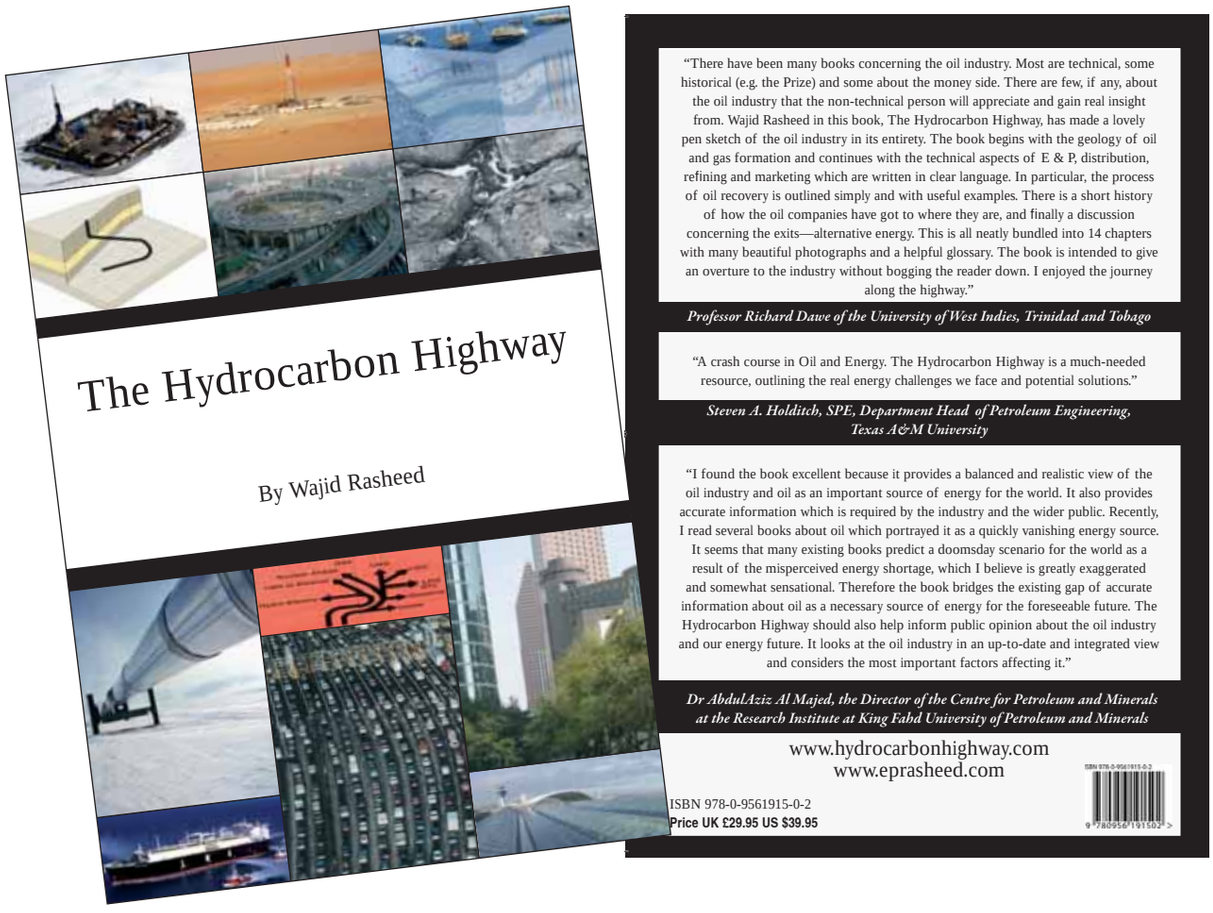

Here we focus on the worlds' oil and gas major producers (OPEC and non-OPEC) from an export perspective. We detail the dominant oil companies behind world exports as well as each country's production level, reserves and capacity.

Although conventional oil production and reserves are globally dispersed, the highest concentration is in the Middle East. Since the 1960s, this region averages nearly 30% of total global oil production and controls 61% of world oil reserves. OPEC itself produces 43% of world oil production and controls 75% of proved oil reserves. Of the 15 countries worldwide that produced 2 MMbbl/d or more of total liquids for export, seven were OPEC members[1].

The Oil Is Ours

Any consideration of OPEC must begin with its importance as a reserves holder and major oil exporter. From this perspective, only producers that export more

than 1 MMbbl/d to the global markets are considered (net of any imports for national refining or consumption). Net exporters play an extremely important role in satisfying demand in global markets because their oil supplies are real exports over and above their domestic needs and are therefore known sources of future oil supply.

Every Move You Make

Undoubtedly, every move made by OPEC gets as much headline ink around the world as any Central Bank decision. It is watched by the major press agencies who have assigned some of their brightest minds to cover the decisions that usually come out of the Austrian capital. Sitting permanently as an inter-governmental organization, OPEC has 11 members: Algeria, Indonesia, the Islamic Republic of Iran, Iraq, Kuwait, the Socialist People's Libyan Arab Jamahiriya, Nigeria, Qatar, Saudi Arabia, United Arab Emirates and Venezuela. The combined population of OPEC countries is just over half a billion people and most are dependent on oil revenues for sustaining their economies. For these countries, oil is the platform for economic, social and political growth[2].

OPEC currently produces about 43% of the world's crude oil, but that is forecast to grow to more than 50% in the next quarter of a century. OPEC has 75% of the world's oil reserves and this will enable it to expand oil production to meet the growth in demand. In order to expand OPEC output, the oil industry needs the oil price to remain at a profitable level. Oil producers invest billions of dollars in exploration and infrastructure (drilling and pumping, pipelines, docks, storage, refining, staff housing, etc.) and a new oil field can take three to ten years to locate and develop. Commercialisation and profitability are complex issues which are dealt with—in the next Chapter[3].

All OPEC countries are sensitive to oil-price fluctuations because of the large contribution oil revenues make to state coffers. As one would expect, high oil prices yield larger gains in revenues from oil exports; the opposite is also true.

Before getting into detail about the major OPEC exporters of oil, it is worth mentioning the Gas Exporting Countries' Forum (GECF). This forum was formed in Teheran, Iran in 2001 with a view to managing global gas reserves and providing a stable and transparent energy market. The GECF consists of 15 gas-producing countries: Algeria, Bolivia, Brunei, Egypt, Equatorial Guinea, Indonesia, Iran, Libya, Malaysia, Nigeria, Qatar, Russia, Trinidad and Tobago, the United Arab Emirates and Venezuela. Five of these countries – Russia, Iran, Qatar, Venezuela and Algeria – control nearly two-thirds of the world's gas reserves and account for 42% of its production. The GECF has a liaison office in Qatar which is 'formulating a gas-trading model to share knowledge of supply and demand and create a level playing field in negotiations with international operators'. It is likely that the GECF will become a gas OPEC. Russia has offered to permanently host the organisation at the most recent meeting in Moscow where Equatorial Guinea and Norway were attending as observers[4].

Saudi Arabia

Saudi Arabia produced a daily average of 10.4 million barrels of oil (MMbbl) in 2007, consumed 2.15 MMbbl/d and exported 8.25 MMbbl/d.

Famous for its ability to 'swing' world markets into 'equilibrium', Saudi Arabia is commonly recognised as the world's leading oil exporter. It sits atop a quarter of world oil reserves, a fifth of international exports and more than a tenth of total world production. It has a refining capacity of 3 MMbbl/d. One of the Kingdom's goals is to maintain sufficient spare production capacity so that it can stabilise the market in a given situation. Leaving production capacity idle, and therefore forfeiting revenues, is commendable on the part of Saudis. Whether such ability continues to exist, and averts the energy crises resulting from supply level, will be dependent on investment in refining capacity and technology.

Geology

The Saudi Geographical Survey identifies the Phanerozoic cover as the geologic range of interest for oil and gas reserves. The Phanerozoic ranges from the Saudi Arabian Paleozoic (540-250 millions of years ago [Ma]) to the Cenozoic (65 Ma to recent) and it crops out as relatively flat beds of sedimentary rocks such as sandstone, siltstone, limestone, evaporites (salt deposits), and volcanic rocks. The youngest deposits in the region include coral limestone and unconsolidated sand, silt, gravel and sabkhah, which accumulated in the sand seas of the Rub al Khali and An Nafud and were deposited on to dried-up lake beds, valleys (wadis) and coastlines.

Reserves

Estimates place Saudi Arabia's proven reserves by the end of 2007 as at least 264.2 billion barrels including new finds and the mega-projects listed below. This is

a consensus figure based on the inclusion of probable and possible reserves based on the Society of Petroleum Engineers (SPE) reserves criteria[5].

Although there has been recent speculation of a lower volume of reserves primarily due to watercut, this is a red-herring as the occurrence of increased water production and re-injection are standard reservoir conditions and secondary recovery mechanisms. This is discussed more fully in *Chapter 9: Mature Fields*. Based on current reserves data, it is fair to say that the last barrel of oil will likely be from Saudi Arabia.

Saudi Aramco

Saudi Aramco is the modern day legacy of the Arab American Company. It is as technically sophisticated and diverse as any major oil company with approximately 86% of its staff as Saudis and the remaining 14% employees from more than 50 countries. Saudi Aramco has invested heavily in reservoir and E & P technology and runs one of the world's largest carbonate research centres encompassing reservoir modelling, dynamics and visualisation. Contrary to the popular belief that low-cost onshore environments have limited technology applications, Saudi Aramco runs the latest in downhole drilling and completions technology such as rotary steerables, high-end logging and formation evaluation tools as well as maximum reservoir contact wells (see *Chapter 7: Pregnant Ladies and Fish Bones*). The company's flagship Research and Development Centre (R&DC) employs 350 research staff working on seismic, drilling, completion and production projects[6].

In spite of the recent surge in its oil income, stabilisation funds and foreign investments, Saudi Arabia is seeking to diversify its industrial and financial base beyond petroleum and has initiated several knowledge and industry based projects such as the King Abdullah University of Science and Technology[7].

Iran

Iran produced 4.4 MMbbl/d through 2007. It still made net oil exports of 2.78 MMbbl/d considering that Iranian domestic oil consumption was 1.62 MMbbl/d[8].

Iran's oil and gas sector is dominated by the National Iranian Oil Company (NIOC). Foreign companies are active in Iran and include Gazprom, Japanese National Oil Company (JNOC), PETRONAS, StatoilHydro and Total. Oil and gas ventures are subjected to 'buy-back' arrangements whereby ownership is retained by the Iranian state. NIOC has made several large discoveries, notably the Azadegan field which is yet to be developed and has recoverable reserves of 9 billion barrels (bbls). Other noteworthy fields include Ferdowsi (30.6 billion bbls), Moud (6.63 billion bbls), Zagheh (1.3 billion bbls), Bangestan (600 MMbbls) and Kushk. Iran relies heavily on oil export revenues for approximately 80% of total export earnings and 40% of the government budget[9].

Venezuela

Venezuela produced 2.63 MMbbl/d in 2007 and consumed 596,000[10] MMbbl/d, therefore it exported 2.03 MMbbl/d[11].

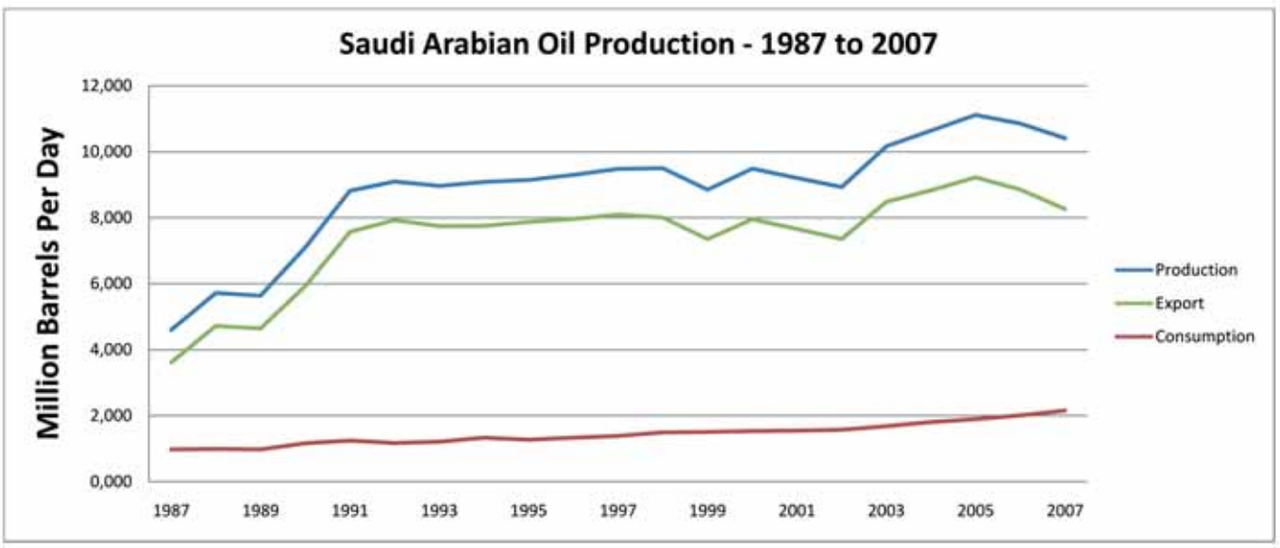

Table 1 - Saudi Arabian Oil Production (1987 to 2007)

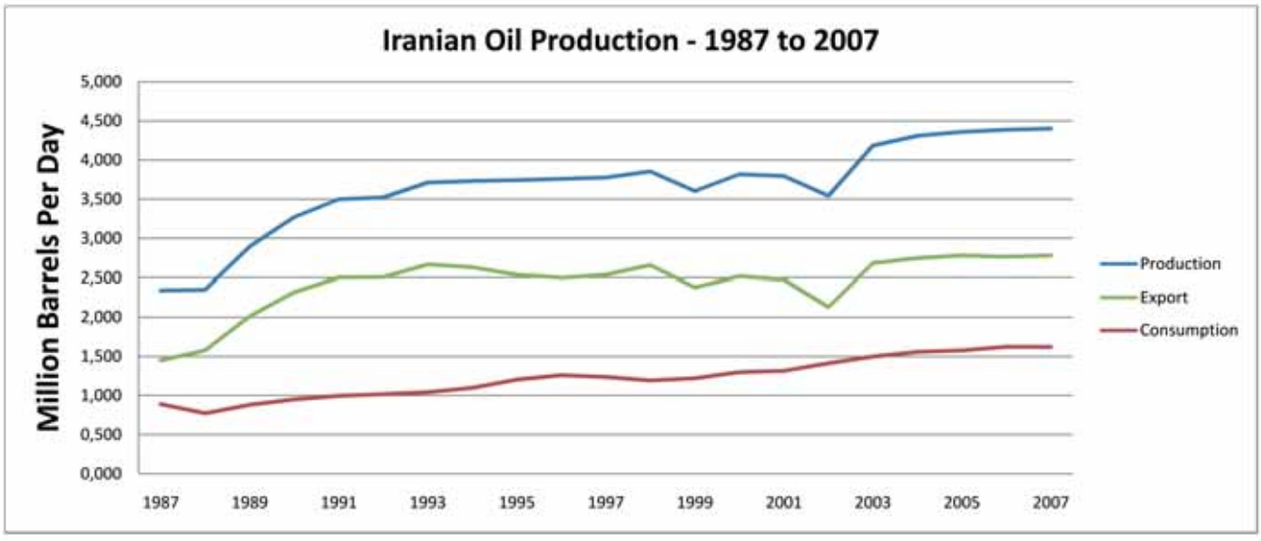

Table 2 - Iranian Oil Production (1987 to 2007)

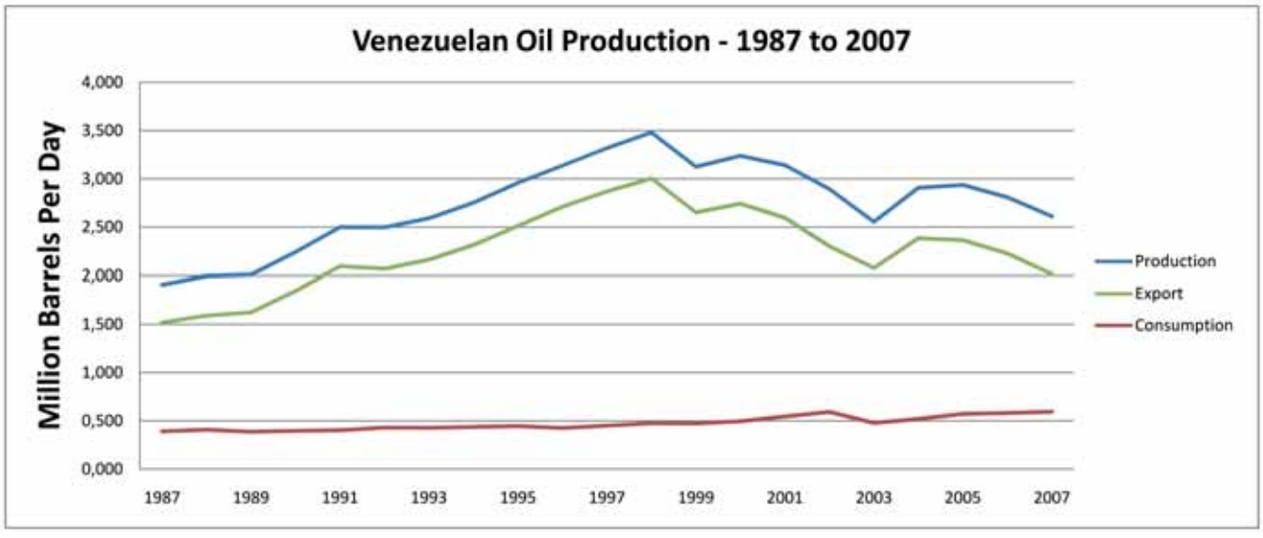

Table 3 - Venezuelan Oil Production (1987 to 2007)

Petróleos de Venezuela S.A. or PdVSA is the state-owned oil company of the Bolivarian Republic of Venezuela and it is responsible for the majority of oil production. Although IOCs such as ConocoPhillips, Chevron and Petrobras are present, they must work with PdVSA.

The country is split into two oil provinces: Maracaibo in the West and the 'Oriente' (Spanish for East), both of which share the same prolific source rock. Oil accumulations are found in Cretaceous limestones and in overlying tertiary sandstones. The East Venezuela Basin is asymmetrical with a long, gently-dipping, southern flank. Oil has migrated up this flank to shallow depths where it has been weathered and has generated sizeable heavy oil and bitumen deposits at depths of 1640 to 4921 ft (500 to 1500 m) along the Orinoco River[12].

Oil export revenues are important for Venezuela because as much as 45% of government revenues come from oil[13].

Based on company figures, PdVSA aims to raise the country's crude oil production capacity to 5.5 MMbbl/d by 2010[14].

UAE

In 2007, the United Arab Emirates or UAE produced 2.9 MMbbl/d, consumed 0.45 MMbbl/d and exported a total of 2.45 MMbbl/d[15].

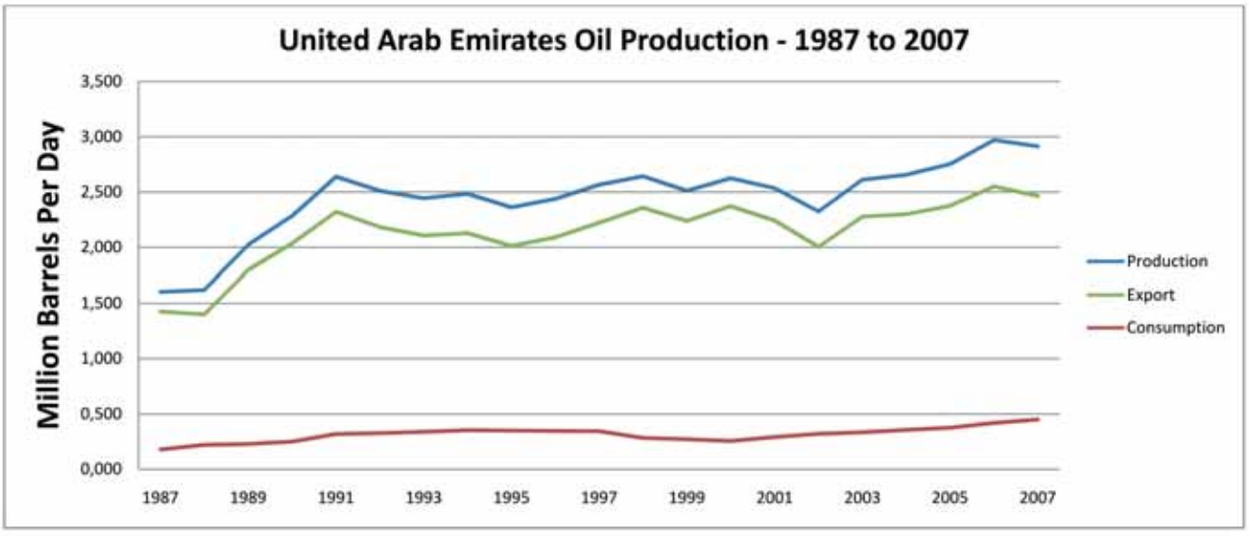

Table 4 - UAE Oil Production (1987 to 2007)

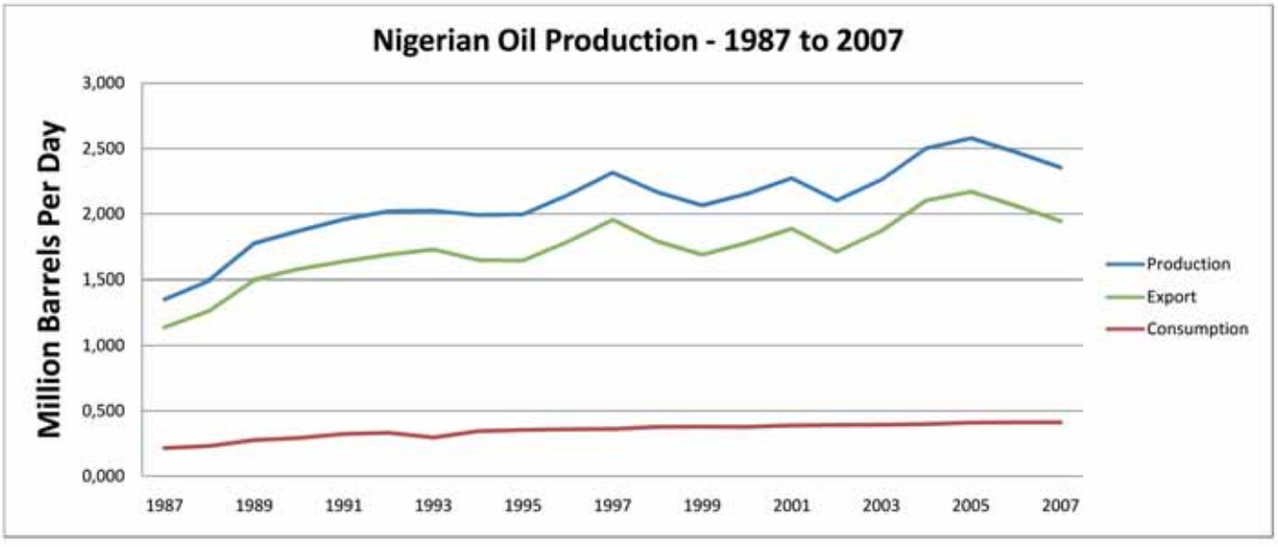

Table 5 - Nigerian Oil Production (1987 to 2007)

The Abu Dhabi National Oil Company (ADNOC) is the major oil and gas producer in the UAE. It is responsible for all operations in Abu Dhabi and owns the Abu Dhabi Company for Onshore Oil Operations (ADCO), which operates in onshore and shelf waters in the Emirates.

ADCO produces oil from five main fields: Asab, Bab, Bu Hasa, Sahil and Shah. The Zakum Development Company (ZADCO) is responsible for oil development and production from the Upper Zakum field. It also operates Umm Al Dalkh and Satah on behalf of its partners. There is also the National Drilling Company (NDC) for onshore and offshore drilling. As with other OPEC countries, relatively strong oil prices and revenues in recent years have helped to significantly improve the UAE's economic, trade, and budgetary situations[16].

The UAE economy is relatively diversified and is in transition from a purely oil-based economy to one that is increasingly moving towards services such as tourism, banking, re-exports, information technology, etc. Privatisation has moved ahead relatively quickly, and the country has set up various Free Zones to encourage foreign trade and investment. These moves have helped to moderate the effects of fluctuating oil prices and revenues[17].

Nigeria

Nigeria produced 2.36 MMbbl/d in 2007 and is estimated to have consumed 0.4 MMbbl/d, hence exporting approximately 1.96 MMbbl/d[18].

Most of Nigeria's crude oil production, comprising ten major crude streams (including condensate), is light sweet crude, API grades 21º-45º, with a low sulphur content. Nigeria's marker crudes on the international oil market are Bonny Light and Forcados. Numerous fields are known across the Niger Delta, and some of the more marginal fields have become the focus of redistribution with the debate favouring private local companies[19].

Nigeria's oil and gas industry is funded through Joint Ventures (JVs), with the National Petroleum Corporation (NPC) as a major shareholder and each oil company holding a share. The largest JV is operated by the Shell Petroleum Development Company (SPDC) and produces nearly half of Nigeria's crude oil, with an average daily output of approximately 1.1 MMbbl/d. Other companies working with the NPC, include ExxonMobil, Chevron, ConocoPhillips, Total and Agip. The remaining funding arrangements comprise Production Sharing Contracts (PSCs), which are mostly confined to Nigeria's deep offshore development programme.

A number of the oil companies prospecting in the offshore blocks in the Niger Delta, have built up considerable deepwater experience in the Gulf of Mexico (GOM), the Gulf of Guinea (particularly in Angola), and the North Sea. Technology developments have reduced the cost of exploration and production, although profitability is reckoned at levels exceeding 5,000 bbl/d per well.

A number of major discoveries have been recorded with Shell's Bonga and Chevron's Agbami field both estimated to hold one billion barrels each. These successes have turned the focus of Nigerian exploration into deep waters which remains a highly prospective area[20].

Kuwait

Kuwait produced 2.62 MMbbl/d in 2007 and consumed 0.28 MMbbl/d allowing it to export 2.34 MMbbl/d.

The Kuwait Petroleum Corporation (KPC) was founded in 1980 with the Government of Kuwait as its sole owner. It owns most of the oil and gas concerns in Kuwait such as the Shuaiba, Al Ahmadi and Mina Abdulla refineries. It is a shareholder, along with BP, of the Kuwait Oil Company (KOC) which produces approximately 2 MMbbl/d. KOC aims to increase production by developing more of the country's light oil and gas reserves in the Jurassic and Paleozoic formations respectively[21].

Iraq

Iraq's oil production fell severely from 2000, from 2.61 MMbbl/d to a low in 2003 of 1.34 MMbbl/d. Iraq's

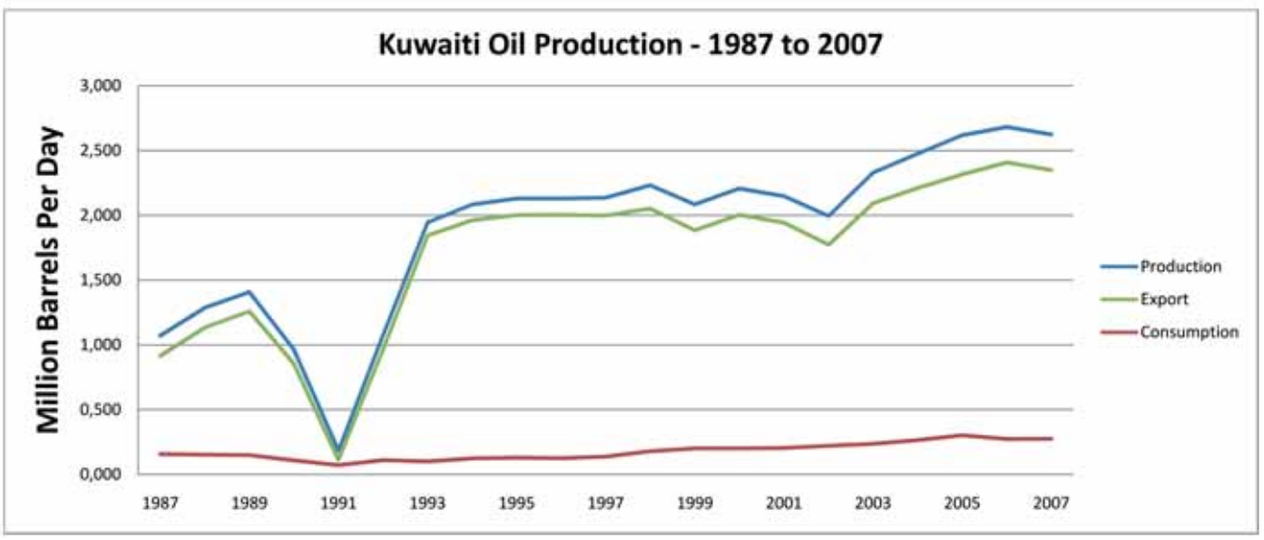

Table 6 - Kuwaiti Oil Production (1987 to 2007)

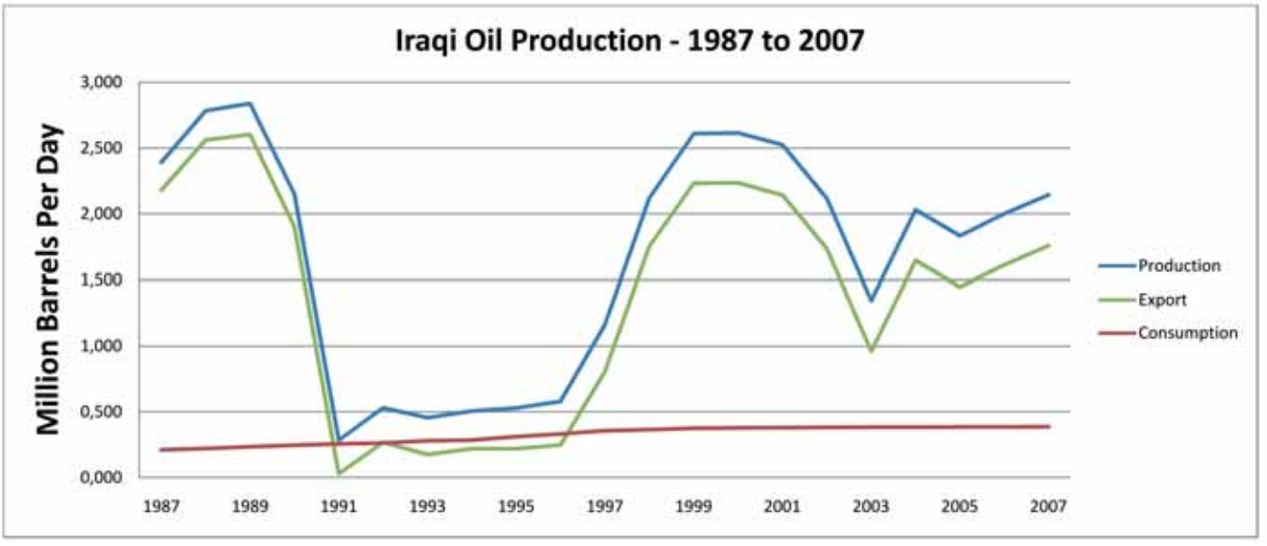

Table 7 - Iraqi Oil Production (1987 to 2007)

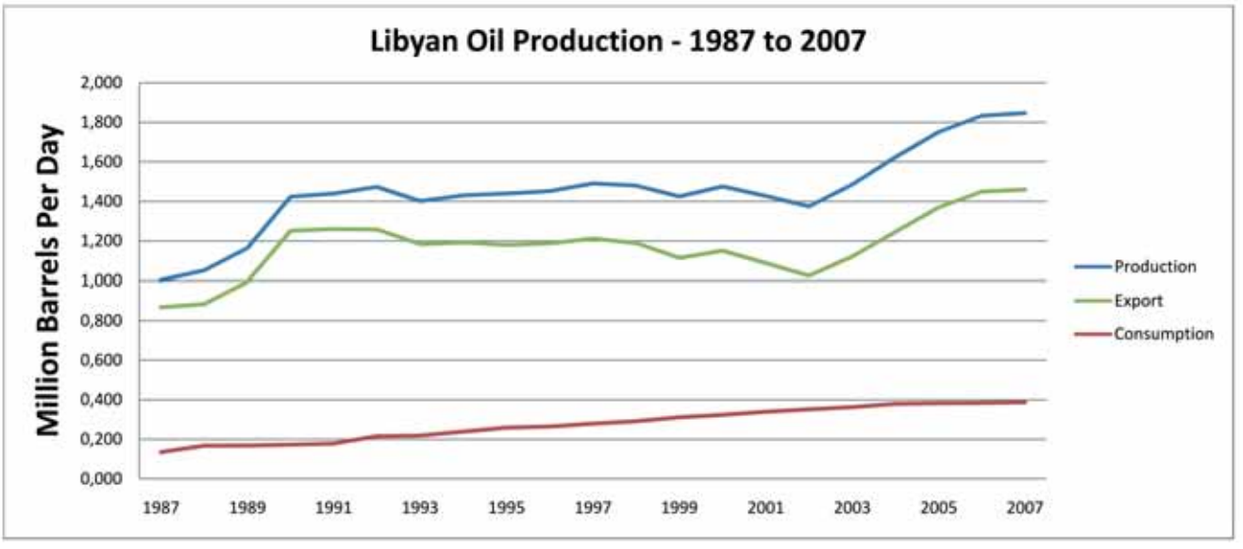

Table 8 - Libyan Oil Production (1987 to 2007)

oil production, however, has regained capacity and it is worth noting that Iraqi E & P costs are amongst the lowest in the world and, given the application of commonly available technology, the country has the potential to produce at far higher levels.

During 2007, Iraq produced 2.145 MMbbl/d and is estimated to have consumed 0.38 MMbbl/d. It is therefore estimated that Iraq exported 1.76 MMbbl/d[22]. Iraq has 115 billion barrels of proven oil reserves, placing it third worldwide after Saudi Arabia and Iran. Oil production in Iraq is concentrated in two oilfields: Rumaila which has 663 producing wells and Kirkuk which has 337 producing wells.

Libya

In 2007, Libya produced 1.85 MMbbl/d and was estimated to have consumed 0.30 MMbbl/d, thereby exporting 1.5 MMbbl/d[23].

Exploration onshore is concentrated in the Sirte, Murzuq and Ghadames Basins as well in the areas of Kufra and Cyrenaica.

Among Libya's largest onshore fields are the Amal field and the Gialo field, both with reserves of over four billion barrels of oil. Other large fields occur in the Sarir complex in southern Cyrenaica which is in the south-eastern margin of the Upper Cretaceous-Tertiary Sirte

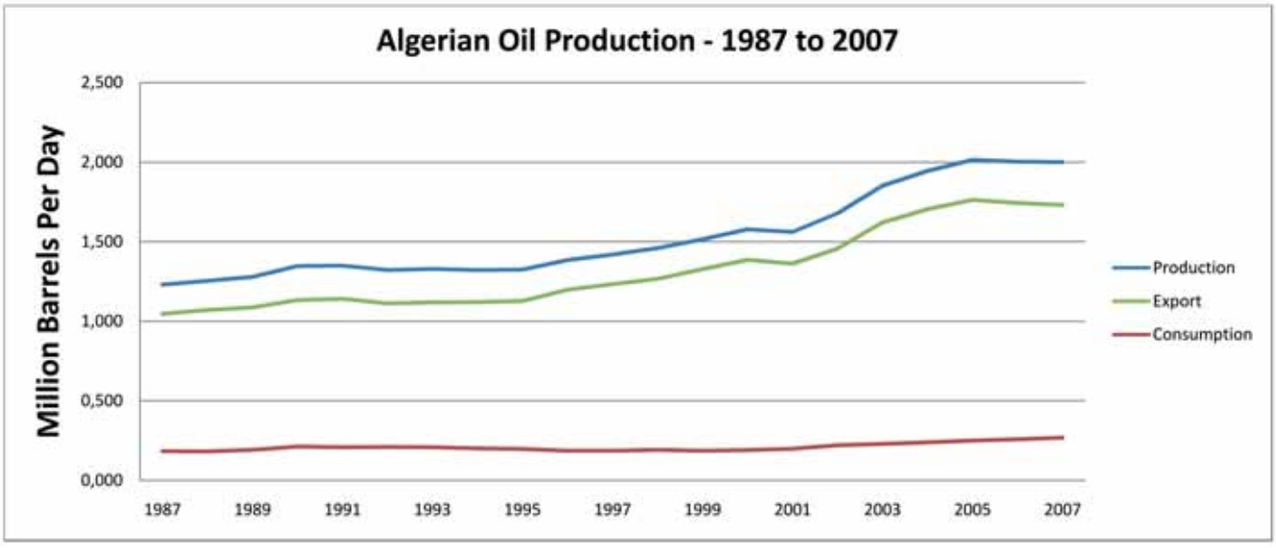

Table 9 - Algerian Oil Production (1987 to 2007)

Basin, which is one of the most highly productive oil basins in North Africa[24].

The majority of Libya's oil and gas is found onshore in three geological trends of the Sirte Basin. In the West, the known fields are Samah, Beida, Raguba, Dahra-Hofra and Bahi. In the north-centre of the country, there are the giant oilfields of Defa-Waha and Nasser and also the large Hateiba gas field and an easterly trend containing Sarir, Messla, Gialo, Bu Attifel, Intisar, Nafoora-Augila and Amal[25].

In early 2005, Libya held its first round of licences with Occidental, Woodside Petroleum, the UAE's Liwa and Petrobras gaining licences. The country continues to attract foreign investment and now has a relatively diverse E & P sector.

Algeria

In 2007, Algeria produced 2.0 MMbbl/d, consumed 0.27 MMbbl/d, and exported 1.73 MMbbl/d. Additionally, Algeria is an established Liquefied Natural Gas (LNG) exporter serving European and US markets.

The petroleum sector is dominated by the NOC Sonatrach which is owned by the Algerian government. Through its subsidiaries, the company has a domestic monopoly on oil production, refining, and transportation. Upstream activities, how-ever, are open to foreign companies, who must work in partnership with Sonatrach, with the company in question usually holding majority ownership in production-sharing agreements. The most notable of these companies are Anadarko, BHP, BP and Repsol[26]. Algeria's Saharan Blend oil is a preferred sweet and light crude approximately 46° API. As of 2007, Algeria had 160 trillion cubic feet (Tcf) of proven natural gas reserves. Hassi Messaoud is the country's largest oilfield and is owned by Sonatrach with average production of 0.350 MMbbl/d of sweet and light 46° API crude. The Hassi Messaoud complex is reckoned to hold six billion barrels and is expected to provide approximately 0.7 MMbbl/d over the next five years. Sonatrach also operates the Hassi R'Mel field, which produced 0.18 MMbbl/d of 46.1° API crude. Anadarko produces approximately 0.5 MMbbl/d from the Hassi Berkine and Ourhound fields in eastern Algeria and is also developing further assets.

Major non-OPEC Producers

Major non-OPEC producer countries are the US, Russia, Mexico, China, Canada and Norway. The focus here, however, should be on producers that make significant oil exports after allowing for their national consumption: for example, in 2007 the US produced 6.9 MMbbl/d (8% of world crude oil) and China produced 3.7 MMbbl/d (4.8%. of world crude oil)[27]. These countries , however, consume far more than they produce. In 2007, oil consumption for the US was

20.7 MMbbl/d and for China 7.89 MMbbl/d, making these two countries the world's largest net oil importers. In the case of Canada, the oil produced was 3.30 MMbbl/d and consumption was 2.30 MMbbl/d, making net exports 1.0 MMbbl/d in 2007[28].

Consequently, after stripping out domestic consumption, significant non-OPEC* net oil exports lie in the hands of four countries: Russia, 7.28 MMbbl/d; Norway, 2.34 MMbbl/d; Mexico, 1.45 MMbbl/d; and, Kazakhstan, 1.27 MMbbl/d.

Considering net exports, the importance of OPEC exports becomes strikingly clear as ten of the world's major oil exporters (more than one MMbbl/d) belong to OPEC, a total which is roughly double that of the combined non-OPEC exports[29,30,31].

Non-OPEC and OPEC Major Net Exporters of Oil 2007

Non-OPEC oil production has risen in the past few years, notably from Russia which briefly displaced Saudi Arabia as the world's foremost crude oil producer in 2006 and from rising exports from central Asian states such as Kazakhstan[32]. It is recognised, however, that only Saudi Arabia retains the existing spare capacity required to meet the predicted total world oil demand growth over the next five years. Other areas such as Offshore West Africa (Angola) and Offshore East Brazil are increasing production, with Brazil reaching a narrow margin of self-sufficiency in April 2006. Neither, however, is likely to make a major impact on world oil exports over the next decade especially considering the high costs associated with these deepwater developments[33].

A Wider OPEC?

It is often reported that the ripples of OPEC decisions are always most keenly felt by consumers 'at-the-pump' in importing countries; however, OPEC decisions can equally affect oil exporting countries. OPEC decisions can influence oil price trends (other things remaining equal), which can affect the revenues realised by oil exporters. This has been noted by certain non-OPEC countries which may see certain advantages of some degree of co-ordinated production policies with OPEC. Russia and Norway are two examples, although they have not always actually carried out co-ordination.

While the stated volumes of non-OPEC production (or export) restrictions have usually been small, the participation of these non-member countries can lead to accentuated effects as market analysts attribute value to such actions and can lead to even greater cohesion with OPEC in restricting output. In this way, the effect of wider co-ordination with OPEC policies is not often recognised[34]. High or increasing oil prices since 2000, however, have led non-OPEC to maximise production rather than restrict output. Whether intended or not, since 2000 there have been similar actions from OPEC and non-OPEC exporters. Since 2003, Mexico, Norway, Russia, Oman and Angola have all pushed to maintain or increase production in the high price environment. The peak prices of mid 2008 of US $147 and the subsequent collapse of oil prices to US $35 by the end of 2008 prompted dramatic production cuts from OPEC. Russia participated as an 'observer' in OPEC meetings, but made no production cuts.

World Oil Consumption

Of the 85.22 MMbbl/d of oil consumed worldwide in 2007, OPEC countries together consumed approximately 7.6 MMbbl/d, which again shows their importance in sustaining production. Of the world's top ten oil consumers in 2007, only Russia has significant net oil exports. The remaining top consumers are listed as the world's largest oil importers, with the exception of Brazil, which reached oil self-sufficiency in April 2006[35].

Estimates of proven oil reserves vary, but the essential fact remains that most of the world's proven oil reserves are held by OPEC. According to OPEC statistics, world proven reserves are 1.15 trillion barrels of proven reserves, of which OPEC holds 0.9 trillion barrels[36]. According to BP's statistical review, world proved reserves are 1.2 trillion barrels, of which 0.9 trillion are held by OPEC[37] and 0.30 trillion are held by non-OPEC members. According to the US Energy Information Association (EIA) which bases it figures on the Oil and Gas Journal, total reserves are 1.3 trillion of which 0.85 trillion are held by OPEC[38]. The remaining reserves are split between Russian, the Former Soviet Union (FSU) and Canada.

Non-OPEC reserves include Canadian unconventional reserves which have higher production costs[39]. In the future, the inclusion of unconventional oil reserves for other countries may positively affect OPEC member Venezuela, as well as non-OPEC countries such as Canada, Brazil and Australia. The reserves of non-OPEC countries are being depleted more rapidly than OPEC reserves. Non-OPEC reserves-to-production ratio – an indicator of how long proven reserves will last at current production rates – is approximately 26 years for non-OPEC. OPEC re-

serves-to-production is 73 years based on 2007 crude oil production rates. Combining the longer reserves life and the high net oil exports figures, it is clear to see just how important OPEC production is over the long term[40].

Refinery Capacity

Countries that have high petroleum demand tend to have large refinery capacities due to proximity to end consumers. Exemplifying this, the US is the world's largest consumer and has the highest refinery capacity in the world, with 20% of the world's crude oil refinery capacity (17.59 MMbbl/d of a total 87.91 MMbbl/d).

Russia's refinery capacity stands at an estimated 5.58 MMbbl/d. Japan (4.56 MMbbl/d) and China (7.5 MMbbl/d) are the only remaining countries with refinery capacities exceeding 3 MMbbl/d[41]. There are several countries that are important to world trade in refined petroleum products despite very low (or non-existent) levels of crude oil production. For instance, Caribbean nations (including US and European territories) have very limited oil production (233,000 bbl/d in 2007), but a refinery capacity of about 2.6 MMbbl/d. Much of this refined product is exported to the US[42].

Review of Major Non-OPEC Oil Exporters

Russia

Russia produced 9.98 MMbbl/d in 2007 and consumed 2.7 MMbbl/d in the same period. The country therefore exported 7.28 MMbbl/d during 2007 making it the second largest oil exporter after Saudi Arabia.

After the break-up of the Soviet Union in the early 1990s, the nature of the Russian oil industry changed dramatically. From being geographically dispersed and technically fragmented with numerous state-owned entities, the State set about vertically integrating these companies in the likeness of IOCs. Behind the scenes inter-related forces were at work. Central Asian states such as Kazakhstan became sovereign nations and were developing their respective oil and gas industries rapidly and independently. These Central Asian Republics had succeeded in attracting and retaining oil and gas investment capital. The Russian government acted to restructure its own industry, not only to attract investment, but also to integrate its NOCs so that they could compete both at home and overseas. It also acted to counter market volatility by channelling windfall oil revenues into a stabilisation fund that came into effect in 2004[42].

Today, several Russian oil companies compete globally and the stabilisation fund is believed to be worth almost US $60 billion—approximately 7.5 percent of the country's Gross Domestic Product (GDP). Taxes on oil exports have been raised significantly and private oil companies complain that the higher export taxes are hindering efficient allocation of profits into exploration and development[43].

The decision to develop Shtokman without foreign partners is a signal as strong as any of Russia's move to-

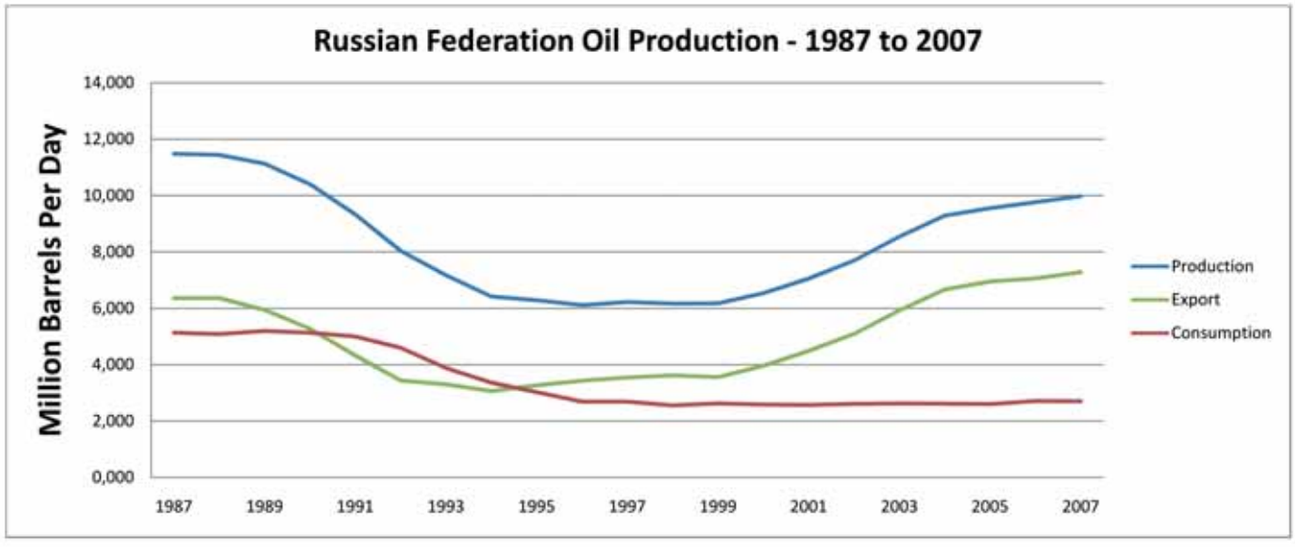

Table 10 - Russian Federation Oil Production (1987 to 2007)

ward nationalisation and emergence as an independent energy power. IOCs such as Chevron, ConocoPhilips, Total and Norwegian company StatoilHydro were excluded from the development and this came as a surprise as it was commonly thought that partnership with a foreign company would occur, especially one with technical expertise, in the harsh conditions of the Barents Sea[44].

Major Russian oil companies that have majority state holdings are Rosneft, Gazprom, Transneft and Rosgas. Other privately-owned companies such as Lukoil are locally owned, while TNK is a BP owned venture and Sakhalin Energy is a consortium of major oil companies.

Rosneft

Rosneft's E & P efforts have been growing steadily and were strengthened by the US $9.3 billion acquisition of Yuganskneftegaz (ex-Yukos), which established the company's proved oil and gas reserves at 21.69 billion barrels of oil equivalent (boe) in 2007 (including gas condensates and gas). Rosneft is also the world's seventh largest producer (in comparison to publicly traded oil companies) and Russia's second largest producer. Average daily output in 2007 was 2 MMbbl/d[45].

Central to Rosneft's cash flow and portfolio is Yuganskneftegaz, which represents approximately two thirds of the company's annual oil production and over 70% of its proved SPE oil reserves. Purneftegaz is Rosneft's second largest production asset. With large non-associated natural gas reserves at the Kharampur field, it is likely to increase in importance as Rosneft seeks to further monetise its gas reserves. Additional exploration in the Timano-Pechora oil province and expanded export capacity at the Arkhangelsk terminal have helped Rosneft grow[46].

Rosneft holds more than a third of Sakhalin's total offshore oil and gas resources. It holds sizeable stakes in all five stages of development. While still at the early stages of exploration, it holds stakes in the Sakhalin-3, Sakhalin-4 and Sakhalin-5 of 49.8%, 51% and 51%, respectively. Rosneft holds a stake in the Sakhalin-1 project, which is currently being developed under a Production Sharing Agreement (PSA) implemented in 1996 with ExxonMobil and Sodeco of Japan (and, since 2001, with India's ONGC). Sakhalin-1 began oil and gas production in late 2005 and is anticipated to experience substantial growth over the next several years[47].

Rosneft also holds interests in Eastern Siberia, in the form of the Vankor field in Krasnoyarsk and with TNK-BP, the Verkhnechonsk field in the Irkutsk.

Other resources on the Black Sea shelf, Sea of Azov and the Kurmangazy structure in Kazakhstan could help the company's future plans for growth[48].

Gazprom

In 2007, GazpromNeft's oil production was 660,000 bbl/d. It comprises nearly half a million shareholders with the Russian Federation controlling a majority of 50.002%. According to the company, it employs some 300,000 people in different operations[49]. Gazprom and its producing subsidiaries hold more than 40 oilfield exploration and development licences in the West Siberian petroleum basin, as well as in Omsk and Tomsk in Chukotka. It acquired Sibneft which has 80% of its reserves concentrated in Noyabr'sk with four large fields – Sugmutskoye, Sutorminskoye, Vyngapurovskoye and Sporyshevskoye – accounting for nearly 50% of Sibneft's reserves. Sibneft was also active in upstream oilfield services and is active in the geophysical arena through OJSC Noyabr'skneftegazgeophysica – a geophysical services company that offers borehole logging, perforation and seismic data preparation[50]. During recent years, Sibneft has spun-off several service companies that were formerly production divisions including Service Drilling Company LLC and Well Workover Service Company LLC. These service companies compete with other Russian and international drilling and service contractors, providing drilling and well work over services[51].

Gazprom – Natural Gas

Russia has the largest natural gas reserves in the world, 1.58 trillion cubic feet (Tcf). In 2007, Russia was the world's largest natural gas producer (58.8 billion cubic feet [Bcf]), as well as the world's largest exporter (16.3 Bcf)[52].

Russia's natural gas infrastructure, however, needs updating and its natural gas industry has not experienced the success of its oil industry, with limited growth in gas production and consumption[53].

Three major fields in Western Siberia – Urengoy, Yamburg, and Medvezh'ye – comprise more than 70% of Gazprom's total natural gas production, but these fields are now in decline. Although the company projects increases in its natural gas output between 2008 and 2030, most of Russia's natural gas production growth will come from inde-

pendent gas companies such as Novatek, Itera and Northgaz. Barents Sea Exploration of the Russian Barents Sea began in the 1970s and to date discoveries in the area consist of ten significant gas and condensate fields, as well as a total of 125 identified fields or potential structures. Total reserves are estimated between five and ten trillion cubic metres[54].

The largest deposit is the Shtokman (Shtockmanovskoye) gas and condensate field, discovered in 1988, with total reserves of 3 trillion m^3, and with estimated recoverable reserves (C1+C2) of 2.5 trillion m^3. Gazprom plans to develop the Shtokman field on its own and expects it to become the resource base for the export of gas to Europe through the Nord Stream pipeline (which is currently under construction)[55]. The energy resources of north-west Russia remain largely unexploited. The total hydrocarbon resources of the Russian Arctic shelf are estimated at about 100 billion tonnes of oil equivalent (toe). The natural gas reserves in north-west Russia form the most important strategic energy resource in the region. Estimates placed on Barents Sea reserves vary from 2 trillion m^3 to 5 trillion m^3. In any event, these reserves offer a major supply contribution to European energy needs. In addition, it is expected that there are also oil deposits in the eastern and northern areas of the Barents Sea. Furthermore, the so-called 'grey zone', formed by the sea boundary claims of Norway and Russia, is considered a promising gas or oil province.

The Timan-Pechora oil and gas region has estimated total oil resources of over 4,800 million tonnes, of which over 1,400 million tonnes is estimated to be recoverable. The Republic of Komi has 520 million tonnes of oil resources. Perhaps the most significant deposit found in the Pechora Sea is the Prirazlomnoye oil field, with estimated reserves of 56-62 million tonnes. The licence for the development of the field is held by JSC Rosshelf, and the Australian company BHP is participating in the development of this field. The exploration of Barents Sea oil resources is still at an early stage[56].

The Timan-Pechora province is considered the third most important oil producer of the Russian Federation, and there is a significant development potential in the area. If the above-mentioned oil reserves are compared world-wide, they are equivalent to Norway's North Sea reserves; however, most of the approximately 200 fields in the region are quite small. Gas reserves are rather small compared to the Barents Sea reserves, for example, which means that they are mainly of local importance[57].

Transneft Russia needs to expand export capacity for its oil and gas in order to monetise growing production. Crude oil exports via pipelines, however, are under the jurisdiction of Russia's state-owned Transneft. The Transneft system cannot meet export needs with an excess of approximately three million barrels of its total seven million barrels transported by road, rail and river routes[58]. This means substantial investments must be made to ensure growing levels of production can reach the markets, especially foreign ones.

Several proposed oil pipeline routes and pipeline expansion projects are planned including the Baltic Pipeline System (BPS), which carries crude oil from Russia's West Siberian and Timan-Pechora oil provinces westward to the newly completed port of Primorsk in the Russian Gulf of Finland[59].

Sakhalin Island

Several IOCs entered into PSAs to develop the resources in Sakhalin Island, Okhotsk Sea (see *Chapter 8: Extreme E & P*). Oil reserves in the area are estimated at around 14 billion barrels, and natural gas reserves at approximately 2.6 trillion cubic metres[60].
The Sakhalin-1 project was led by Exxon Neftegaz, in conjunction with consortium members SODECO, ONGC Videsh, Sakhalinmorneftegaz and RN Astra. The Sakhalin-2 project was developed by Shell, Mitsubishi and Mitsui, and entails the development of Russia's first LNG facility to be built on the southern tip of the island. Sakhalin-2 will also be used to supply natural gas to the United States, Korea and Japan in 2008. Sakhalin 3-6, North and South East of Sakhalin Island, are at the planning stages of development[61].

Norway

Norway had 8.2 billion barrels of proven oil reserves at the end of 2007, the largest in Western Europe. Norway's oil reserves are located offshore on the Norwegian Continental Shelf (NCS), which is divided into the North Sea, the Norwegian Sea and the Barents Sea[62].

Oil and Gas Exports

Norway produced 2.56 MMbbl/d in 2007 and consumed 221,000 bbl/d in the same period. The country therefore exported 2.34 MMbbl/d during 2007. Norway has significantly increased its natural gas production; in 2007 it produced 8.7 bcf and consumed 0.4 bcf[63].

The United Kingdom is the largest importer of Norway's oil and gas having imported 814,500 bbl/d from

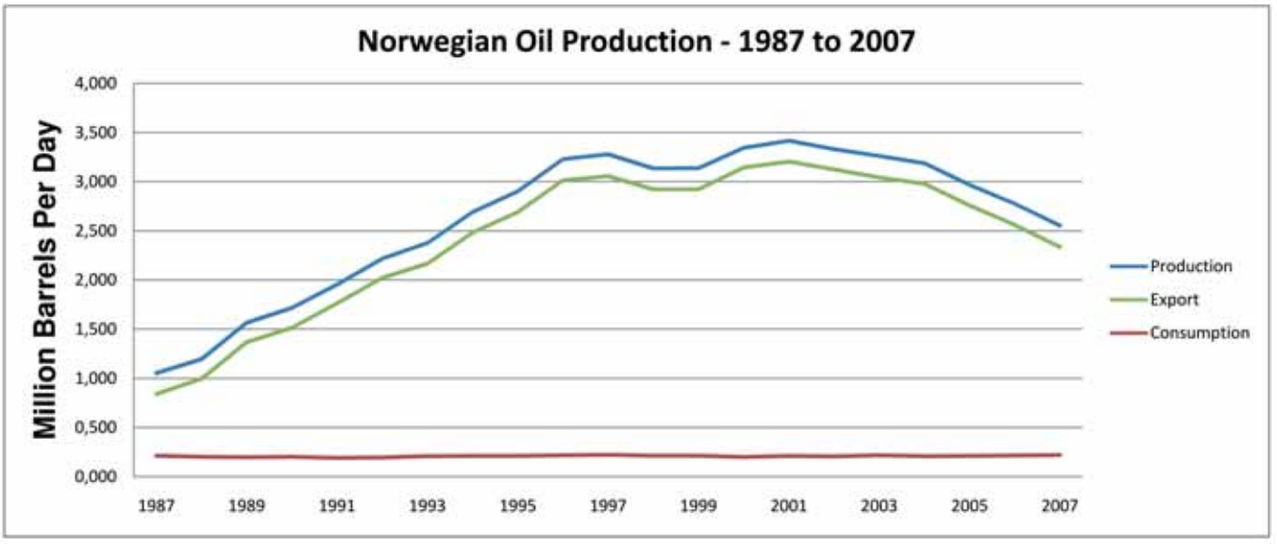

Table 11 - Norwegian Oil Production (1987 to 2007)

Norway, or 34 % of Norway's 2007 total exports.

In contrast to its maritime neighbour, the UK, Norway's government holds a dominant stake in the oil sector and controls 66.42% of StatoilHydro (the remainder of the shares are owned by international, institutional and private stockholders)[64].

StatoilHydro itself holds more than 80% of Norway's oil and gas production. Additionally, Norway's government owns approximately 40% of the country's total oil production through the State Direct Financial Interest (SDFI). State-owned Petoro administers these ownership interests, while StatoilHydro is responsible for managing actual production from SDFI assets[65].

IOCs do have a sizeable presence in the NCS, but they must act in partnership with StatoilHydro. The largest private oil producers in Norway are ConocoPhillips, ExxonMobil and BP. Petoro is the state limited company which is responsible for managing, on behalf of the government, SDFI[66].

While the state has the ownership of the SDFI's assets, Petoro acts as the licencee in production licences, pipelines and land-based plants on behalf of the government. The primary objective of Petoro's administration of the SDFI portfolio is to achieve the highest possible income for the state. The SDFI arrangement involves the state paying a share of all investments and operating costs in projects which correspond to its direct financial interest. On the same terms as the other owners, the government then receives a matching share of revenues from the sale of production and other income sources.

The licencees, and in particular the operator, are responsible for developing discoveries which are made within the boundaries of a licence. Should there be a need for research and technology development to overcome technological challenges in developing the discovery, the tax system provides favourable conditions to ease the burden of such efforts. Relevant expenditures on research are fully deductible against tax and there is a special tax scheme aimed at stimulating research and development in industry ('Skattefunn'). Due to the nature of oil exploration and production in the NCS, the region has traditionally been accessible only by international oil majors. Because of harsh weather and operating conditions, projects in the NCS require sizable initial investments. Further, the structure of Norway's petroleum taxes means that smaller, marginal fields often are not profitable. Finally, stringent environmental, safety, and labour regulations further increase operating costs[67].

Technology Development

The Ministry in Norway funds petroleum-related research programmes which are administered by the Norwegian Research Council. The two most important programmes are called Petromaks and Demo 2000. Petromaks deals with basic and applied research and

Demo 2000 covers the demonstration/application of new technology. The main aim of both programmes is to increase value creation on the Norwegian Continental Shelf and to increase the export of Norwegian oil and gas technology. The Ministry has also established OG 21, 'Oil and Gas in the 21st Century', which provides overall guidance on priorities for the public research and technology programmes, as well as for related activities in universities, research institutes and industry through a comprehensive national R & D strategy. The OG 21 board consists of members from oil companies, the supply industry, research institutions and academia. The implementation of the OG 21 strategy is largely based on the activities of the Petromaks and Demo 2000 programmes and on joint industry projects[68].

As with any development project on the Norwegian Continental Shelf, the Ormen Lange and Snøhvit developments have been driven by commercial interests. The Ministry's role in development projects is to coordinate the administrative procedures and approval processes, ensuring that the projects comply with sound resource management practice, as well as balancing all interests with regard to value creation, environmental concerns and the fisheries. With regard to Snøhvit, minor tax regime adjustments were made to facilitate the development of the LNG projects[69].

Production

The bulk of Norway's oil production occurs in the North Sea, with smaller amounts in the Norwegian Sea. In 2007, LNG production of the Snøhvit field was scheduled to commence which brought development to Hammerfest. Most of the Barents Sea is unexplored and activity there will always be subject to high costs associated with a harsh offshore area and environmental concerns as the seas have abundant fish stocks and are considered unpolluted. The Barents Sea is likely to contain oil and gas reserves, but the question remains one of delineation. To this end, the Norwegian government has restarted licensing in the Barents Sea and companies such as StatoilHydro are looking keenly to what some consider as a new frontier for the Norwegian Petroleum Industry[70].

Exploration and Production

Norwegian oil production rose dramatically from 1980 until the mid-1990s, remained flat since (see Table 11) and has now started to decline. During the first six months of 2005, for example, Norway's oil production averaged 2.95 MMbbl/d, while in 2007 the average figure was 2.55 MMbbl/d. As North Sea fields continue to mature, Norwegian oil production will focus on mature fields, though it is expected that new developments in the Barents Sea will offset some of this decline.

One of the largest oil fields in Norway is the Troll complex operated by StatoilHydro. Other important fields include Ekofisk (ConocoPhillips), Snorre (StatoilHydro), Oseberg (StatoilHydro), and Draugen (Shell). ConocoPhillips, ExxonMobil and BP operate oilfields in Norway. There is a great emphasis on increasing production from existing projects, including the incorporation of smaller satellite fields that will take advantage of the existing infrastructure[71].

As was the case with the United Kingdom, however, many oil majors have begun to withdraw from the NCS in order to pursue projects in high-growth regions. StatoilHydro have begun to sell NCS interests in order to pursue projects in Latin America and Africa.

Mexico

Pemex (Petróleos Mexicanos) was created as a result of the 1938 Mexican President Cardenas' nationalisation of the oil industry.

Today, the company is responsible for all petroleum production in Mexico which is 3.48 MMbbl/d (2.02 MMbbl/d consumption) and 4.5 bcf of gas production (5.2 bcf consumption). The United States is the destination of over 70% of Mexico's 1.46 MMbbl/d exports[72].

A highly prospective area for Mexico are the Mexican waters of the 'Gulf of Mexico' or GOM which to date have only been developed within the US territorial jurisdiction. Mexico's reservoirs are mostly high permeability limestone reservoirs, while the US tends to be lower permeability sandstones. This in part accounts for the higher average Pemex production well rates of approximately 6000 bbl/d per well. The onshore Burgos Basin on the Mexico-U.S. border shares similar gas prone characteristics with its onshore South Texas neighbours[73].

Mexico must prove its deeper GOM trends and in recent times has issued new discoveries such as Noxal. It has been said that it could be a difficult and longwinded task for Mexico to develop its own deepwater expertise, but this argument fails to recognise that many service provisions could be made by service and supply companies rather than oil companies. However, by bringing in reputed deepwater oil companies, the best

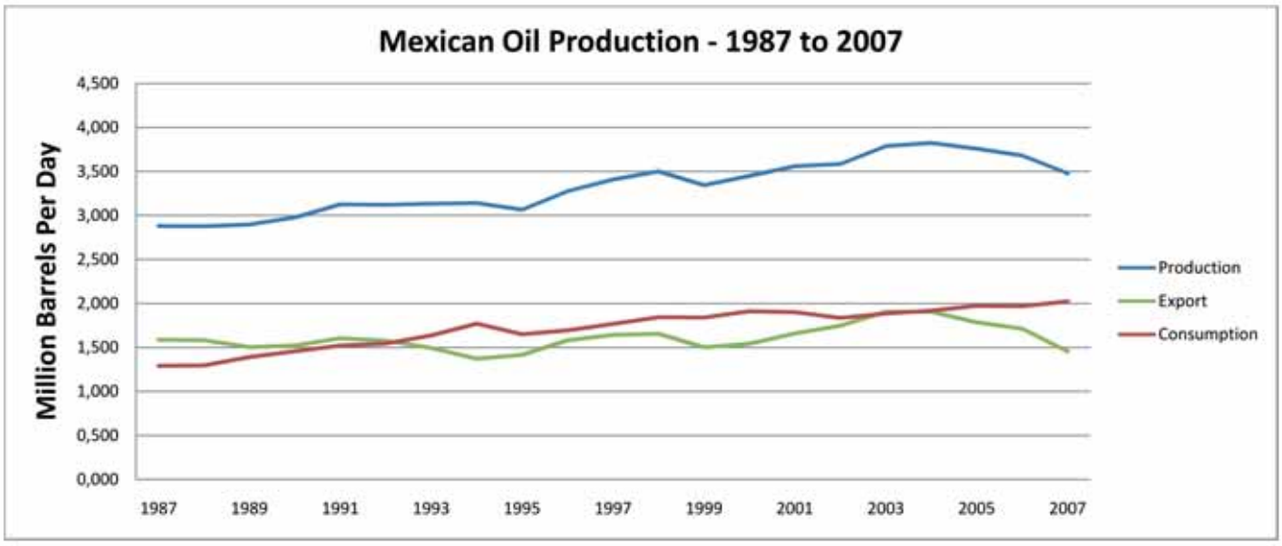

Table 12 - Mexican Oil Production (1987 to 2007)

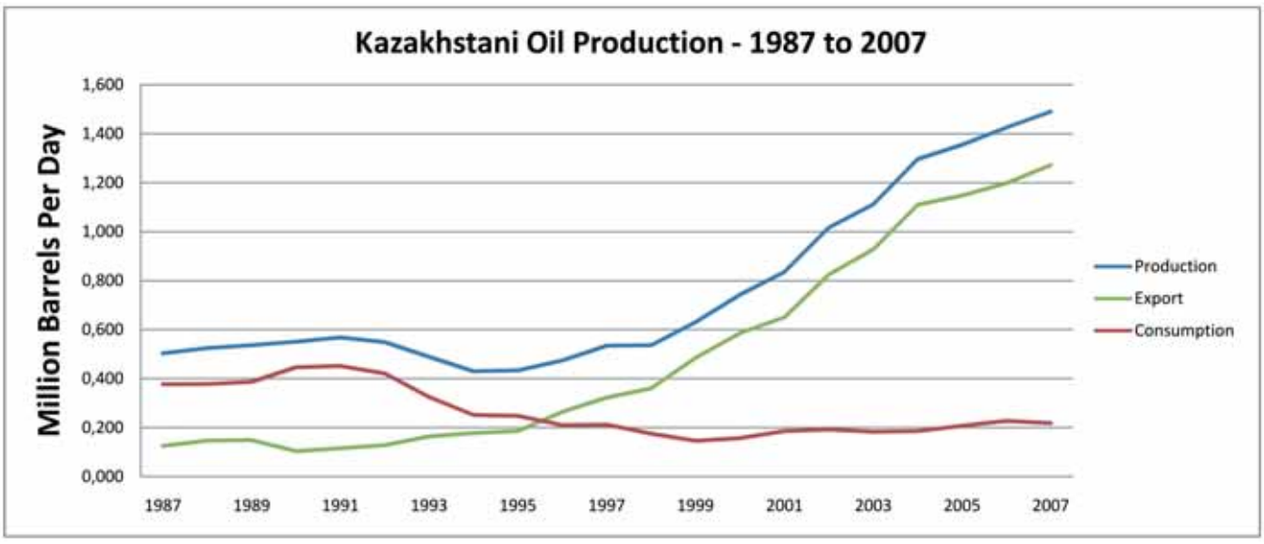

Table 13 - Kazakhstani Oil Production (1987 to 2007)

development strategies could be applied to the GOM Mexican deepwaters.

Kazakhstan

The Caspian Sea contains six separate hydrocarbon basins and has attracted much foreign investment as most of its oil and natural gas reserves are undeveloped and unexplored with the notable exception of Kashagan, which is the flagship project in the North Caspian Sea. High prospectivity is the cause of interest in the Caspian Sea region, but for net oil exports Kazakhstan alone is relevant (although Azerbaijan and Turkmenistan are worth noting for future production growth)[74].

Kazakhstan produced 1.49 MMbbl/d in 2007 and consumed 219,000 bbl/d in the same period. The country therefore exported 1.27 MMbbl/d during 2007.

Proven Kazakhstani oil reserves are 39.8 billion barrels (defined as oil and natural gas deposits that are considered 90% probable) and gas reserves are 67.2 Tcf. The figure for the Caspian sea is much higher but is split between several states. Kazakhstan's reserves are very much a work-in-progress as the country is relatively unexplored and untapped. Even relatively high-profile Kashagan does not have any final proven oil reserves figures as it is still undergoing appraisal and exploratory well drilling. After Russia, Kazakhstan was

the largest oil-producing republic in the Soviet Union and has successfully attracted foreign investment in its oil sector to increase oil production to 1.49 MMbbl/d in 2007, most of which came from two large onshore fields (Tengiz, and Karachaganak) and the offshore complex of Kashagan which is still under appraisal and first oil is not expected before 2011. The Tengiz oil field is estimated to contain recoverable oil reserves of six to nine billion barrels. The Kashagan complex has an unitisation agreement that covers the Kalamkas, Aktoty and Kairan blocks[75]. North Caspian Operating Company (partners include ExxonMobil, Shell, Total, Eni, ConocoPhillips, Inpex and National Oil Company KazMunaiGas) is developing the Kashagan complex. The field was discovered in June 2000, when the first exploration well (KE-1) was drilled with 13 billion tonnes of oil potentially recoverable with the use of gas re-injection[76].

Now that we have in-depth knowledge of where our oil and gas resources are located, we need to think about how one actually gets access to these resources. Does one need to buy the land from those who own it? Are there procedures and policies in place that need to be followed? What are the legal requirements? Who can actually acquire oil or gas fields? Who are the major players in this area?

References

1. BP Statistical Review 2008 page 8.

2. Considering the contributions oil revenues make to GDP

3. Concerns regarding commercialisation and profitability are the main reasons why insufficient refining capacity.

4. The GECF was widely covered in the press.

5. BP Statistical Review 2008 defined as proved reserves.

6. Saudi Aramco Annual Report 2008. For specifics of technologies see editions of Saudi Aramco Journal of Technology.

7. King Abdullah University of Science and Technology (KAUST) is being built in Saudi Arabia as an international, graduate-level research university dedicated to inspiring a new age of scientific achievement in the Kingdom that will also benefit the region and the world. KAUST will be merit-based and will recruit men and women from around the world.

8. BP Statistical Review 2008 page 8.

9. EIA/IEO www.eia.doe.gov/pub/oil_gas/petroleum/analysis_publications/oil_market_basics/supply

10. BP Statistical Review 2008 page 8.

11. BP Statistical Review 2008 page 11.

12. Rice University Energy Study: Latin America the Orinoco Heavy Oil Belt in Venezuela (Heavy Oil To The Rescue?) Manik Talwani Schlumberger Professor of Earth Science.

13. EIA/IEO www.eia.doe.gov/pub/oil_gas/petroleum/analysis_publications/oil_market_basics/supply

14. PdVSA Annual Report 2008.

15. BP Statistical Review 2008 page 8.

16. Oil wealth has undoubtedly helped the UAE especially Abu Dhabi secure commercial growth.

17 See Dubai's Strategic Plan

18. BP Statistical Review 2008 page 8.

19 See Niger Delta Development Commission Master Plan 2001 which states 'There have been many attempts and many plans made in the past to improve the lives of the people of the Niger Delta Region of Nigeria. Sadly, each ended with very little to show for the time and resources spent. Therefore it is understandable that the people of the Niger Delta are quite disillusioned with 'plans' at this time. The disenchantment of the people not withstanding, it must be stated that the Niger Delta Master Plan is different in its goals, focus and approach, and will not suffer the fate of the others before it'.

20. Depositional Control on Hydrocarbon Accumulations in Deepwater Nigeria By Xijin (CJ) Liu Conoco Phillips Search and Discovery Article #40226 (2006)

21. Kuwait Petroleum Corporation (KPC) Annual Report 2008.

22. Any number for consumption will be controversial

for those who require an explanation see "Scramble to carve up Iraqi oil reserves lies behind US diplomacy," Observer, October 6, 2002.

23. BP Statistical Review 2008 page 8.

24. Sarir, Sirte Basin, Desert Surprise Then and Now Some Keys to Revisit of Libya Compiled from articles by C. J. Lewis (1990) and R. M. Sanford (1970).

25. Framework for the Exploration of Libya: An Illustrated Summary Compiled by Jingyao Gong.

26. Sonatrach Annual Report 2007.

27. BP Statistical Review 2008 page 8.

28. Idem.

29. Idem.

30. OPEC Annual Statistical Bulletin 2008.

31. EIA IEO 2008 outlook.

32. EIA IEO 2008 outlook states Kazhakstan as exporter to note.

33. The deepwater developments are particularly susceptible to the low oil price environment.

34. Perhaps wider co-ordination is simply due to market forces.

35. See Brazil Oil and Gas Issue 3 – Petrobras and Self Sufficiency (www.braziloilandgas.com/issue3).

36. BP Statistical Review 2008 page 8.

37. OPEC Annual Statistical Bulletin 2008.

38. EIA IEO 2008.

39. This is a well known fact regarding Canadian Tar Sands.

40. There is no doubt regarding OPEC's future importance.

41. BP Statistical Review 2008 page 18.

42. Idem.

43. The Stabilization fund of the Russian Federation was established on January 1, 2004 as a part of the federal budget to balance the books in the event of the oil price falling below a cut-off price, currently set at US $27 per barrel. Furthermore, the Fund is to serve as an important tool for absorbing excessive liquidity, reducing inflationary pressure and insulating the economy from the volatility of export earnings.

44. Widely reported in the press.

45. Rosneft Annual Report 2008 converted from tonnes.

46. Ditto above.

47. Sakhalin Report 2006.

48. Rosneft Annual Report 2008.

49. GazpromNeft Annual Report 2008.

50. OJSC Noyabrskneftegazgeophysica—Company Profile 2006.

51. Sibneft Annual Report 2005.

52. GazpromNeft Annual Report 2008.

53. Recently Russia is investing more in its Gas infrastructure.

54. Offshore Magazine Feb 1997 RUSSIA Barents Sea still languishing in political limbo Gazprom, Rosshelf, and partners predicting production post-2000 Dev George Managing Editor.

55. Nordstream Facts Newsletter Issue 9/1—2009.

56. Barents Sea field delineated 2008-12-08 StatoilHydro.

57. Idem.

58. CGES Pipeline Advisory Service bulletin No. 23 2006 6th November 2006.

59. Baltic Pipeline System (BPS) was built to transport the crude from fields in Western Siberian, Timan-Pechora and Volga-Urals petroleum provinces to a terminal on the coast of the Gulf of Finland for export. The system includes an existing oil pipeline, which links Haryaga and Usa, trunk pipelines from Usa to

Ukhta to Yaroslavl to Kirishi, new trunk pipelines between Haryaga and Usa and between Kirishi the coast of the Gulf of Finalnd, and finally the new oil export terminal in the city of Primorsk.

60. The Federation of Russian States Oil and Gas Activity and Concession Map—2nd Edition —2007.

61. Sakhalin-1 Project Receives Award for Excellence from International Petroleum Technology Conference Kuala Lumpur, December 3, 2008.

62. The Norwegian Petroleum Directorate is administratively subject to the Ministry of Petroleum and Energy, and advises the Ministry on matters concerning the management of the petroleum resources on the Norwegian continental shelf. The Directorate holds all the important data in connection with the petroleum activity in Norway, including a complete, up-to-date survey of resources, production, costs and other relevant information.

63. BP Statistical Review 2008 page 8.

64. Norway StatoilHydro shareholders.

http://www.statoilhydro.com/en/InvestorCentre/Share/Shareholders/Top20/Pages/default.aspx

65. Petter Osmundsen Commitment at home and abroad 30.4.2007 Merging Statoil and Hydro's petroleum business will benefit the international involvement of the new company, since size is significant in this business. But any reduction in activity on the NCS would be a very poor socio-economic outcome for Norway.

66. See Petoro Perspective Sveinun Sletten. The Norwegian government has been involved as an owner from the early days of the country's oil adventure – through Statoil and Hydro. And from 1985 also through the State's Direct Financial Interest (SDFI).

67. The Norwegian Petroleum Directorate shall contribute to creating the greatest possible values for society from the oil and gas activities by means of prudent resource management based on safety, emergency preparedness and safeguarding of external environment.

68. The Research Council for Norway, Funding for Petroleum Research Adviser Tor-Petter Johnsen PETROMAKS.

69. Offshore Magazine April 2002 Norway: NKr 46 billion Snøhvit scheme brings LNG to northern Norway By Nick Tedre, Contributing Editor.

70. StatoilHydro Annual Report 2008.

71. 2000 NWECS Report by Wajid Rasheed.

72. BP Statistical Review 2008 page 8.

73. US Country Analysis Brief of Mexico http://www.eia.doe.gov/emeu/cabs/mexico.html

74. US EIA DOE Caspian Sea Analysis Report January 2007.

75. Authors discussion with Kazhak expert.

76. See www.eia.doe.gov/emeu/cabs/Kazakhstan/pdf

مدينة الملك عبدالعزيز
للعلوم والتقنية KACST
Oil and Gas Research Institute

Seismic Analysis Center

Our Vision Is to be the leading soultion provider for seismic processing and imaging in the arabian peninsula

SAC - KACST - P.O. Box. 6086 Riyadh 11442
Tel. : +966 1 4814324 - FAx : +966 1 4814314

www.sac.edu.sa

Find More, Produce More with Baker Hughes Geoscience Services

With our geoscience technologies and expertise, we can help maximize the value of your project with timely, accurate reservoir answers.

We can improve hydrocarbon recovery by bringing together highly skilled, multidisciplinary teams of experts in a service environment. Employing cutting-edge collaboration tools, our specialists in geology, geophysics, petrophysics, reservoir engineering and related fields apply advanced techniques in an integrated environment—helping you cut costs, reduce risks and increase production.

Choose an integrated, seamless, and user-friendly service that empowers you to work more efficiently than ever and collaborate as a virtual team. Make the right decision for your reservoir and contact your Baker Hughes representative today.

www.bakerhughes.com

BAKER HUGHES